

Lab-on-a-Chip Technology and its Application to Drug Analysis

**Dissertation zur Erlangung des Doktorgrades
der Naturwissenschaften
der Fakultät für Chemie und Pharmazie
der Universität Regensburg, Deutschland**



vorgelegt von

Kamal M. A. Tolba

aus Ägypten

September 2007

Lab-on-a-Chip Technology and its Application to Drug Analysis

**Dissertation zur Erlangung des Doktorgrades
der Naturwissenschaften
der Fakultät für Chemie und Pharmazie
der Universität Regensburg, Deutschland**



vorgelegt von

Kamal M. A. Tolba

aus Ägypten

September 2007

Lab-on-a-Chip Technology and its Application to Drug Analysis

Doctoral Dissertation

by

Kamal M. A. Tolba



**Faculty of Chemistry and Pharmacy,
University of Regensburg, Germany**

September 2007

This study was performed at the Max-Planck institute of carbon research in Mülheim an der Ruhr and the institute of analytical chemistry, chemo- and biosensors of the University of Regensburg between October 2004 and July 2007 under the supervision of Prof. Dr. Detlev Belder.

Date of defense: 12.09.2007

Committee of defense (Prüfungsausschuss):

Chairperson (Vorsitzender): Prof. Dr. Georg Schmeer

First expert (Erstgutachter): Prof. Dr. Detlev Belder

Second expert (Zweitgutachter): Prof. Dr. Jörg Heilmann

Third expert (Drittprüfer): Prof. Dr. Achim Göpferich

List of publications

- 1- Belder, D., Kohler, F., Ludwig, M., **Tolba, K.**, Piehl, N., Coating of powder-blasted channels for high-performance microchip electrophoresis, *Electrophoresis* 2006, 27, 3277–3283.
- 2- **Tolba, K.**, Belder, D., Fast quantitative determination of diuretic drugs in tablets and human urine by microchip electrophoresis with native fluorescence detection, *Electrophoresis* 2007, 28, 2934–2941.
- 3- **Tolba, K.**, Belder, D., Fast determination of central nervous system stimulant drugs in tablets and human urine by microchip electrophoresis with fluorescence detection, in course of submission.

This thesis is dedicated to:

my parents, my wife and my daughters

Acknowledgements

I would like to thank my supervisor Professor Detlev Belder for his useful advice and guidance in this work. When he assigned me to my first microfluidic project, I did not realize that this research is multi-disciplinary as it contains many areas of science including biology, physics, material science, surface chemistry. It requires a broad basic understanding of these areas to be able to communicate with collaborators. However, with his guidance, I managed to navigate through the problems of this research area and understood how we can use microfluidics technology to solve some of these problems. He always emphasized the need to keep abreast with recent advances in analytical technologies and I would like to thank him for sending me to Doktorandenseminar in Hohenroda to present and keep up with cutting edge research. I would also like to thank the chromatography group in Max-Planck institute of carbon research in Mülheim an der Ruhr. I would also like to thank all my colleagues in the lab and friends in Germany for making my stay enjoyable and memorable. Also I would like to give my deep appreciation to the department of chemistry, Regensburg University for giving me the opportunity to broaden my knowledge.

I would like to thank my wife for supporting me through all these years and keeping me balanced. I also thank my family for their unwavering support of this undertaking. The financial support of the Ministry of Higher Education of Egypt and the National Organization for Drug Control and Research (NODCAR, Cairo, Egypt) is gratefully acknowledged.

Table of contents

Dedication.....	i
Acknowledgements.....	ii
List of figures.....	v
List of tables.....	vii
List of abbreviations.....	viii
Chapter 1 Introduction.....	1
1.1 Surface modification project.....	1
1.2 Therapeutic and abuse drugs analysis project.....	2
Chapter 2 Theoretical background.....	4
2.1 History of capillary electrophoresis (CE).....	4
2.2 Basic principles of CE.....	5
2.2.1 Electrical double layer.....	8
2.2.2 Electroosmosis.....	10
2.2.3 Electrophoresis.....	10
2.2.4 Flow profile in CE.....	11
2.2.5 Efficiency.....	13
2.2.6 Resolution.....	14
2.3 Factors affecting peak resolution in CE.....	15
2.3.1 Electrodispersion.....	15
2.3.2 Joule heating.....	16
2.3.3 Solute-capillary wall interactions.....	17
2.3.4 Running buffer.....	17
2.3.5 Applied voltage.....	18
2.3.6 Injection plug length.....	19
2.4 Modes of capillary electrophoresis.....	19
2.4.1 Capillary zone electrophoresis.....	20
2.4.2 Micellar electrokinetic capillary chromatography.....	20
2.5 Fluorescence detection in CE.....	21
2.6 Capillary electrophoresis on microchip.....	23
2.6.1 Chip materials and fabrication.....	24
2.6.1.1 Photolithography and wet chemical etching.....	25

2.6.1.2 Powder blasting.....	26
2.6.2 Detection in MCE.....	27
2.6.3 Chip layout.....	28
2.6.4 Pinched injection.....	29
Chapter 3 Experimental part.....	32
3.1 CE instrumentation and capillary.....	32
3.2 MCE-instrumentation.....	32
3.3 MCE-LIF coupling.....	35
3.4 Microchip.....	36
3.5 Chip handling and storage.....	37
3.6 Chip coating.....	38
3.7 Derivatization and solutions.....	38
3.8 Chemicals.....	41
3.9 MCE experiments.....	42
Chapter 4 Results and discussion.....	43
4.1 Surface modification.....	43
4.2 Application to drug analysis.....	56
4.2.1 Application to central nervous system stimulant drugs.....	56
4.2.1.1 Method development.....	57
4.2.1.2 Application to pharmaceutical formulations.....	63
4.2.1.3 Application to human urine.....	69
4.2.2 Application to diuretic drugs.....	74
4.2.2.1 Method development.....	75
4.2.2.2 Quantitative analysis of diuretics in tablets.....	81
4.2.2.3 Analysis of diuretics in human urine.....	87
Chapter 5 Summary and conclusions.....	89
Chapter 6 Curriculum vitae.....	91
References.....	92

List of figures

2.1	Cross-sectional view of a fused silica capillary.....	7
2.2	Schematic diagram of a classical capillary electrophoresis system.....	7
2.3	Schematic diagram of the electrical double layer.....	9
2.4	Mobility of ions in an applied field.....	12
2.5	Hypothetical flow profiles.....	12
2.6	Calculation of efficiency and resolution from an electropherogram.....	15
2.7	Electrodispersion due to mismatched sample and buffer conductivities.....	16
2.8	Schematic diagram of MEKC principle.....	21
2.9	Schematic diagram of the Argos system.....	22
2.10	Number of publications in scientific journals.....	23
2.11	Photolithography process.....	26
2.12	A schematic diagram of the powder blasting process.....	27
2.13	Microchip layouts.....	29
2.14	Schematic drawing of the pinched injection.....	30
2.15	Video images of the pinched injection process.....	31
3.1	Photo of MCE-system.....	33
3.2	Instrumental setup of a modular MCE.....	34
3.3	Chip mount and electrode cover plate.....	34
3.4	MCE-laser coupling.....	35
3.5	Simple cross microchip layout and channel dimensions.....	37
3.6	Schematic drawing of the coating device.....	38
3.7	Excitation-emission spectra of AF350.....	39
3.8	Excitation-emission spectra of FITC.....	40
4.1	Scanning electron microscope micrographs for wet chemical and powder blasted channels.....	43
4.2	Chemical structure of the AF350-amine test compounds.....	45
4.3	Electropherogram of the AF350-amine test compounds.....	45
4.4	Video image of the leakage through the 100 μm channel.....	46
4.5	Baseline drifts due to leakage through the 100 μm channel.....	47
4.6	Video images of the injection process using uncoated wc- and pb-chips.....	48
4.7	Electropherograms of AF350-labeled amines.....	48
4.8	Efficiencies of separation of AF350-labeled amines.....	49

4.9 Effect of dynamic coating on the separation of AF350-labeled amines.....	51
4.10 Chemical structure of the FITC-amine test compounds.....	52
4.11 Efficiencies and resolutions of separation of FITC-labeled amines.....	53
4.12 Chiral separation obtained on pb-chips.....	55
4.13 Chemical structure of (-)-ephedrine and (+)-pseudoephedrine.....	56
4.14 Electropherograms of FITC labeled stimulant drugs obtained using CE.....	58
4.15 Electropherograms of FITC labeled stimulant drugs obtained in different chips.....	60
4.16 Electropherograms of FITC labeled stimulant drugs obtained in BF and FS chips.....	61
4.17 Electropherograms of FITC-ephedrine in different BGE.....	62
4.18 Electropherograms of ephedrine and pseudoephedrine at LOD.....	63
4.19 Standard calibration plots for standard ephedrine and pseudoephedrine.....	64
4.20 Electropherograms of standard ephedrine and pseudoephedrine at LOQ.....	65
4.21 Electropherograms of ephedrine and pseudoephedrine in commercial tablets....	67
4.22 Standard calibration plots for ephedrine and pseudoephedrine in human urine.....	70
4.23 Electropherograms of labeled ephedrine and pseudoephedrine in vitro human urine.....	71
4.24 Electropherograms of standard ephedrine and pseudoephedrine in human urine at LOD.....	72
4.25 Electropherograms of labeled ephedrine and pseudoephedrine in vivo human urine.....	73
4.26 Chemical structure of the diuretic drugs.....	74
4.27 3-D measurements of the excitation-emission spectra of the diuretics.....	75
4.28 Comparison of electropherograms of diuretics obtained with CE and MCE.....	76
4.29 Electropherograms of diuretics using different pH buffers.....	77
4.30 Electropherograms of diuretics using some additives.....	79
4.31 Comparison of sensitivities obtained with different light sources for excitation in MCE.....	80
4.32 Standard calibration plots for standard diuretic drugs.....	82
4.33 Electropherograms of standard diuretics at LOD.....	83
4.34 Electropherograms of standard diuretics at LOQ.....	84
4.35 Electropherograms of the diuretics in commercial tablets.....	85
4.36 Electropherogram of the standard diuretic drugs in human urine.....	87

List of tables

2.1 List of commonly used buffers with their characteristics.....	18
4.1 Method validation for quantitative determination of ephedrine and pseudoephedrine.....	66
4.2 Determination of ephedrine and pseudoephedrine in pharmaceutical formulations...	68
4.3 Determination of ephedrine and pseudoephedrine in human urine.....	70
4.4 Method validation for quantitative determination of diuretic drugs.....	82
4.5 Determination of diuretics in pharmaceutical formulations.....	86

List of abbreviations

CE	Capillary electrophoresis
CZE	Capillary zone electrophoresis
MEKC	Micellar electrokinetic capillary chromatography
HPCE	High-performance capillary electrophoresis
MCE	Microchip capillary electrophoresis
EOF	Electroosmotic flow
SDS	Sodium dodecyl sulfate
HV	High voltage
PI	Isoelectric point
PMT	Photomultiplier tube
ACN	Acetonitrile
DMSO	Dimethyl sulfoxide
PAHs	Polyaromatic hydrocarbons
CD	Cyclodextrin
PDMS	Polydimethylsiloxane
PMMA	Polymethylmethacrylate
pb	Powder blasted
wc	Wet chemical
LOC	Lab-on-a-chip
PVA	Polyvinyl alcohol
TRIS	Trisamine
MES	2-Morpholinoethanesulfonic acid
CHES	N-cyclohexyl-2-aminoethanesulfonic acid
PIPES	Piperazine-1,4-bis(2-ethanesulfonic acid)
HEPES	N-(2-hydroxyethyl)-piperazine-N'-2-ethanesulfonic acid
i.d.	Internal diameter
o.d.	Outer diameter
BI	Buffer inlet
BO	Buffer outlet
SI	Sample inlet
SO	Sample outlet

SEM	Scanning electron microscope
LIF	Laser induced fluorescence
LOD	Limit of detection
LOQ	Limit of quantification
IR	Infrared
BF	Borofloat
FS	Fused-silica
AF350	Alexa flour 350
FITC	Fluorescein-5-isothiocyanate
HP- γ -CD	Hydroxypropyl- γ -cyclodextrin
HPMC	Hydroxypropylmethylcellulose
POC	Point-of-care
CNS	Central nervous system
E	Ephedrine
PE	Pseudoephedrine
RSD	Relative standard deviation
BFMTZ	Bendroflumethiazide
HCTZ	Hydrochlorothiazide
BGE	Background electrolyte

Chapter 1 Introduction

Lab-on-a-chip (LOC) is a term for devices that integrate multiple laboratory functions on a single chip of only millimeters to a few square centimeters in size and that are capable of handling extremely small fluid volumes down to less than pico liters [1]. Miniaturization of chemical analysis systems using microchips is an emerging new technology. In order to achieve widespread applications of those systems other materials (polymers) than silicon are required as the basis of the chips. Currently, glass is frequently used as a substrate material due to its favorable electrical and optical properties and its ease of structuring by wet chemical etching or powder blasting techniques.

Microfluidic devices have been applied to electrophoretic separations for a variety of biochemical and chemical analysis [2-8]. Microchip capillary electrophoresis (MCE) is often regarded as a higher miniaturized version of capillary electrophoresis (CE) and a lot of applications can easily be transferred from classical CE to the microchip format.

This thesis is divided into two main projects. The following two sections briefly discuss the motivations of each project.

1.1 Surface modification project

In order to obtain the desired microstructures in glass, generally a fabrication technique based on photolithography is used [9]. Its main disadvantages are the health hazards involved with hydrogen fluoride (HF) and the clean room facilities required for the photolithographic process, leading to relatively high fabrication costs [10].

A cheap and simple process to obtain microstructures in glass was developed in the last decade which is known as the “powder blasting” process [11]. The main drawback of powder-blasted chips in comparison to hydrogen fluoride (HF)-etched fluidic channels is the higher roughness of the channel surface, which, in general is at least a few μm for powder blasting and below 100 nm for HF-etching [10]. It was also found that the resolution in electrophoretic separation obtained in powder-blasted (pb) devices is lower compared to wet chemical etched (wc) chips, which is attributed to the much higher surface roughness inducing band broadening [10].

Surface modification is of great importance in chip-based microfluidic devices especially in highly miniaturized and integrated systems due to the high surface area-to-volume ratio [12]. Motivations for surface manipulation are similar to those for classical capillary electrophoresis. However, surface modification appears to be even more important in microchip capillary electrophoresis for the following reasons:

(i) Control of the electroosmotic flow (EOF): Stabilization of the electroosmotic flow is required in MCE because most of the injection processes such as pinched and gated injections rely on the reproducibility of the EOF. Furthermore, stabilization of EOF is not only important in order to improve the precision of migration times but also necessary for a robust injection process with predefined potentials avoiding back leakage of the sample and ensuring injection of a reproducible sample plug.

(ii) Reduction of analyte-wall interaction: Application of appropriate surface coatings reduces the analyte-wall interaction, elevates separation efficiency and enhances resolution.

This project focuses on improving the resolution obtained using powder blasted (pb) chips. Coating materials such as polyvinyl alcohol (PVA) and hydroxypropylmethylcellulose (HPMC) are used to cover the channel walls of the chips. These coated pb-chips are utilized in a chip electrophoresis. The obtained data are then compared to those based on classical wet chemical etched (wc) chips.

1.2 Therapeutic and abuse drugs analysis project

Drug analysis is undertaken during various phases of pharmaceutical development such as formulation, stability studies, toxicological and pharmacological testing [13-16]. In hospitals, drug analysis is performed on patients' samples in support of clinical trials (bioavailability and pharmacokinetic studies), in monitoring therapeutic drugs and drugs of abuse [17-20]. All these investigations require reliable and validated analytical methods in order to measure drugs in complex media such as formulations and biological fluids.

For drug analysis, a variety of analytical techniques have been developed involving immunoassays [21, 22], spectrophotometry [23, 24], thin-layer chromatography (TLC) [25], gas chromatography (GC) [26, 27] and high performance liquid chromatography (HPLC) [28-42]. Furthermore, 42 references are found in literature

[43] describing some methods for doping control analysis. Most of these methods are based on chromatographic techniques [44-51]. These methods, however, require large amounts of analytes, are time consuming, use bulky instrumentation and generate large quantities of organic waste. Capillary electrophoresis (CE) has also been used as an alternative separation method for the analysis of pharmaceutical compounds [52 – 58]. More recently, considerable interest has been directed to the use of MCE [59] due to the fact that MCE has the potential to achieve very rapid analysis (typically seconds), easy integration of multiple analytical steps and parallel operation [60-68]. For these reasons, MCE would speed up quality control of drugs and thus would shorten the time of a drug to enter the market remarkably.

This project focuses on the development and validation of fast methods based on MCE to detect some drugs of abuse such as central nervous system stimulant drugs and diuretics, which are prohibited by the International Olympic Committee [69], in pharmaceutical formulations and human urine. The linearity, reproducibility and applicability of those methods are evaluated. Such methods can be used in clinical toxicology, therapeutic drug monitoring, forensic science and doping control.

Chapter 2 Theoretical background

2.1 History of capillary electrophoresis

The history of the development of capillary electrophoresis (CE) started at 1879 when Helmholtz applied an electric field to the ends of a horizontal glass plate. Afterwards, he observed a very important phenomenon, which led to the principle of capillary electrophoresis, where the bulk liquid flows towards the negative electrode. Based on this observation, he could conclude that the plate wall acquired a negative charge while the solvent close to the wall surface was positively charged. A second scientist who described a similar phenomenon is called Lodge [70]. He also observed the migration of H^+ in a tube of phenolphthaline in the presence of an electric field. After that Kohlrausch [71] described that the passage of an electric current through a uniform electrolyte solution does not provide concentration changes in the system. In 1932, Tiselius explained the moving boundary method for the electrophoresis of proteins in a U-shaped tube [72]. In 1937, he introduced a new way of studying proteins and used electrophoretic methods to separate the chemically similar proteins of blood serum, an achievement that was especially cited in the Nobel award. Therefore he was awarded the Nobel Prize for chemistry in 1948.

In 1967, Hjerten described zone electrophoresis in free solution [73]. He described two methods of the problem of eliminating convection in free solution. One of these methods is based on rotation (40 rpm) of the horizontal capillary around its long axis while the other is based on the use of a stationary capillary with a narrow bore (the latter method is now called high-performance capillary electrophoresis). Hjerten's work mainly focused on the first method. At that time (1967) no UV detectors were available that would be sensitive enough to detect zones in a tube with a diameter below 1 mm. Hjerten was the first to describe the coating technique of the capillaries and the advantages of coated capillaries for improving the separation. He also explained the effect of sample conductivity on the separation of metal ions, nucleotides, proteins, nucleic acids, DNA, purine and pyrimidine bases. In his 1967 publication, Hjerten successfully demonstrated the application of free zone electrophoresis ensuring a theoretical understanding of the CZE process and expected that CE could become an alternative technique for different applications. There is another successful demonstration for capillary zone electrophoresis

(CZE) explained by Virtanen [74, 75] who used glass capillaries as separation columns with an internal diameter (i.d.) of 0.2-0.5 mm and a column length of 50-100 cm. The very important evaluation of concentration distribution in zone electrophoresis was explained by Mikkers et al. [76, 77], who demonstrated that rapid and highly efficient separations could be obtained in the absence of diffusional broadening. As a result, he could confirm the theoretical predictions about separation efficiency which was demonstrated by Giddings [78].

Jorgenson and Lukacs [79-81] described a very important explanation which led to the initial demonstration of the power of modern capillary electrophoresis. They described that a high separation efficiency with high-field strength in narrow capillaries (less than 100 μm i.d.) was obtained. They demonstrated also a brief discussion of the theory of dispersion in CE [79]. Since that time CE techniques have been growing fast, and a commercial CE instrument became available at the end of the 1980s. Currently, CE is gaining popularity as an alternative analytical tool for some routine analytical applications.

2.2 Basic principles of capillary electrophoresis

In high-performance capillary electrophoresis (HPCE), separation is performed in narrow-bore capillaries, typically of 10-100 μm inner diameters (i.d.). The length of the capillary differs by different applications, but it is normally in the range of 40-100 cm. Fused-silica capillaries, typically used in CE, are externally coated with polyimide (Figure 2.1) which gives flexibility to the capillary that would otherwise be very fragile. The small bore allows easy control of temperature which improves separation efficiencies. Other types of capillaries such as Teflon and polypropylene capillaries have also been used for some applications. In a CE system, the ends of the capillary are connected to electrodes, which are connected to a high voltage power supply. The capillary ends are placed into buffer reservoirs, and the capillary is filled with a buffer identical to that in the reservoirs as shown in Figure 2.2. The sample is introduced into the capillary by replacing one of the buffer reservoirs with a sample reservoir (usually at the anode end); the sample may be injected either electrokinetically or hydrodynamically. After the buffer reservoir is replaced, the electric field is applied and the separation is performed. Either on-column or end-column optical detection can be made at the cathode end of the capillary.

The time interval between the beginning of the separation and the passage of the analyte zone through the detection point (migration time, t_{mig} , s) is used for identification of the sample components. The information in observed migration times can be made more universally comparable by a conversion to observed migration rates or migration velocity (v_{obs} , cm/s) according to equation 2.1:

$$v_{obs} = \frac{l}{t_m} \quad (2.1)$$

where l [cm] is the length of the capillary between the point of sample introduction and detection. The calculation of migration velocity allows a comparison of migration behavior between capillaries of different lengths. To compare migration data of different capillary lengths and at different applied separation potentials, it is necessary to calculate the observed electrophoretic mobility (μ_{obs} , $\text{cm}^2 \text{v}^{-1} \text{s}^{-1}$):

$$\mu_{obs} = \frac{v_{obs}}{E} \quad (2.2)$$

E [V/cm] is the applied electric field.

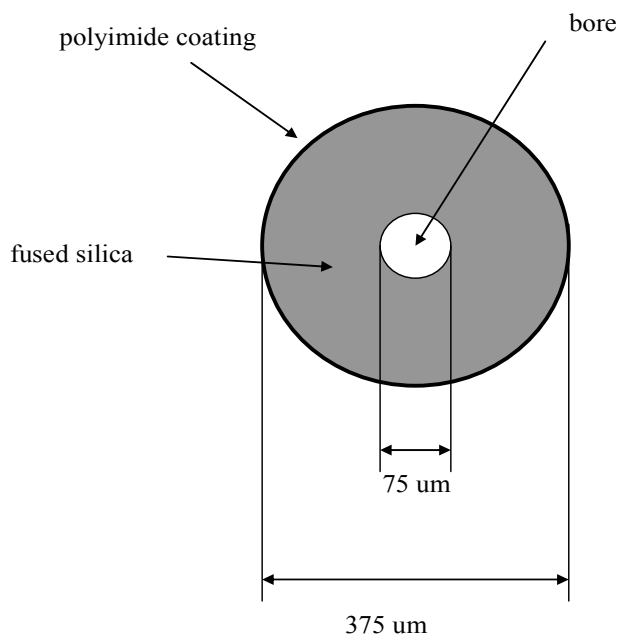


Figure 2.1: Cross-sectional view of a fused silica capillary [82].

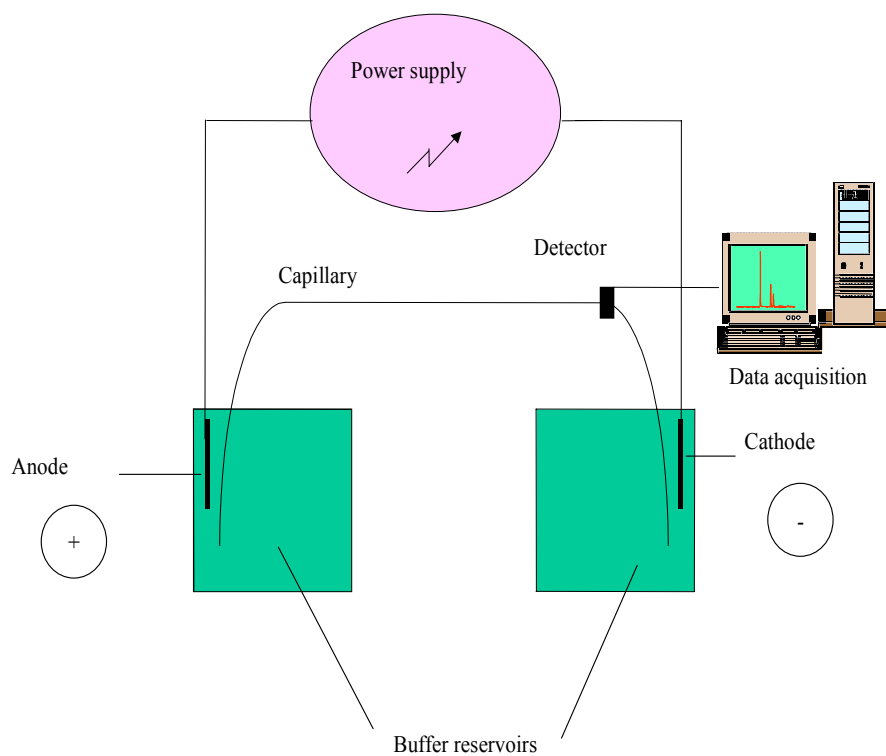


Figure 2.2: Schematic diagram of a classical capillary electrophoresis system [83].

2.2.1 Electrical double layer

The formation and structure of the electrical double layer is important in CE because any change in this layer will change the electrophoretic behavior of ions. The structure of the electrical double layer is shown in Figure 2.3. When the silica surface is negatively charged, counterions tend to adsorb on it by electrostatic attraction which balances the surface negative charge. According to Stern's model (Figure 2.3A), a rigid double layer of adsorbed ions (Stern layer) is in equilibrium with an outer diffuse layer allowing diffusion of ions by thermal motion.

This double layer system provides an electric potential ψ at the interface between silica surface and electrolyte solution. Within the rigid double layer the potential decreases linearly with the distance from the surface and becomes zero in the diffuse layer as shown in Figure 2.3B. The potential at the shear plane is known as the zeta potential (ζ -potential).

A layer of water, about a molecule in thickness, is probably bound to the charged surface, mainly by charge-dipole interaction. The usual location of the surface of shear is therefore just outside the Stern layer and the ζ -potential is generally smaller in magnitude than ψ_d . The electrokinetic potential, which can influence ion migration in CE, is determined by the properties of the electrical double layer [84-86]. The zeta potential is proportional to the surface charge density and the thickness of the double layer. This potential can be influenced by many parameters such as the pH of the separation medium, ionic strength, charge and nature of counterions, surface active agents, and organic solvents [86].

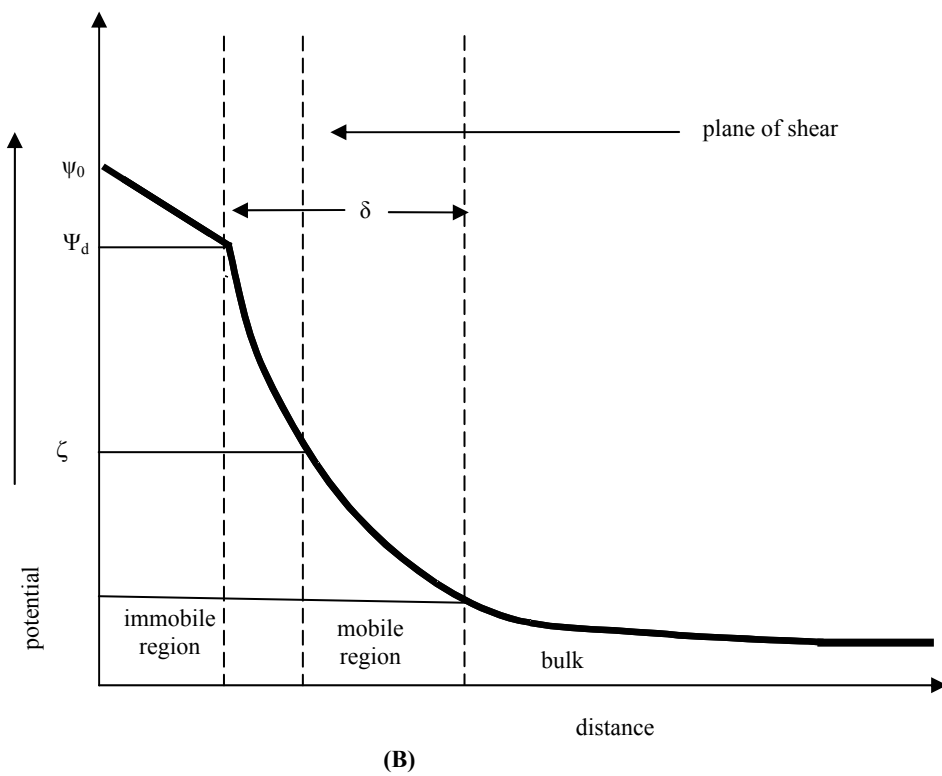
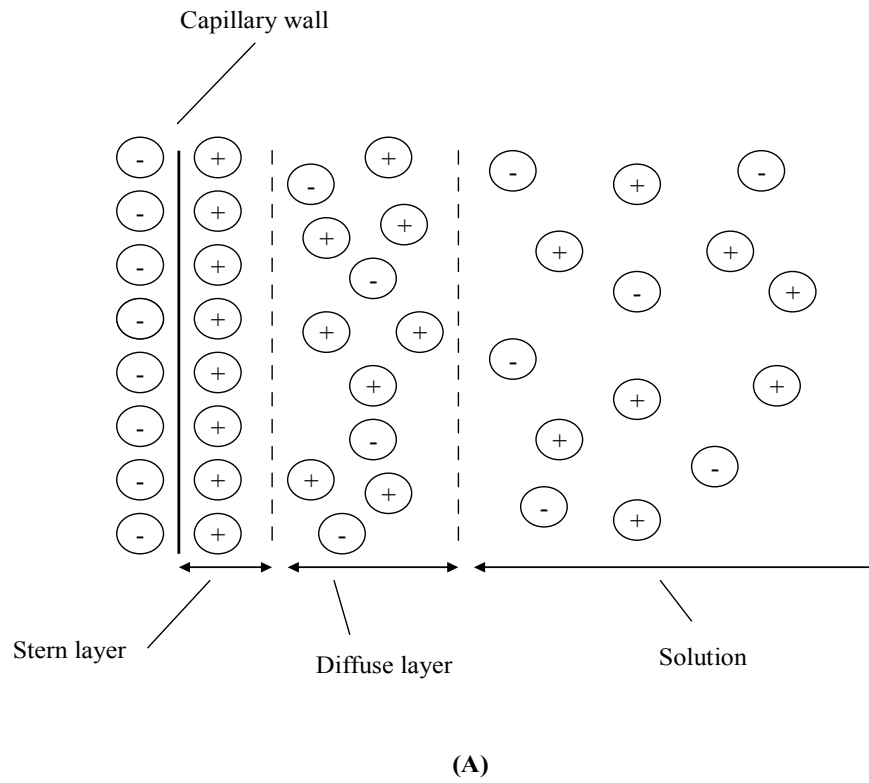


Figure 2.3: Schematic diagram of the electrical double layer. δ and ζ are the thickness of the diffuse layer and zeta potential, respectively [87].

2.2.2 Electroosmosis

Electroosmosis is defined as the movement of liquid relative to an immobile charged surface in the presence of an electric field. The fused silica capillaries that are typically used for separations have ionizable silanol groups in contact with the buffer which fills the capillary.

The negatively-charged wall attracts positively-charged ions from the buffer, creating an electrical double layer. When a voltage is applied across the capillary, cations in the diffuse portion of the double layer migrate in the direction of the cathode, carrying water with them. This results in a net flow of buffer solution in the direction of the negative electrode. Such a phenomenon is called electroosmotic flow (EOF).

The electroosmotic flow (EOF) has a plug form profile as shown in Figure 2.4. The plug form of EOF can result in less peak broadening and higher separation efficiency compared to HPLC separation [88]. The magnitude of the electroosmotic mobility can be calculated by the use of the Smoluchovski equation [89]:

$$\mu_{eo} = -\frac{\varepsilon\zeta}{4\pi\eta} \quad (2.3)$$

Where η is the medium viscosity (Poise), ε is the dielectric constant (Fm^{-1}), and ζ is the zeta potential (V). The EOF can be measured by the injection of a neutral compound (neutral marker).

2.2.3 Electrophoresis

Electrophoresis is defined as the migration of charged species in an electrolyte solution under the influence of an electric field. Ionic solutes are separated based on differences in charge, size and shape. When a charged particle is placed in an electric field it experiences a force which is proportional to its effective charge q and the electric field strength. The transitional movement of the particle is opposed by a viscous drag force which is proportional to particle velocity, hydrodynamic radius r and medium viscosity. When the two forces are counterbalanced the particle moves with a steady state velocity. Electrophoretic mobility of an ion is defined by:

$$\mu_{ep} = \frac{q}{6\pi\eta r} \quad (2.4)$$

This equation is suited only for spherical particles under the assumption that the velocity of the liquid, relative to the particle, vanishes at the particle surface [90, 91]. From equation 2.4 we can see that differences in electrophoretic mobility will be caused by difference in the charge-to-size ratio of ions. In an applied electric field, cations move towards the cathode (negative electrode) while anions move towards the anode (positive electrode). Different ions and solutes have different electrophoretic mobilities; therefore they also have different migration velocities at the same electric field. This could be explained as in a normal situation at $\text{pH} > 3$, the capillary surfaces are negatively charged, and thus the EOF is cathodal. When cations move in the same direction as the EOF (towards cathode), their apparent mobility (μ_{obs}) is larger than their electrophoretic mobility ($\mu_{ep} < \mu_{obs}$). If anions move in the opposite direction to the EOF, their apparent mobility is smaller than their electrophoretic mobility ($\mu_{ep} > \mu_{obs}$), as shown in Figure 2.4A. The corresponding migration order in an electropherogram is shown in Figure 2.4B.

2.2.4 Flow profile in CE

Due to the EOF in CE having a flat flow profile (Figure 2.5A), the peak efficiency in CE is much better than in HPLC. This profile is caused by EOF's driving force being uniformly distributed around the wall of the capillary. In HPLC, the frictional forces at the column walls cause a pressure drop across the column, yielding a parabolic or laminar flow profile, as shown in Figure 2.5B.

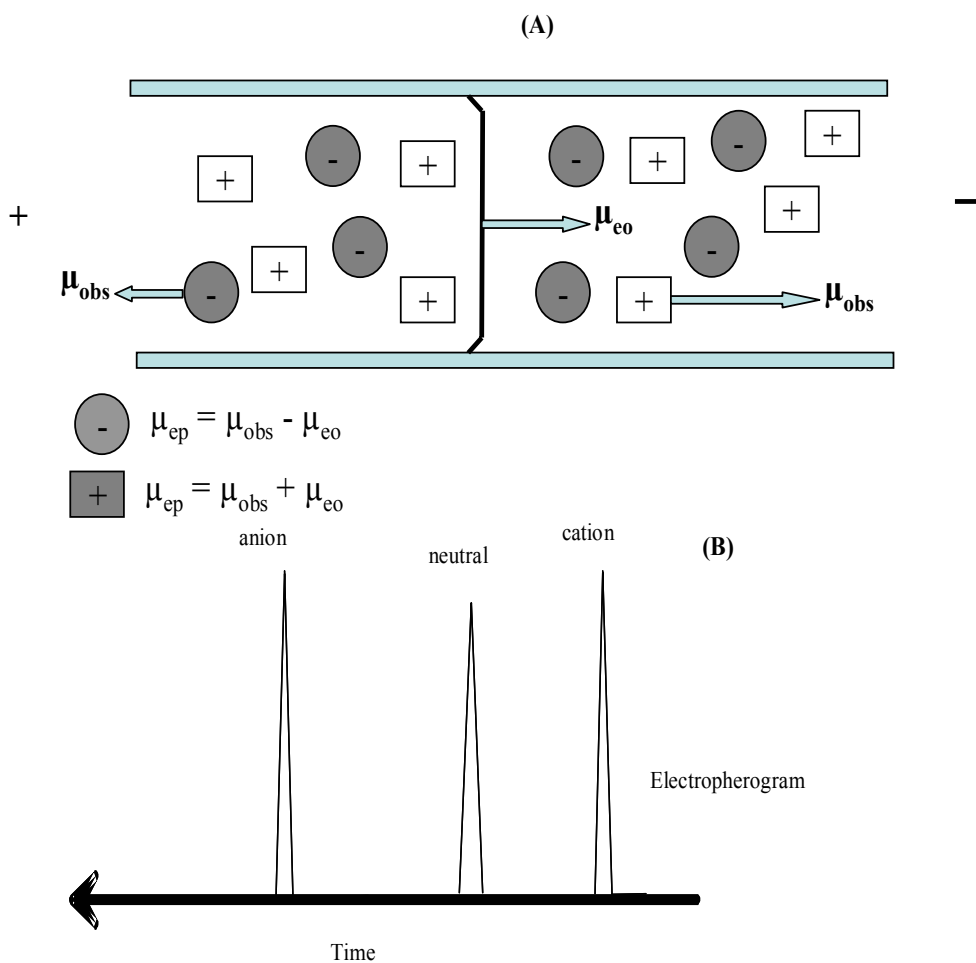


Figure 2.4: (A) Mobility of ions in an applied field where length of arrows represents velocity vectors. (B) Migration order of the analyses [92].

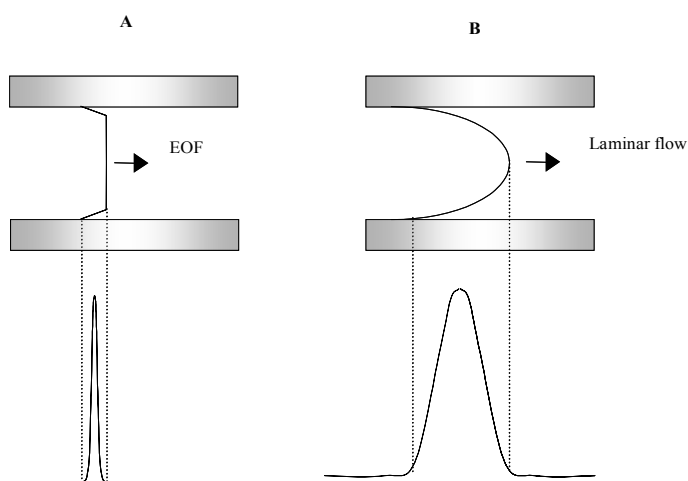


Figure 2.5: Hypothetical flow profiles and corresponding peak forms in case of (A) electrokinetic flow and (B) hydrodynamic flow [93].

2.2.5 Efficiency

In separation science, two related concepts for measuring the efficiency of a separation are widely used namely the plate height (H) and the plate number (N). The width of the analyte zone can be expressed in terms of the plate height [94]:

$$H = \frac{\sigma^2}{L} \quad (2.5)$$

where σ^2 is the variance of the zone and L is the effective separation distance to the detector. In any experiment, the zone broadening of a solute should be kept as small as possible, which means that the variance of a zone (σ) should be kept at a minimum. Low values of H are thus favorable and are in the μm range for high efficiency separations.

An alternative, commonly employed term in electrophoresis is the plate number (N):

$$N = \frac{L}{H} = \frac{L^2}{\sigma^2} \quad (2.6)$$

The plate number for a Gaussian curve (Figure 2.6) can be obtained at half of the height or at the baseline of the peak by use of the following formula:

$$N = f \cdot \left(\frac{t_i}{w} \right)^2 \quad (2.7)$$

where w is the width of the peak at half of the height or at the baseline, t_i is the migration time and the factor f is 5.54 when w is at half of the height and 16 when the width of the peak at the baseline is used. The values of the plate numbers are commonly in the range of 1×10^5 to $5 \times 10^5 \text{ m}^{-1}$ [95].

The efficiency of separation is only limited by diffusion and is proportional to the strength of the electric field as shown in the following equation:

$$N = \frac{\mu V}{2 D_m} \quad (2.8)$$

Where μ is the apparent mobility in the separation medium and D_m is the diffusion coefficient of the analyte.

2.2.6 Resolution

The resolution (R_s) is a quantitative measure of the degree of separation of two species and is defined as [94]:

$$R_s = \frac{2 \cdot \Delta t_{mig}}{(w_1 + w_2)} \quad (2.9)$$

or

$$R_s = \frac{0.589 \cdot \Delta t_{mig}}{(w_{1(1/2)} + w_{2(1/2)})} \quad (2.10)$$

where Δt_{mig} is the difference between the migration times of the analytes and w_1 and w_2 are the widths of the peaks at the baseline; $w_{1(1/2)}$ and $w_{2(1/2)}$ are the peak widths at half of the height. Accordingly, to achieve a high resolution Δt should be large, whereas the zone width should be kept at a minimum. R_s is dependent on the number of theoretical plates and the relative mobility difference between any two species [96]:

$$R_s = \frac{\sqrt{N}}{4} \cdot \frac{\Delta\mu_{app}}{\bar{\mu}} \quad (2.11)$$

where $\Delta\mu_{app}$ is the difference in apparent mobilities of two solutes (for instance, enantiomers) and $\bar{\mu}$ is their average mobility. The R_s is made up of both selectivity ($\Delta\mu / \mu_{app}$) and efficiency (N) terms. The selectivity term is determined by the properties of the analytes and the buffer, whereas the efficiency term is determined by the properties of the buffer and the instrument.

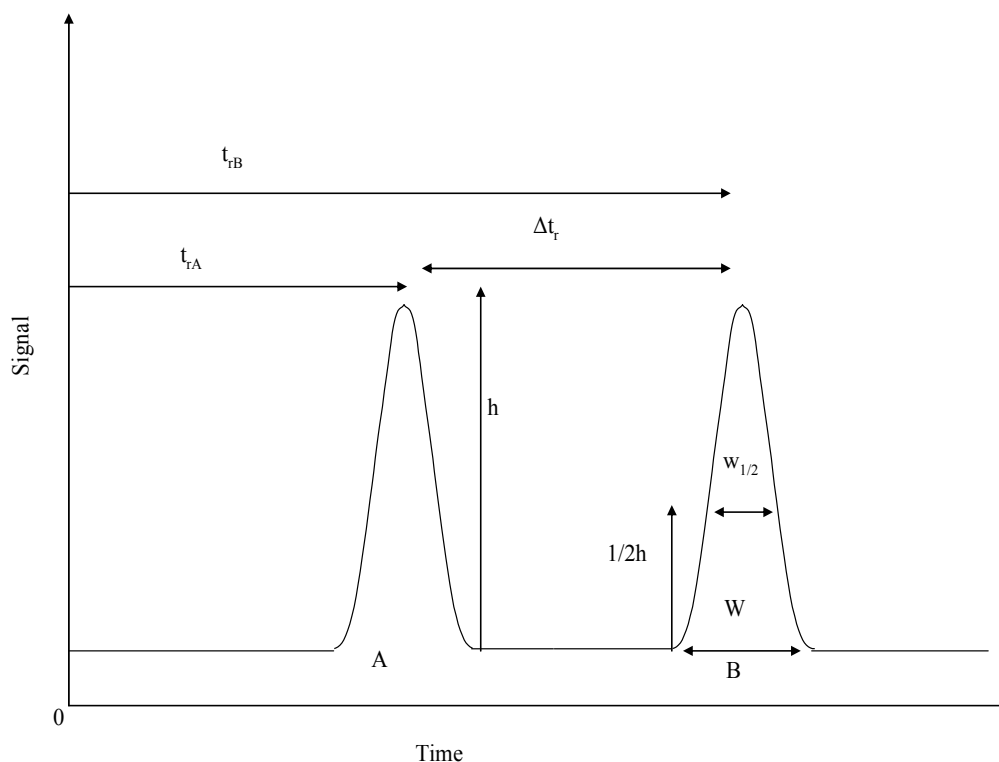


Figure 2.6: Measurements used to calculate efficiency and resolution from an electropherogram. t_{rB} : retention time of peak B, t_{rA} : retention time of peak A, Δt_r : difference in retention of peaks A and B, h : height of peaks, $1/2h$: half height of peaks, w : width of peak at base, $w_{1/2}$: width of peak at half of height [97].

2.3 Factors affecting peak resolution in CE

2.3.1 Electrodispersion

The description of electrodispersion is given by Kohlrausch's regulating function [71]. Differences in sample zone and running buffer conductivity have three major effects. When the solute zone has a higher mobility (i.e. higher conductivity) than the running buffer, the leading edge of the solute zone will be diffused and the trailing edge becomes sharp (Figure 2.7A). Conversely, when the solute zone has a lower mobility than the running buffer, the leading edge will be sharp and the trailing edge diffuses (Figure 2.7C). When the conductivities are equivalent, no such peak distortion will occur (Figure 2.7B). This situation is reversed when anions are analyzed instead of cations. Neutral species are unaffected by this conductivity difference [75].

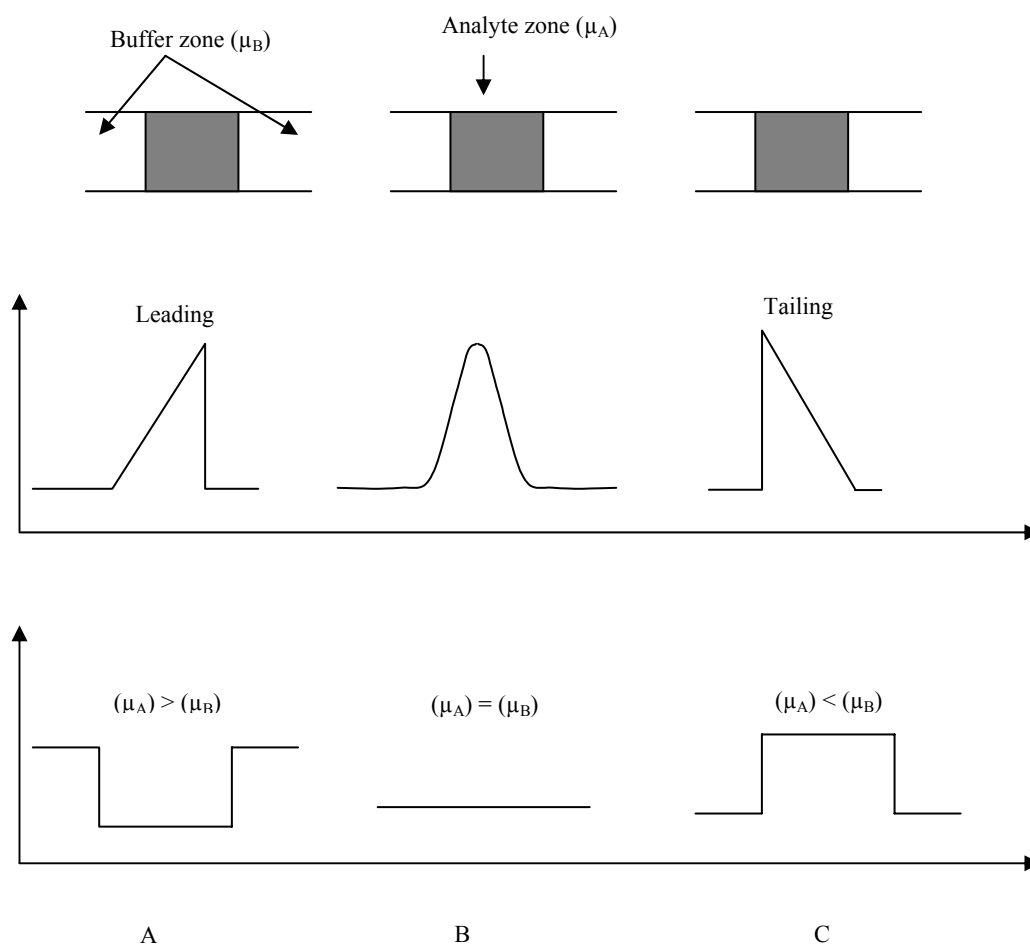


Figure 2.7: Electrodispersion due to mismatched sample and buffer conductivities [93].

2.3.2 Joule heating

When a current passes along an electrolyte solution inside the capillary, electrical energy is partially converted into Joule heating due to frictional collision between mobile ions and buffer molecules. As a result of heat generation the temperature increases within the capillary. The control of the buffer temperature in CE is important for the success of separation. The elevation of temperature inside capillary can lead to problems with reproducible sample injection [98], sample stability [99-101], band broadening [102-105] and quantification [77, 106]. Also, heat generation can lead to undesirable effects such as bubble formation and decreases in conductivity in the capillary.

2.3.3 Solute-capillary wall interactions

The solute-capillary wall interactions phenomena are problematic in CE in term of efficiency. The primary causes of adsorption to the fused silica walls are ionic interactions between cationic solutes and the negatively charged wall. This is due to the fact that fused silica capillaries acquire a negative charge at $\text{pH} > 3$.

As shown by Schure and Lenhoff [107] for the separation of small molecules, where diffusive transport is high, smaller diameter capillaries are clearly more favorable in limiting the potential loss of resolution due to wall adsorption. Various salts, zwitterions and surfactants have been used in buffers to compete with solutes (mostly proteins) for adsorption sites and to minimize adsorption [108-110]. The solute-wall interactions can also be affected by dynamic or permanent coating of the capillary wall [111-114].

2.3.4 Running buffer

The selection of the running buffer is a critical factor in CE because its composition determines the migration behavior of the analytes. A buffer which provides a constant pH is favorable in CE. It enhances the sensitivity of both electrophoretic mobility of the charged species (μ_e) and EOF (μ_{EOF}). A wide variety of buffer systems have been used to effect the required separations. A selection of common buffers is given in Table 2.1.

Some general guidelines can be given for the selection of buffers in CE. Phosphate buffer is widely used in CE because it can be applied in a large pH-range and it also absorbs at a wavelength below 260 nm. For buffers in the basic pH range, TRIS, Tricine and borate are acceptable electrolytes. The advantage of zwitterionic buffers such as MES, PIPES, HEPES and CHES is their low conductivity. This results in a reduction of Joule heating, allowing a higher buffer concentration to be used. This is sometimes useful for minimizing solute-wall interactions, the undesirable effects of electrodispersion and the EOF.

In addition to the type of buffer, its concentration is another principal variable in CE. Theoretically, buffers with high ionic strengths are preferable to minimize solute-capillary wall interactions. On the other hand, highly concentrated buffers have greater conductivity and hence generate more heat; in this case a thermostating/cooling system is necessary.

Table 2.1: List of commonly used buffers with their characteristics [115].

Buffer	pK _a	pH-range	Mobility (10 ⁻⁵ cm ² V ⁻¹ s ⁻¹)	Minimum useful λ (nm)
Phosphate	2.12, 7.21, 12.30	1.14-3.14 6.20-8.20		195
Citrate	3.06, 5.40	3.06-5.40		260
Acetate	4.75	3.76-5.76	-42.4	220
Formate	3.75	2.75-5.75	-56.6	220
MES	6.13	5.15-7.15	-26.8	230
PIPES	6.80	5.80-7.80		215
HEPES	7.51	6.55-8.55	21.8	230
Tricine	8.05	7.15-9.15		230
TRIS	8.30	7.30-9.30		220
Borate	9.14, 12.74, 13.80	8.14-10-14		180
CHES	9.50	9.50		190

2.3.5 Applied voltage

The optimization of the applied voltage (V) in CE is given by the following basic equation [116] for peak resolution (R_s):

$$R_s = \frac{1}{4} \left[\frac{(\mu_{av} + \mu_{EOF})V}{2D} \right]^{1/2} \left[\frac{\Delta\mu}{\mu_{av} + \mu_{EOF}} \right] \quad (2.12)$$

According to equation 2.12, the peak resolution (R_s) is proportional to the square root of the applied voltage. In order to double the resolution the applied voltage should be quadrupled. This can lead to heat generation inside the capillary which limits the value of an increase in voltage for achieving a high resolution in CE. For technical reasons most of

CE instruments operate under a high voltage limit of 30 kV. Although an increase of voltage can improve the peak resolution, attention should be taken to not arrive of the voltage limit (30 kV). A high voltage limit leads to an undesirable effect such as bubble formation.

2.3.6 Injection plug length

During injection it is important to minimize the sample plug length to get high peak efficiency. A practical limit of the injection length is less than 1 or 2 % of the total capillary length [117]. In CE, a solution of analytes is used in a micro- and nanoliter scale. For example the total volume of a 1 m long capillary of 50 μm i.d. is 2 μl . For this reason, even a very small additional volume within the system can lead to strong disturbance of the equilibrium and can cause additional band broadening. Therefore the injected sample plugs should not be too long for a particular separation system. If the sample plug is longer than the dispersion caused by diffusion, the efficiency and resolution will be affected. According to this statement, the plug length for high molecular weight analytes is essentially shorter.

The contribution of the sample volume (σ_s^2) to the total peak dispersion can be expressed as [118]:

$$\sigma_s^2 = \frac{S^2}{12v_R\pi(d_c/r)^4} \quad (2.13)$$

where S is the sample volume, v_R is the linear velocity of the sample injection and d_c is the inner diameter of the cylindrical capillary.

2.4 Modes of capillary electrophoresis

Capillary electrophoresis is used in different applications such as separation of peptides, proteins, oligonucleotides, metal ions and inorganic ions as well as in the analysis of pharmaceuticals and the monitoring of water quality [119-125]. Although the basic principle of CE involves the separation of molecules based on their charge to mass ratio,

there are some modifications to this procedure obtained from existing well-established techniques. This alteration allows the separation of non-charged molecules or even optical isomers. The following sections will outline some of the currently used CE techniques.

2.4.1 Capillary zone electrophoresis (CZE)

Capillary zone electrophoresis (CZE) is the most widely used type of CE because of its simplicity. The separation mechanism of CZE is based on differences in the charge-to-mass ratio of the analytes, this leads to different electrophoretic mobilities of the analytes in free solution under the effect of an electric field.

In CZE the apparent mobility (μ_{app}) of an ion is the sum of the analytes's inherent electrophoretic mobility (μ_e) and the electroosmotic flow (μ_{EOF}) of the capillary.

$$\mu_{app} = \mu_e + \mu_{EOF} \quad (2.14)$$

2.4.2 Micellar electrokinetic capillary chromatography (MEKC)

One limitation of the above described CZE-technique is that only the charged molecules can be separated. Neutral analytes have no electrophoretic mobility and therefore all of those are moving with the EOF. As a result, no separation will occur and all molecules will arrive at the detector at the same time. For this reason, Terabe et al. [126] described MEKC for the separation of neutral analytes. Terabe described that an ionic surfactant micelle is used as a pseudostationary phase that corresponds to the stationary phase in liquid chromatography (LC). A portion of the sample molecules, introduced in the micellar solution, is incorporated into the micelle. The analyte acquires an apparent electrophoretic mobility by interacting with the micelle and a distribution equilibrium is established between the micelle and the surrounding aqueous phase. The analyte that is not incorporated into the micelle migrates at the same velocity of the EOF. The separation of molecules is based on their distribution coefficient between the micellar and the non-micellar (aqueous) phase. Sodium dodecyl sulfate (SDS) is widely used as an anionic surfactant in MEKC because it is easily available in a sufficiently pure form, has good water solubility and is able to solve non-polar molecules [127]. The presence of an anionic micelle based on SDS means that cationic

molecules will associate with the micellar phase while anions will be repelled but migrate to the detector window with the EOF. The separation principle of MEKC with SDS micelles is shown in Figure 2.8.

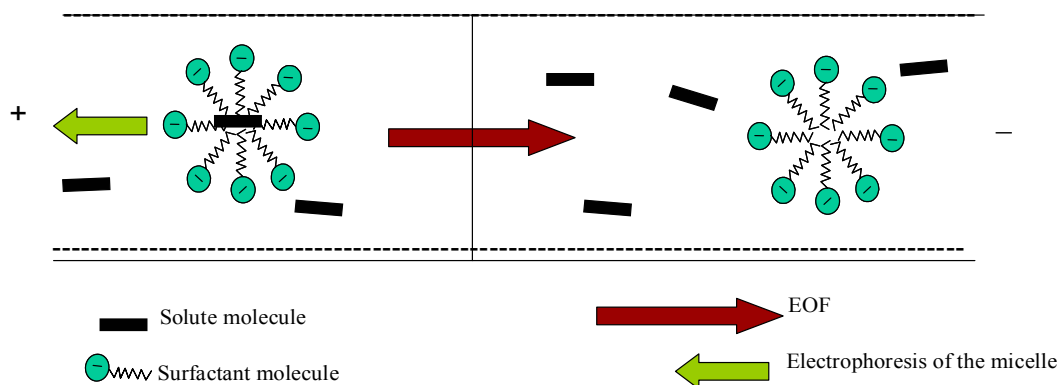


Figure 2.8: Schematic diagram showing MEKC partitioning of neutrals into/out of micelles. The directions of the velocity are given below the capillary [127].

Based on this principle, ephedrine and its diastereoisomer pseudoephedrine are separated using SDS in this work (see chapter 4).

2.5 Fluorescence detection in CE

Fluorescence detection has emerged as one of the most sensitive detection modes used in CE, especially for trace analysis of derivatized amino acids, peptides and oligosaccharides. The high sensitivity of this technique is a result of the low background noise and the direct proportionality between excitation power and emission signal intensity. For fluorescein, a detection limit of approximately 10^{-8} M (S/N=2) has been obtained for conventional fluorescence detection [128]. Using laser-induced fluorescence (LIF) detection, LODs of as low as 10^{-12} M have been realized for fluorescence derivatives of amino acids [129]. A fluorescence detector is comprised of an efficient excitation source, a detection cell and an arrangement to detect the fluorescence signal. Fluorescence detection in CE is mostly performed on-column by aiming the excitation beam at the capillary and collecting the emission on a photo-sensitive device such as a

photodiode or photomultiplier tube.

The Argos 250B (Figure 2.9) is a sensitive fluorescence detector for many applications in capillary electrophoresis. For many compounds the Argos 250B allows increasing sensitivity in CE down to the 1 ng/mL range. The fluorescent light is totally reflected within the capillary in a down-stream direction. This is then diverted by a glass ellipsoid, sleeved over the capillary, at the downstream end of the optical window. In order to allow emitted light to leave the capillary window at the ellipsoid's 1st focus, optical contact is established by applying a tiny amount of glycerol which is held in the contact area by the capillary force. Fluorescence light, which is "trapped" in that way by the ellipsoid, is deflected to its 2nd focus and conducted from there to the photomultiplier in the detector by the emission light guide. In order to keep the optical path free for the emission light guide, the capillary is bent out of the way. This kind of detector is used in this work for different applications such as polyaromatic hydrocarbons (PAHs), central nervous system stimulant drugs and diuretics.

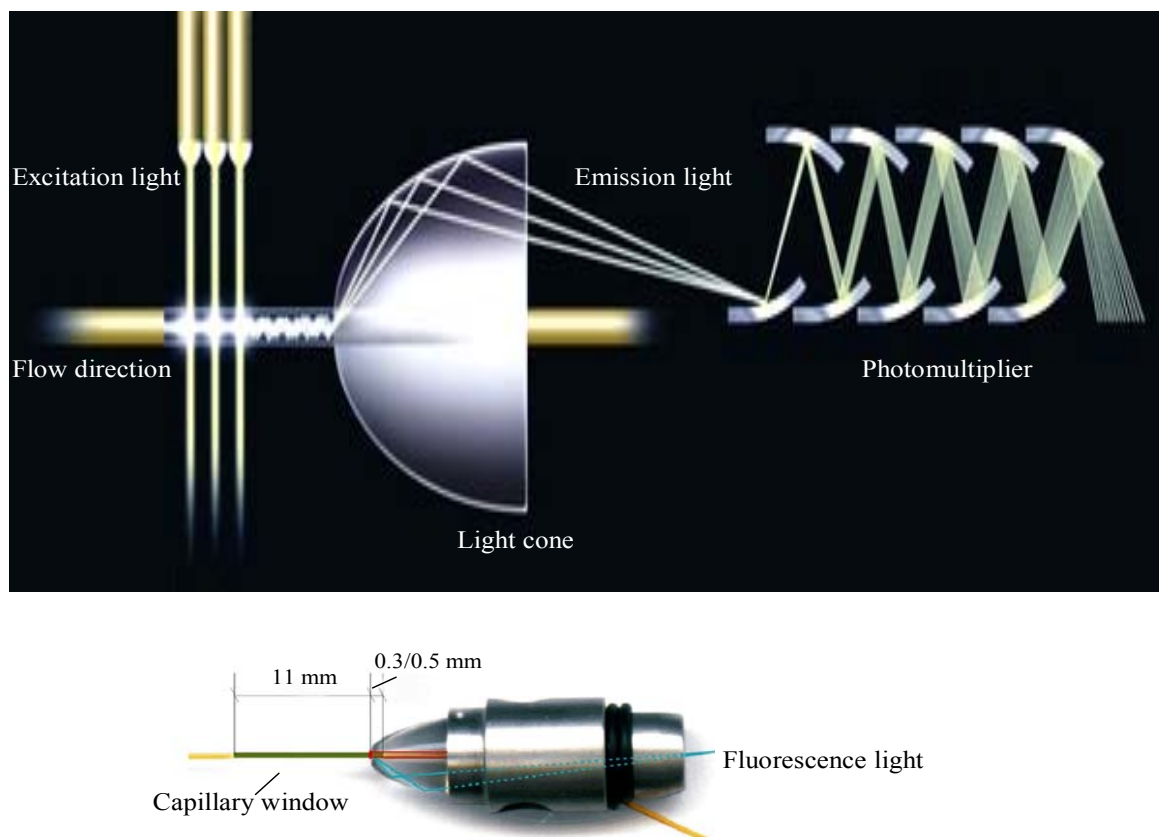


Figure 2.9: Schematic diagram of the Argos system [130].

2.6 Capillary electrophoresis on microchip

The concept of microchip separations is not new. In 1979 [131] the first report of a microfabricated gas chromatography column has been published. In 1990 [132] the first example of a microfabricated gas chromatography system appeared. A little excitement was generated over these early developments, due to the complexity of the operational systems and the generally poor performance of the devices. The first work on microchip capillary electrophoresis was published in 1992 and demonstrated that a significant improvement in speed is obtained by miniaturizing conventional separation methods [133, 134]. The steadily growing number of publications on MCE each year shows the sustained interest and continuing development as shown in Figure 2.10.

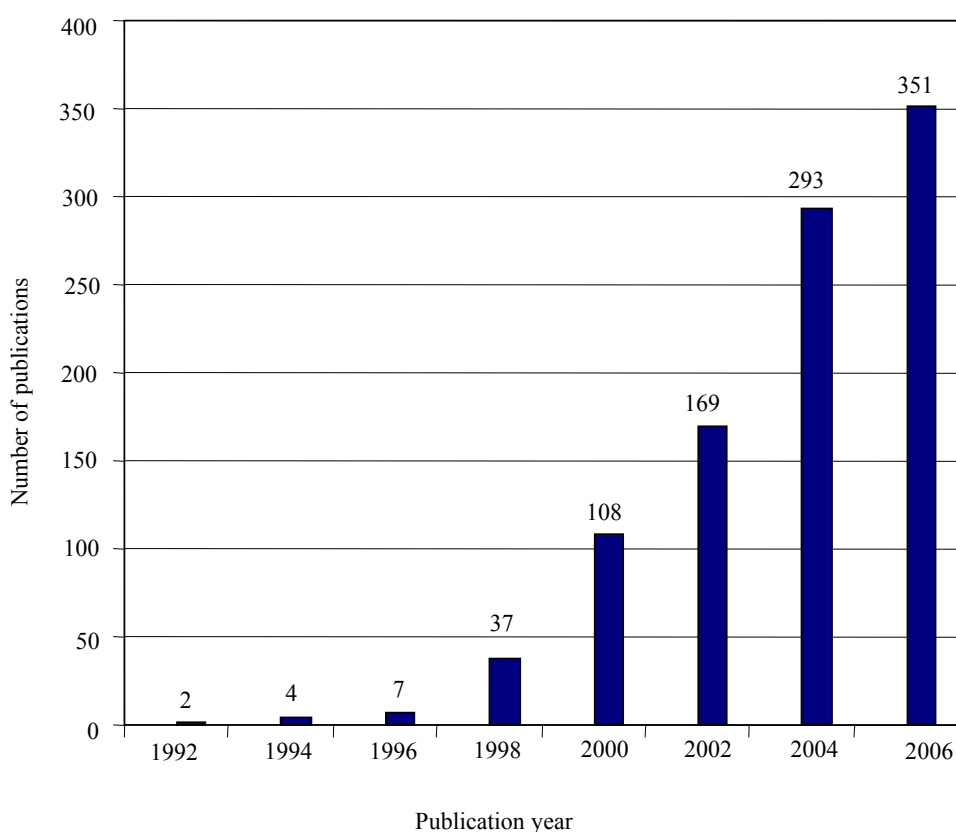


Figure 2.10: Number of publications in scientific journals containing the keywords *capillary electrophoresis and microchip* in the title or abstract [43, 133, 134].

Capillary electrophoresis on a microchip is an emerging new technology that promises to lead the next revolution in chemical analysis. It has the potential to simultaneously assay hundreds of samples in a matter of minutes or less. The use of microfabricated analytical devices is especially attractive when high speed or high throughput is needed. In recent years [135-140], it has become generally accepted that high throughput analytical methods are needed in various emerging application fields of life sciences, especially in the field of genomics and proteomics. It also strongly applies for pharmaceutical analysis due to the growing importance of combinatorial chemistry, parallel synthesis, and high throughput screening in drug discovery. Although microchip electrophoresis is one of the most successful applications of chip based microfluidics, which is also reflected by the introduction of commercial systems, it has only rarely been applied to quantitative analysis of pharmaceuticals [141-144]. This is especially true for so-called “real samples”, such as commercial formulations.

Microchip electrophoresis (MCE) could become an attractive alternative to high-performance liquid chromatography (HPLC) due to its economic properties in terms of the low reagent consumption and high speed of analysis. Furthermore chip electrophoresis has a great potential for multiplexed separations [67, 68] as well as for complex lab-on-a-chip systems integrating chemical synthesis and analysis on a single microfluidic device [145].

2.6.1 Chip materials and fabrication

Most microchip devices have been fabricated from glass, quartz, silicon, or polymer materials [146]. The standard procedure for fabrication of a microchip device involves a photolithography process adapted from the micro-electronics industry. More recently, powder blasting has shown the simplicity of the production of microchips with a complex structure.

The advantages of using a glass substrate microchip in comparison to a polymer chip are summarized as:

- 1- Better hydrophilicity
- 2- Chemical inertness
- 3- Optical clearness
- 4- Non-porous

5- Suitable for prototyping

Beside these advantages, the etched glass surface provides high electroosmotic flow (EOF), its surface chemistry is well understood, contain many reactive silanol groups and many methods of modifying glass surfaces are available. Glass substrates, however, suffer from some limitations such as adsorption of analytes to a negatively charged wall, metal ion impurities, being fragile and slow fabrication.

In order to overcome limitations of glass, the development of polymer microfluidic devices is an active and growing area of research. Polymer substrates are generally less expensive than glass substrates and there are a wider variety of fabrication methods that are faster and easier. Fabrication methods of polymers include laser ablation for polystyrene, polycarbonate, cellulose acetate, poly (ethylene terephthalate), replica molding for PDMS, injection molding and hot embossing imprinting for polymethylmethacrylate (PMMA) [147, 148]. However, most polymers are not chemically inert and may dissolve in some organic solvents. Most polymers also tend to be hydrophobic, exhibit poor wettability and need to be coated as well to minimize surface interactions with proteins.

2.6.1.1 Photolithography and wet chemical etching

Photolithography is a process where a pattern is transferred to a substrate by optical means. For microfluidic devices, the pattern is a 2D layout of the channels and reservoirs. A chromium/gold film is distributed onto the surface of the substrate. A positive photoresist is spin-coated on the chromium surface, and the channel design is transferred to the substrate using a photomask and UV exposure of the photoresist [9]. When ultraviolet light strikes the photoresist, it weakens the polymer in the portions exposed to the light. These portions are washed away during developing and the image of the mask is transferred to the photoresist layer. After exposing and developing the photoresist the metal films are etched by using KI/I_2 for gold and $K_3Fe(CN)_6/NaOH$ for Cr. The channels are then etched into the glass substrate with a HF/HNO_3 solution. A summary of the process is outlined in Figure 2.11.

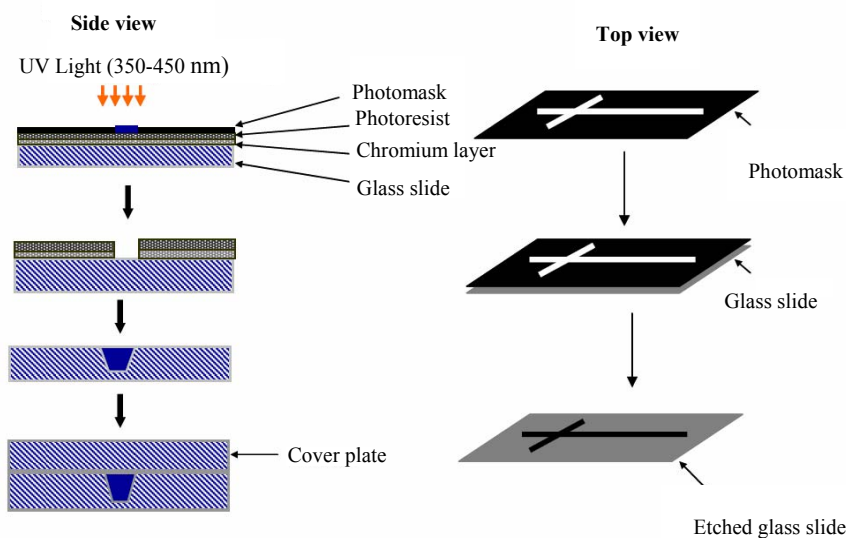


Figure 2.11: Photolithography process [9].

2.6.1.2 Powder blasting

Powder blasting is a fast and inexpensive method of making holes, cavities and channels for brittle materials such as glass, silicon and ceramics [11]. This micro patterning process relies on mechanical erosion of a masked material by a high velocity powder beam (Figure 2.12). Powder blasting is a relatively fast process, with erosion rates of 100 $\mu\text{m}/\text{min}$, which is more than 100 times faster than wet chemical etching. This makes the technique especially attractive for fast prototyping.

Powder blasting has been evaluated to structure microfluidic chips for electrophoresis [149-152]. It is shown that such devices can in principal be applied in chip electrophoresis. It was, however, found that the resolution in electrophoretic separation obtained in powder-blasted (pb) devices is generally lower compared to wet chemical etched (wc) chips. This is attributed to the much higher surface roughness of the pb-chip wall [153].

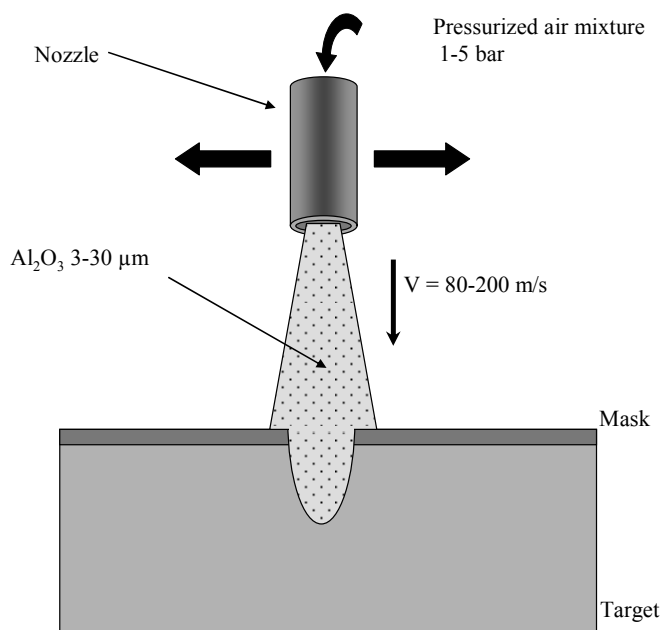


Figure 2.12: A schematic diagram of the powder blasting process [11].

2.6.2 Detection in MCE

Although MCE has several advantages with regard to separation performance, size and chemical integration, detection is one of the disadvantages in MCE. The small dimensions of a microchip result in a small sample volumes that require an extremely sensitive detection technique. Therefore development of suitable detection methods providing higher sensitivity for a wide variety of analytes is a challenge in MCE. The most commonly used detection technique in MCE is fluorescence detection due to its high-sensitivity and can easily be implemented in the experimental setup. The key to ultrasensitive fluorescence detection is the ability to maximize signal while minimizing background.

Currently, LIF detection is a widely utilized mode in microchip devices [154, 155], due to its high sensitivity and compatibility with the typical chip dimensions (i.e. the ease of focusing a laser beam onto the μm -sized channels). However, these conventional lasers are generally expensive, relatively instable and have short lifetimes (3000 h) [156].

Various LIF detection systems based on a HeCd laser (325 nm), argon ion laser (488 nm) and frequency quadrupled Nd:YAG laser (266 nm), were developed and have been successfully applied in microfluidic devices.

In the literature, Ramsey's group [157] reported a detection limit of 1.7 pM rhodamine 6G and 8.5 pM rhodamine B in a chip-based system with a LIF detector. Harrison's group developed a series of epifluorescence microscope systems for microchip LIF detection, in which LODs are 300 fM for fluorescein [158] and 9 pM for Cy-5 [159]. Recently, Schulze et al. [160] described a deep UV fluorescence method for the detection of unlabeled basic proteins on a chip based on their native fluorescence. The use of a lamp-based system with flexible variable wavelength detection was also reported [161].

A disadvantage of fluorescence detection is that most of the analytes have to be derivatized prior to analysis, which is not only inconvenient and sometimes troublesome. If the analyzed compounds exhibit native fluorescence at the excitation wavelength troublesome labeling can be avoided. This is described in chapter 4 where diuretic drugs exhibited native fluorescence and thereby the labeling process was avoided.

Most lasers are significantly larger in scale than microchips and not portable or disposable, limiting their use in point of care testing applications.

2.6.3 Chip layout

An attractive feature in utilizing microfabricated structures is the integration of different kinds of fluid manipulation on a single device. The first chip design consisted of microchannels with a cross layout geometry. Afterwards the design of microchips provided significant development from simple single-channel structures to complicated ones. Design rules for many channel geometries and separation length were developed using computer-aided design tools. Currently, microchip design allows reaction and separations on a single microchip with multiple channels [145]. Different chip layouts are shown in Figure 2.13.

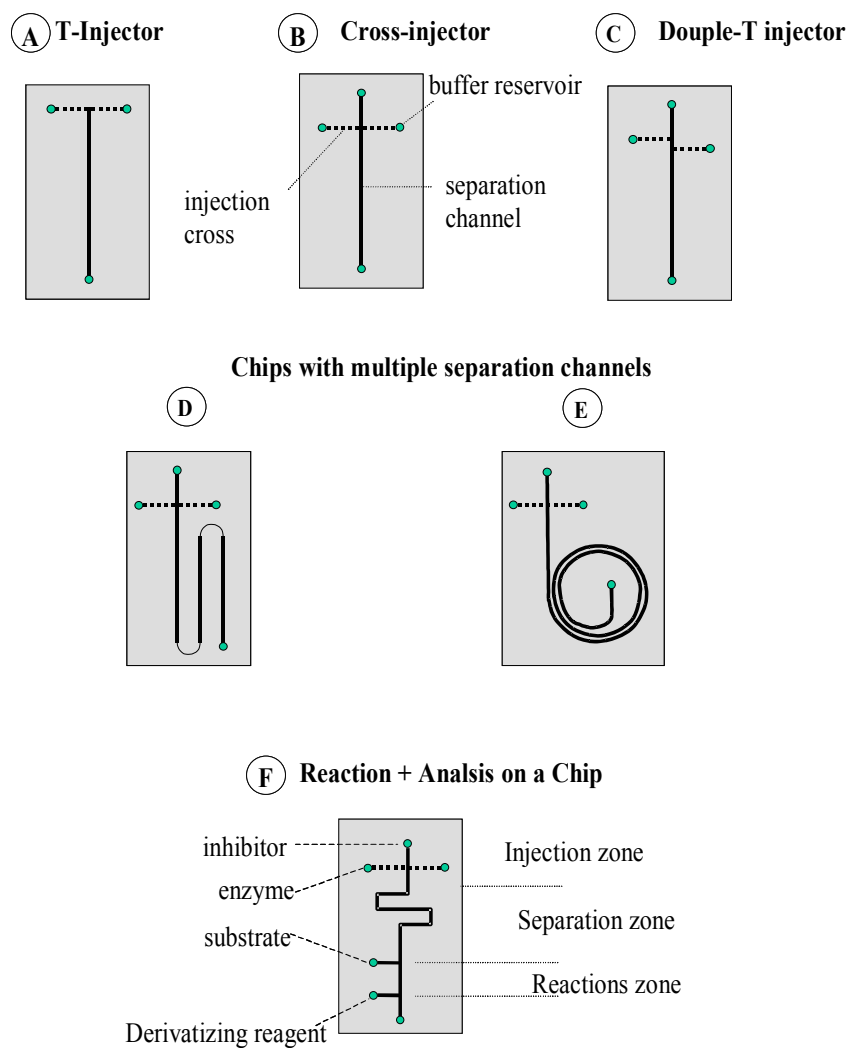


Figure 2.13: Microchip layouts [162].

2.6.4 Pinched injection

The pinched injection is performed using electrokinetic forces to restrict the sample in the loading step. Then the sample is injected as a plug. Ideally, a short well defined sample plug is required to achieve high separation efficiencies as given by equation 2.15:

$$\sigma_{inj}^2 = \frac{I_{inj}^2}{12} \quad (2.15)$$

σ_{inj} is the variance due to injection plug length I_{inj} .

Samples are easily introduced into the channels by applying high voltage without the necessity to use high-pressure pumps avoiding a laminar flow profile. Pinched injection allows the injection of very narrow sample plugs. This is achieved by pinching potentials which are applied at the buffer inlet and outlet, inducing buffer flows to the sample outlet which is grounded. This prevents sample leakage into the separation channel and band broadening during injection. In Figure 2.14, a schematic drawing of the pinched injection process and the following separation is shown. The complex fluid handling is performed by directed manipulation of the applied voltages at the reservoirs due to electroosmosis and electrophoresis [140]. The pinched sample plug is time dependent therefore relative long injection times are required for the analytes to fill the intersection (about 15 s). Once a stable sample plug is achieved (Figure 2.15), the high voltage is switched to the injection mode in which the analytes move under the influence of the EOF to the detector end and the separation is performed.

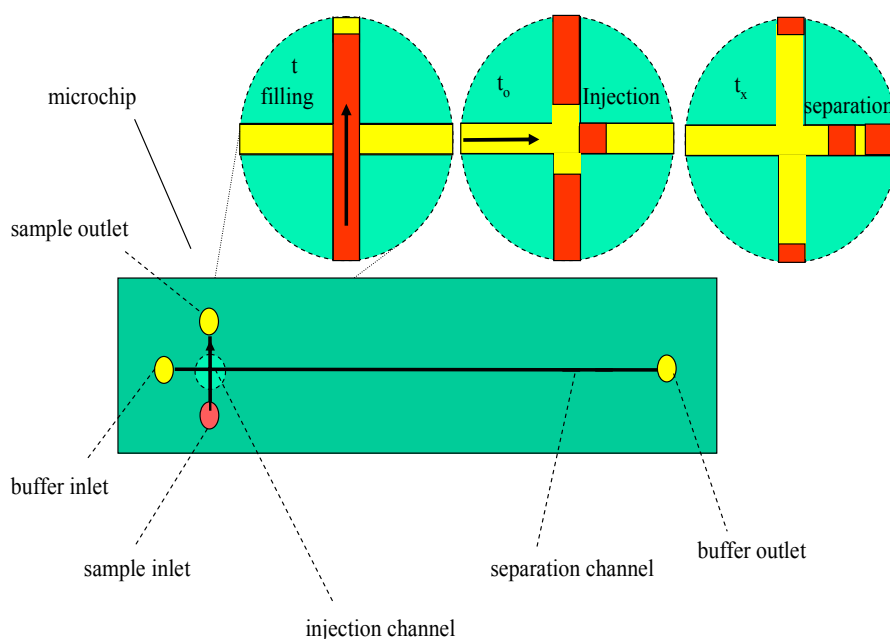


Figure 2.14: Schematic drawing of the injection/separation process in MCE applying pinched injection [140].

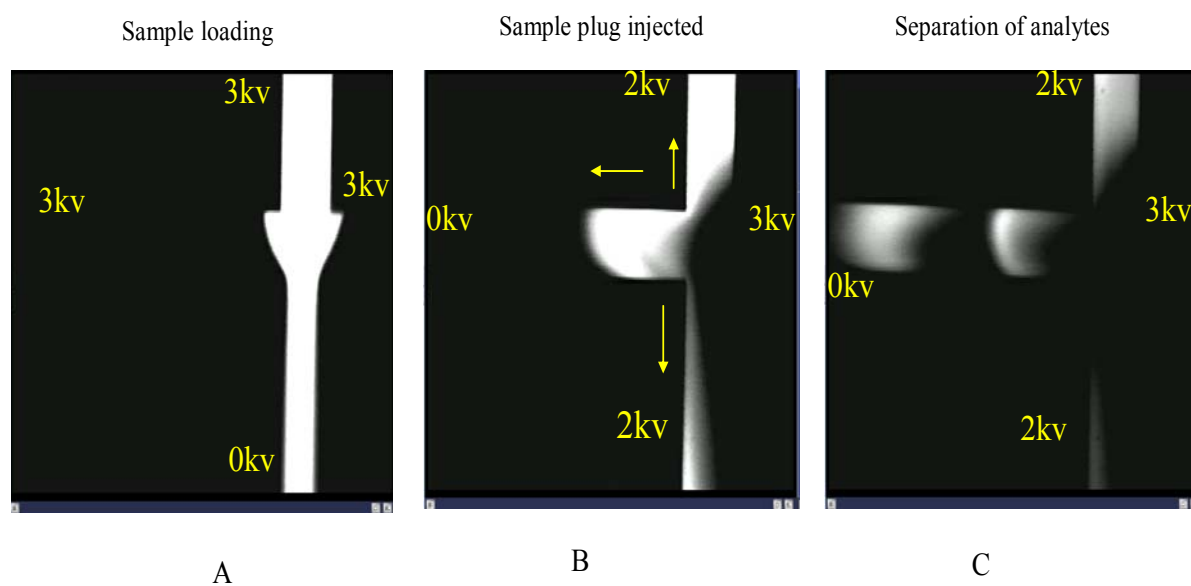


Figure 2.15: Video images of the pinched injection process.

Chapter 3 Experimental part

3.1 CE instrumentation and capillary

For classical CE measurements in this thesis, a home-build CE instrument is used. Untreated fused-silica capillaries 50 μm i.d. \times 375 μm o.d. (BGB Analytik Vertrieb, Germany) are used for separation. For on-column detection, an Argos 250B fluorescence detector (Flux Instruments, Basel, Switzerland) is used.

3.2 MCE-instrumentation

High-voltage source

A programmable bipolar four-channel high-voltage source (type HCV 40M-10000, FUG-Elektronik, Rosenheim, Germany) is used [161]. Using this type of power supply, the electrical potential (-10 to $+10$ kV) per channel can be adjusted using a manual program mode (see photo 3.1).

Optical and mechanical parts

The schematic drawing of the instrumental setup including the HV-source and the optical setup is shown in Figure 3.2. The optical parts consist of an epifluorescence microscope (Olympus IX 50) fitted with a video camera (PCO Computer Optics, Kehlheim, Germany) for imaging the flows in microchannel [161]. The two standard objectives Lucplan FI 10X and 40X are equipped with the microscope setup. The latter is used to visualize the fluorescence emission during separation. Fluorescence excitation is performed using a 100W mercury lamp which is attached to the microscope. For wide range of applications, three different fluorescence excitation filter blocks are used. These excitation filters are 330–380, 360–370 and 450–480 nm with the corresponding emission filters of 420, >420 and >515 nm and dichroic mirrors of 400, 400 and 500 nm, respectively. A photomultiplier tube (PMT) (Hamamatsu 7711–03) is attached at the side place of the microscope (see photo 3.1) to detect the fluorescent light. An adjustable optical aperture (viewfinder, Till

Photonics, Gräfelfing Germany) is installed in front of the PMT which allows to restrict the detection area with a rectangular aperture. The viewfinder is equipped with various mirrors and filters and with a video camera which enables to visualize the fluorescence detection area on a video monitor [161].

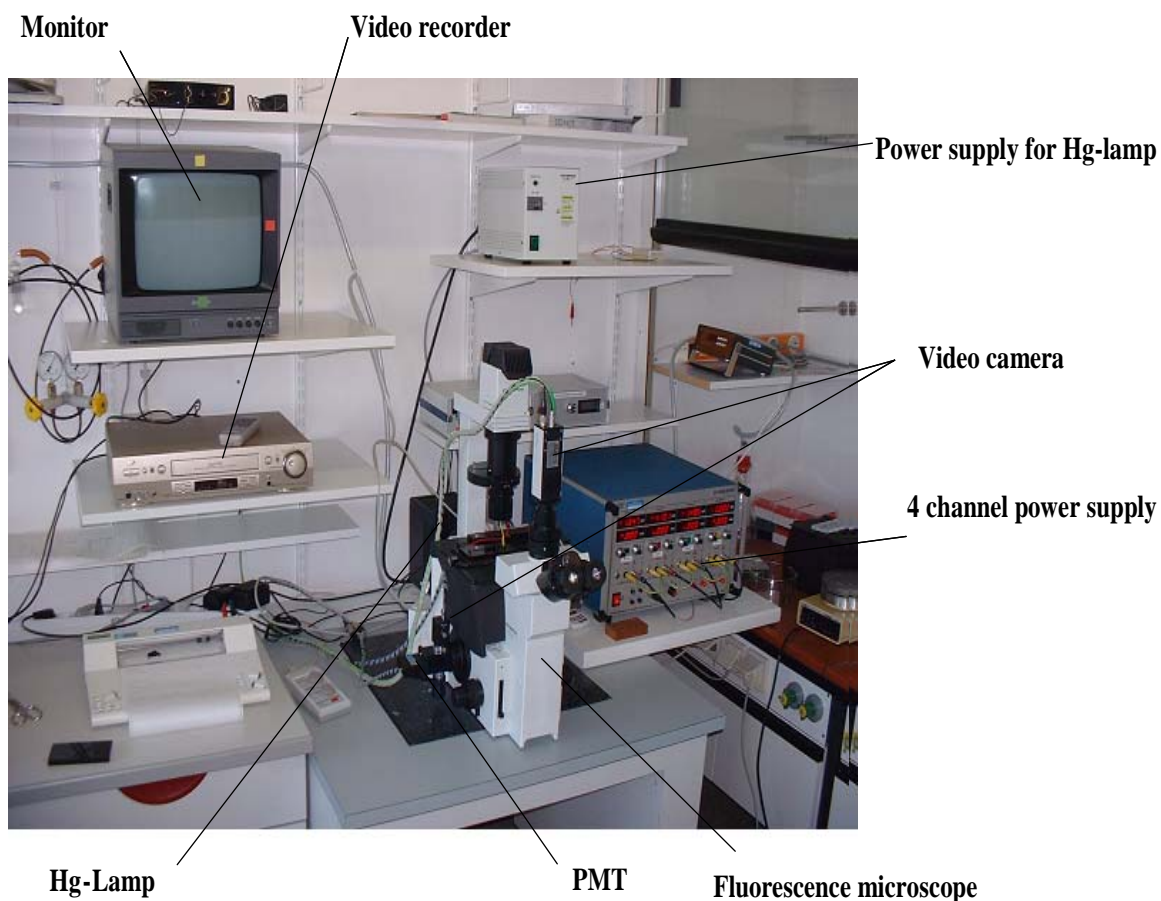


Figure 3.1: Photo of the MCE-system.

The microchips are placed in a chip mount (Figure 3.3A) which is made from Vitronit (Vitron, Jena, Germany). The chip mount is made of glass ceramic with very low electric conductivity and high mechanical stability [146]. The electrode cover plate (Figure 3.3B) is made of Plexiglas with a built-in IR-high pass filter which contains four chemically inert pt electrodes. These electrodes are designed to fit the microchip layout (simple cross layout). This setup allows a safe operation protecting the environment from the high voltages and the UV-irradiation [161].

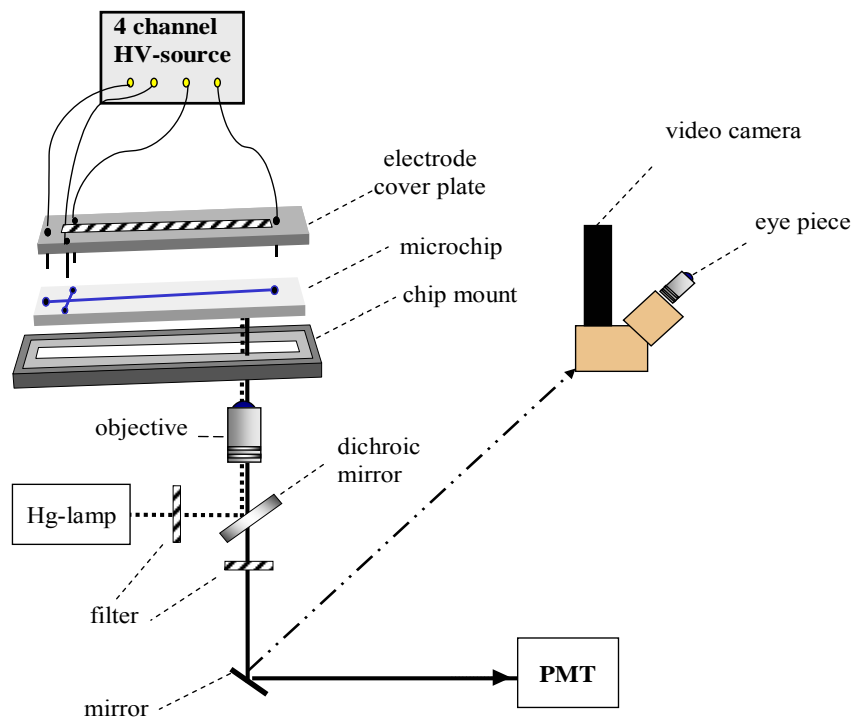


Figure 3.2: Instrumental setup of a modular MCE [161].

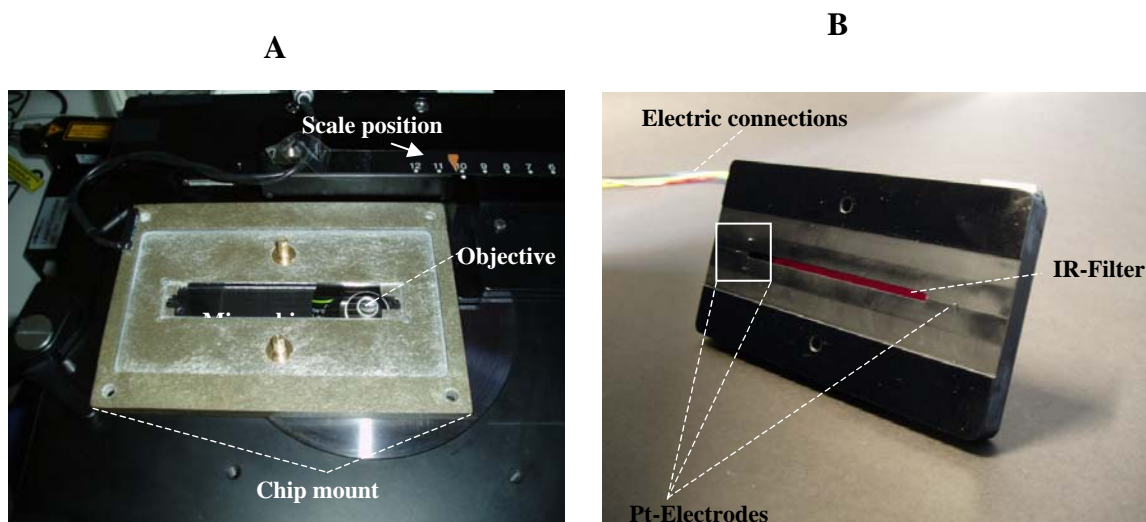


Figure 3.3: (A) Chip mount, (B) electrode cover plate [162].

3.3 MCE-LIF coupling

The flexibility of the experimental set up allows to use different light sources for fluorescence excitation which is a real benefit for the development of various applications [141]. The following sections will describe some types of lasers used in this thesis.

Frequency quadrupled pulsed laser operating at 266 nm

To enable microchip electrophoresis with deep UV-LIF detection, the standard objective in the microscope setup (Figure 3.4) is replaced by a filter cubus holding the fused silica objective (Partec GmbH Münster, Germany). A fiber coupled pulsed, frequency quadrupled Nd:YAG laser (type FQSS266-Q; 4 mW) purchased from Crystal GmbH (Berlin, Germany) is used as excitation light source [160].

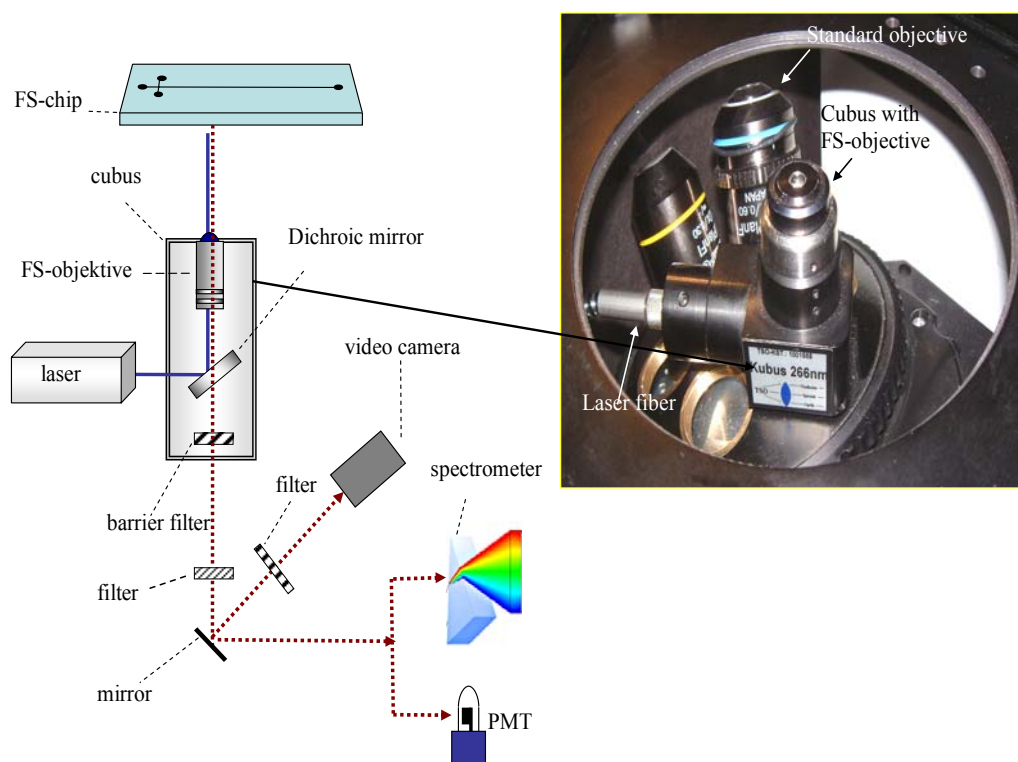


Figure 3.4: MCE-laser coupling [160].

HeCd laser operating at 325 nm

For coupling a HeCd laser operating at 325 nm with an emission filter >350 nm (Series 74, Model No. 3074-EOS-A01, 20 mW, Laser 2000, Wessling, Germany), a similar setup as in the pervious section is used. The dichroic mirror reflects light with wavelength of <335 nm, whereas light of >340 nm is transmitted.

Argon-ion laser operating at 488 nm

For coupling of the argon-ion laser operating at 488 nm with an emission filter at 520 nm (Series N129239Q, Model No. 163-D1241, 25 mW, Spectra-Physics, USA), an adapted filter cubus holding the fused silica objective is developed.

3.4 Microchip

All microchips used in this thesis have a simple cross layout as shown in Figure 3.5. Two types of microchips are used in this thesis, a wet chemical etched chip (wc) and a powder blasted chip (pb).

Wet chemical etched microchips

The microchips made from low-fluorescent borofloat glass (BF) are purchased from Micalyne (Edmonton, Canada) with outer dimensions of $90 \times 15 \times 2.2$, a separation channel length of 85 mm and an injection channel length of 8 mm. At the end of each channel there is a 1.1 mm deep hole with 2 mm in diameter. These holes are labeled as buffer inlet (BI), buffer outlet (BO), sample inlet (SI) and sample outlet (SO). High grade fused-silica (FS) microchips (channels were 20 μm deep and 50 μm wide at the top as shown in Figure 3.5) are also used.

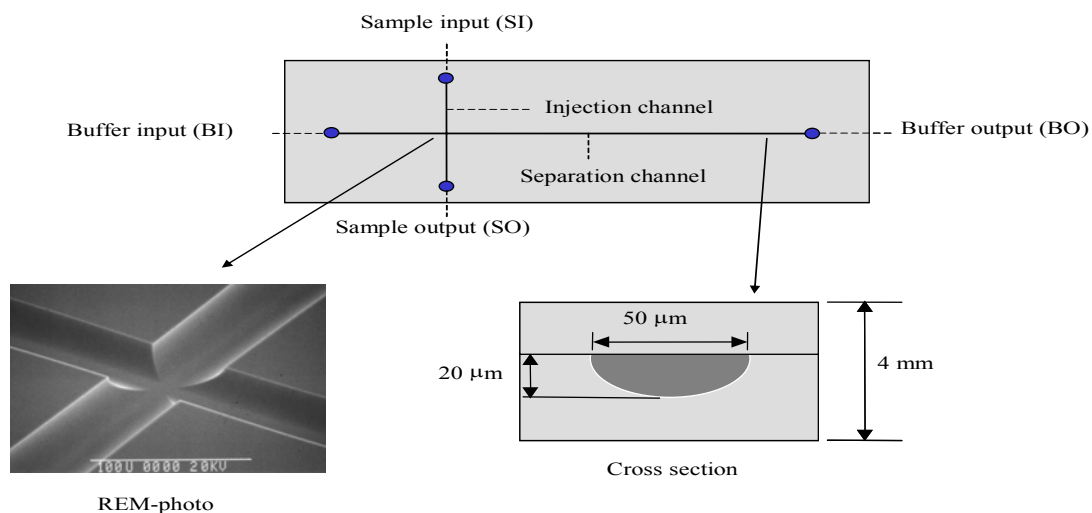


Figure 3.5: Simple cross microchip layout and channel dimensions [163].

Powder blasted microchips

Powder blasted (pb) glass chips are purchased from Micronit (Enschede, The Netherlands). Microchannels have been blasted [1] in borofloat substrates with 9 μm aluminum-oxide powder. One substrate has been blasted with 5.6 bar compressed air, the other with 4.0 bar. The blasted channels are 38 μm (5.6 bar) or 43 μm (4.0 bar) deep and 100 μm wide at the top.

3.5 Chip handling and storage

At the beginning, 1 M NaOH is used as an etching solution to remove the undesirable adsorbed materials in uncoated chips. This solution is left inside the microchannel for 1 h to ensure a complete etching process. After etching, the holes are emptied by applying a vacuum at the buffer outlet. Afterwards, the channel is rinsed using deionized water for 2 min followed by emptying the channel. Finally, the microchannel is rinsed with the running buffer for 2 min. For cleaning and storage, the chip is filled with 96% H_2SO_4 /30% H_2O_2 (3:1) overnight. PVA-coated chips are rinsed with water only for 2 min and stored dry.

3.6 Chip coating

Before coating, the chips are etched with 1 M NaOH for 1 h followed by a rinsing step with deionized water for 1 min. Afterwards a 1% w/w aqueous PVA coating solution is slowly injected through the four holes using a 50 μL syringe [164]. After complete filling the channels are emptied by applying gas pressure (N_2 , 5 bar). Then, the chip is inserted into a metallic connection device and connected with a FS capillary as shown in Figure 3.6. The channels are dried under a 5 bar nitrogen flow for 15 min. To immobilize the PVA layer on the channel wall, the chip in the metallic device is placed in a GC oven and heated to 70 $^\circ\text{C}$ with 15 $^\circ\text{C}/\text{min}$ for 1 h. Finally the chip is heated to 160 $^\circ\text{C}$ with 15 $^\circ\text{C}/\text{min}$ for 10 min while the channels are flushed with 1.5 bar nitrogen flow. Then, the chip is allowed to cool down to room temperature inside the oven.

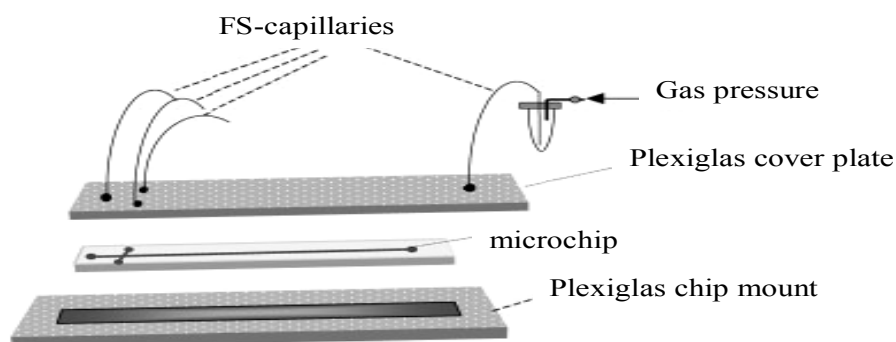


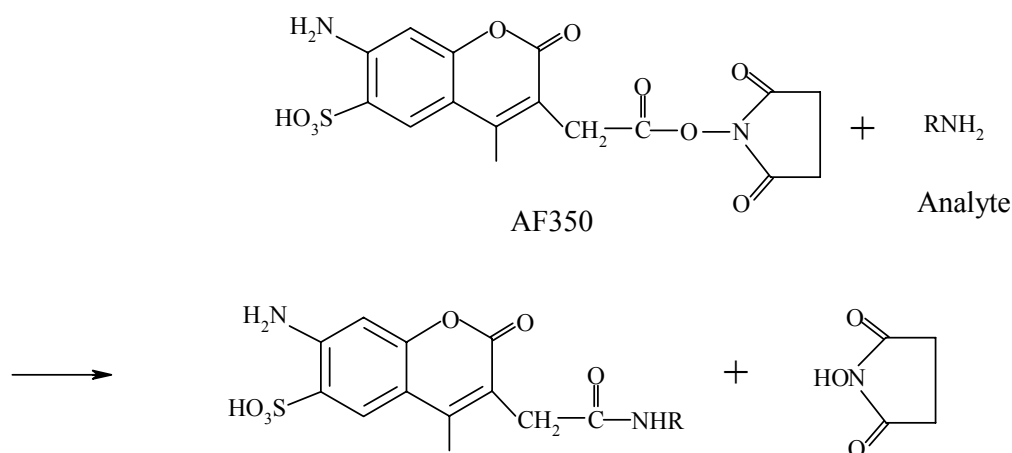
Figure 3.6: Schematic drawing of the coating device [164].

3.7 Derivatization and solutions

Derivatization of amines with Alexa Flour 350

To prepare the Alexa flour 350 (AF350)-amine stock solutions, 100 μL of an amine solution (0.5-1 μM in ACN or methanol) is mixed with 20 μL of a AF350-solution (1 mg/mL in dried DMSO) and 50 μL borate buffer (20 mM, pH 8.5). The reaction is carried

out for 4 h in the dark. All stock solutions are stored at -20°C . Scheme 3.1 shows the reaction of the AF350 with an amine.



Scheme 3.1: Analyte derivitization with Alexa Fluor 350.

Excitation-emission spectra of AF350

AF350 is optimally excited at 346 nm and exhibited bright blue fluorescence at 442 nm [165] as shown in Figure 3.7.

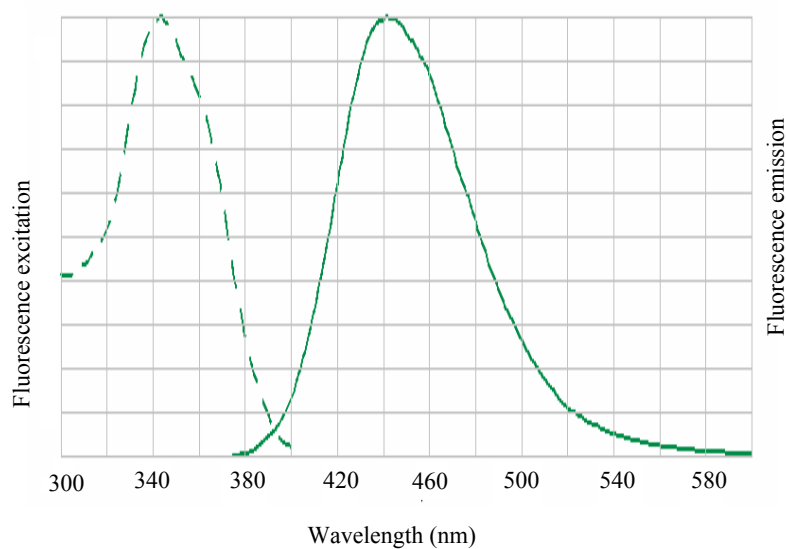
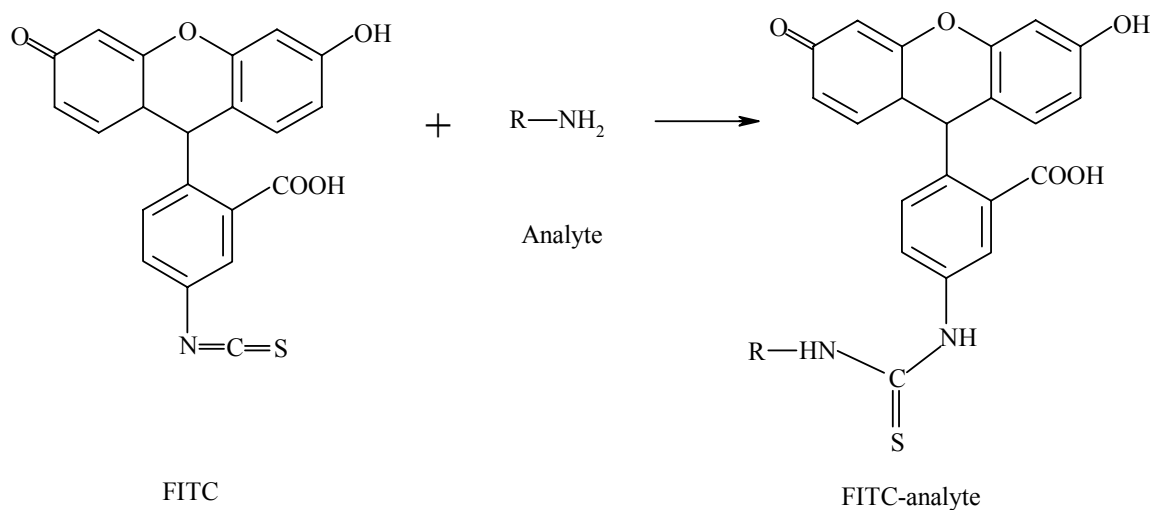


Figure 3.7: Excitation-emission spectra of AF350 [166].

Derivatization of amines with FITC

A 100 μL aliquot of an amine solution (1 mg/mL in methanol) is mixed with 12.7 μL of a FITC-solution (10 mg/mL in acetone) and 50 μL borate buffer (20 mM, pH 9.2). The reaction is performed for 2 h in the dark. The reaction of the FITC with an amine is shown in scheme 3.2.



Scheme 3.2: Analyte derivatization with FITC.

Excitation-emission spectra of FITC

FITC-dye is used for the derivatization of primary and secondary amines. Its excitation/emission wavelengths (488/520 nm) are shown in Figure 3.8.

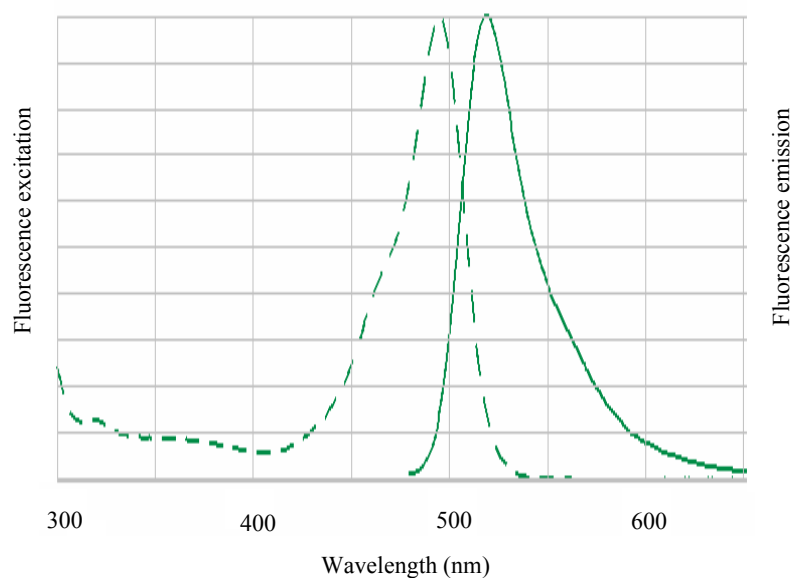


Figure 3.8: Excitation-emission spectra of FITC [166].

Derivatization of ephedrine and pseudoephedrine in tablets

The commercially available tablets Asmoline (20 mg/tablet ephedrine) and Congestal (60 mg/tablet pseudoephedrine) are used. One tablet of each drug is powdered and dissolved in methanol according to the declaration of the product to obtain 1 mg/mL stock solutions. Prior to derivatization, the extract is centrifuged and filtered through a 0.45 μm membrane filter. The remaining procedure is performed analogous to that described under the derivatization of amines with FITC.

Derivatization of ephedrine and pseudoephedrine in human urine

1 mL of human urine is diluted with 1 mL of water and 1 mL of 20 mM borate buffer pH 9. Ephedrine and pseudoephedrine reference compounds are dissolved in diluted urine to obtain 1 mg/mL stock solutions and the derivatization is completed as mentioned above.

Standard diuretics stock solutions

The stock solutions of diuretics are prepared to give the concentration of 0.2 mg/mL in methanol and stored at 4 °C.

Stock solutions of diuretic tablets

Hydikal, Epiteps and Edemex tablets, containing 5 mg/tablet amiloride, 30 mg/tablet triamterene, and 1 mg/tablet bumetanide, respectively, are used. One tablet of each drug is powdered and dissolved in methanol according to the declaration of the product to obtain 0.2 mg/mL stock solutions.

3.8 Chemicals

2-Butylamine, 2-octylamine, (R)-(-)/(S)-(+)-1-cyclohexylethylamine, (-)-ephedrine, (+)-pseudoephedrine, HPMC and PVA (*Mr* 89000–98000) are obtained from Aldrich

(Steinheim, Germany). DMSO, FITC (isomer I), sodium hydroxide, sodium tetraborate, sodium dihydrogen phosphate monohydrate, sulfuric acid, SDS and hydrogen peroxide are purchased from Fluka (Neu-Ulm, Germany). HPLC-grade acetone, methanol and ACN are obtained from Merck (Darmstadt, Germany). Amiloride, triamterene, BFMTZ, bumetanide CHES and MES are obtained from Sigma (Deisenhofen, Germany). Native cyclodextrins and hydroxypropyl- γ -cyclodextrin (HP- γ -CD) are from Wacker (Burghausen, Germany). Metoprolol tartrate is kindly donated by Prof. J. Crommen (University of Liège, Belgium). Alexa Fluor® 350 carboxylic acid succinimidylester is obtained from Molecular Probes (Leiden, The Netherlands). Commercially available tablets of Hydikal® (5 mg/tablet amiloride), Epitens® (30 mg/tablet triamterene), Edemex® (1 mg/tablet bumetanide), Asmoline® (20 mg/tablet ephedrine) and Congestal® (60 mg/tablet pseudoephedrine), are kindly donated by the National Organization for Drug Control and Research (NODCAR, Cairo, Egypt).

3.9 MCE experiments

After cleaning the chip using Piranha solution followed by the etching process as previously described (section 3.4), the respective BI, SI and SO holes are loaded with 2 μ L buffer solution. By applying a vacuum at the BO, the channels are completely filled after that 2 μ L buffer solution is added to the BO. Then the SI is emptied and filled with 2 μ L sample solution. After setting up the electrode plate, the sample is injected using pinched injection. This is achieved by a two-step high-voltage program. In the first step (injection mode), a sample plug is placed in the intersection and after 15 s the voltage is switched to the separation mode, where a small sample plug is injected and the sample is separated. For a PVA-coated chip the polarity of the potentials are reversed. Between the runs, the coated/uncoated chips are rinsed with water and buffer for 30 s.

Chapter 4 Results and discussion

4.1 Surface modification

Currently, the lower resolution obtainable in powder blasted (pb) chips restricts the application of the fast and economic powder-blasting process for manufacturing fluidic devices for chip electrophoresis. Therefore, the numbers of publications that use pb-chips are very rare [134-138]. Recently, van den Berg et al. [10] reported that 7–9 times lower plate numbers were obtained on a pb-chip compared to a wc-chip with similar dimensions. As the lower separation performance of pb-chips is attributed to the high surface roughness, this issue can be overcome by the application of immobilized polymer coatings to cover the channel surface.

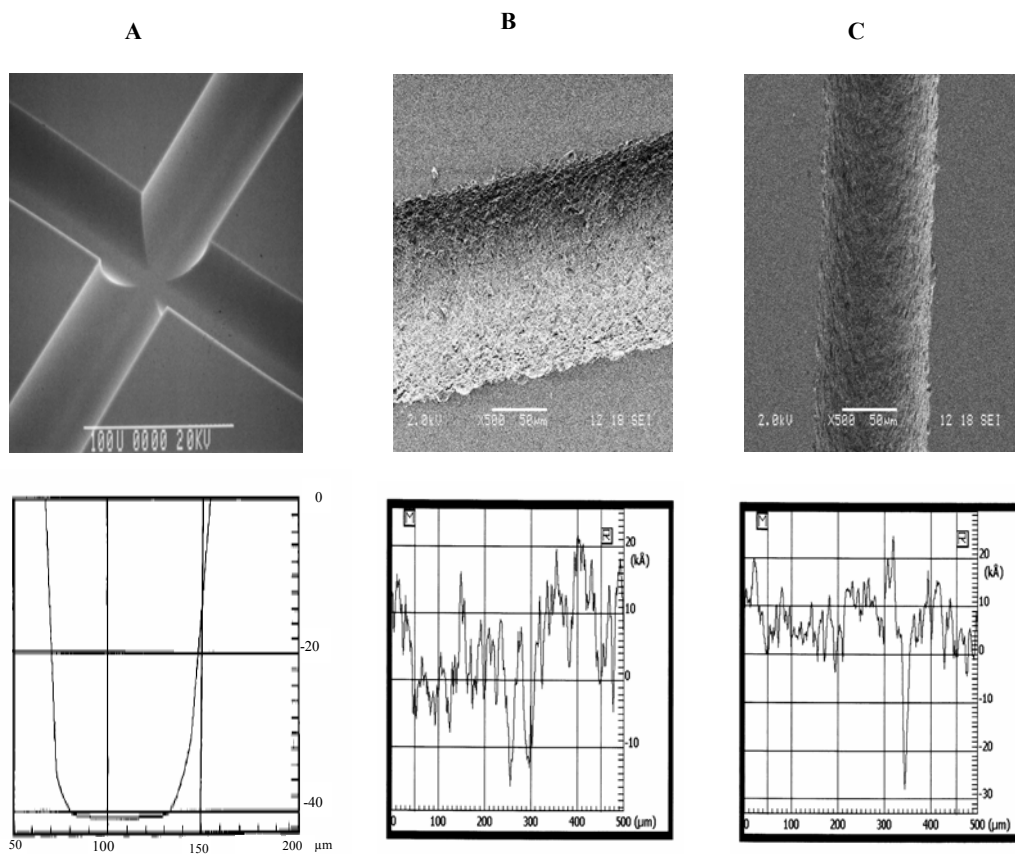


Figure 4.1: Scanning electron microscope (SEM) micrographs (500 times zoomed) and corresponding surface profile scans of wc-(A) and pb-channels. The glass wafer was blasted with 9 µm large Al_2O_3 -particles with 5.6 bar (B) and 4.0 bar (C) compressed air [10, 138].

As shown in Figure 4.1, scanning electron microscopy (SEM) images and data from Dektak measurements visualize the dimensions and surface roughness of the uncoated wet chemical etched (wc) and pb-chips [10, 153]. The surface of the wc-chips is very smooth (Figure 4.1A) while the surface roughness is noticeable for pb-chips (Figures 4.1B,C). Comparing channels blasted with different air pressure, it can be observed that structures generated at lower pressure exhibit, as expected, smoother surfaces (Figure 4C).

Recently, Belder et al described that immobilized poly(vinyl alcohol) (PVA) coatings can greatly improve the separation performance of classical wc-chips [167, 168]. Transferring this coating process to pb-chips can lead to a major achievement for the powder-blasting technique. Such devices would be especially attractive for the analyses of adsorptive proteins where hydrophilic coatings are essential to realize high-resolution free zone electrophoretic separations with glass chips [160].

In this project, permanent PVA coatings as well as dynamic coatings are applied to pb-chips. The coated pb-chips are utilized in chip electrophoresis and the obtained data are compared to the results obtained from classical wc-chips.

AF350-labeled amine test compounds

To evaluate the correlation between increased surface roughness and the separation performance, the separation performance of the different labeled substrates in chip electrophoresis is examined.

For this purpose, some anionic compounds are used in this study including AF350-metoprolol, AF350-dicyclohexylamine, AF350- α -4-dimethylbenzylamine and AF350-2-butylamine as shown in Figure 4.2.

In the first stage of this work, the separation of the four labeled amines (Figure 4.2) is performed with a classical CE using 40 mM phosphate buffer at pH 6. The corresponding electropherogram is shown in Figure 4.3A.

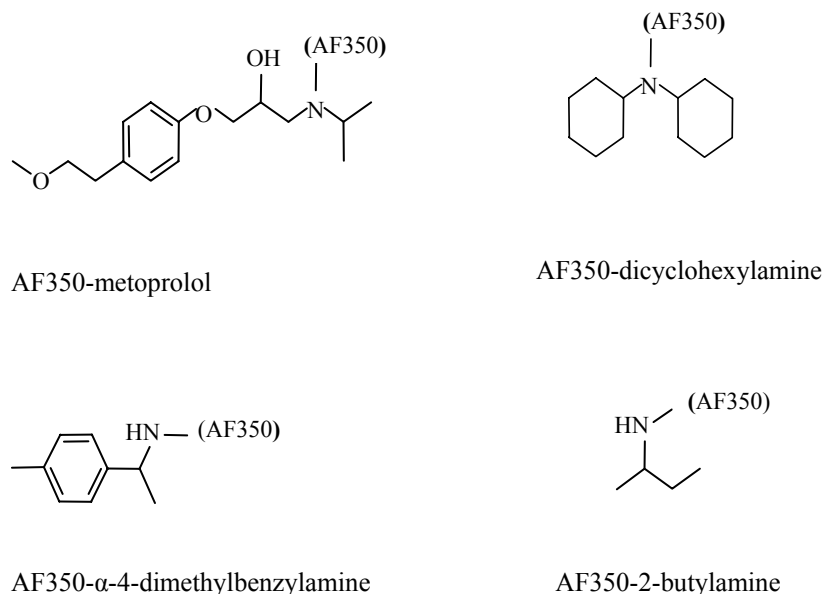


Figure 4.2: Chemical structure of the AF350-amine test compounds.

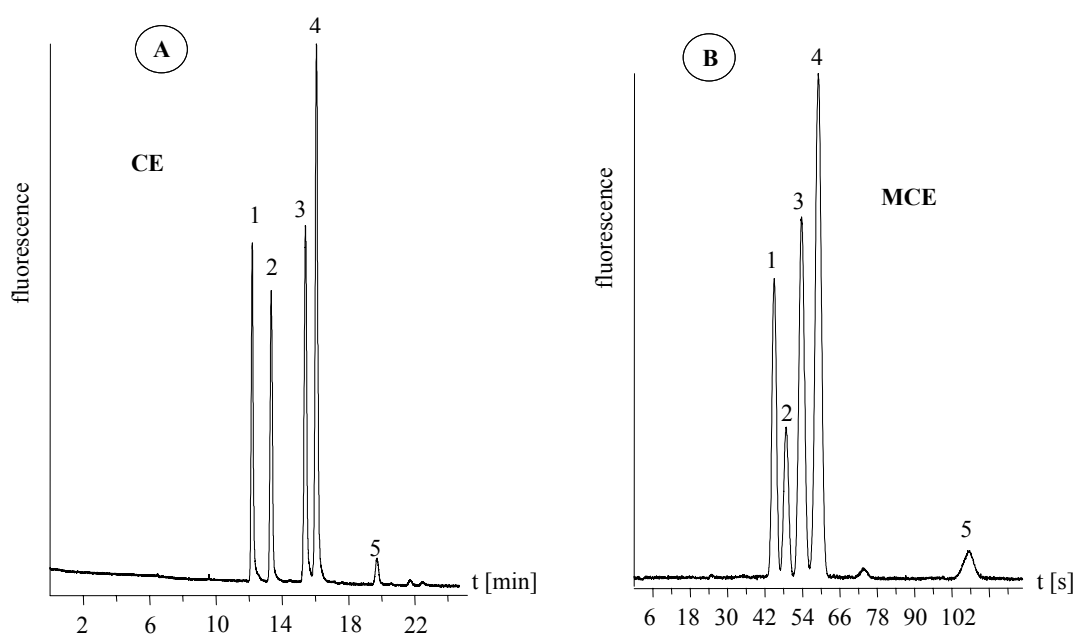


Figure 4.3: Electropherograms of the AF350-amine test compounds using 40 mM phosphate buffer at pH 6. Conditions: (A) Capillary, 50 cm effective, 70 cm total length, 50 μ m i.d. Injection, 10 s hydrodynamic injection. Separation, 30 kV. Detection using Argos system at 360 nm exci/385 nm emis. (B) effective separation length, 3.4 cm; injection potentials, BI 1.06, BO 3.32, SI 1.22, SO 0.0 kV, separation potentials, BI 2.4, BO 0.0, SI 2.00, SO 2.00 kV Peak identification: (1) AF350-metoprolol, (2) 2- AF350-dicyclohexylamine, (3) AF350- α -4-dimethylbenzylamin, (4) AF350-2-butylamine, (5) originating from the fluorescent dye, 29 mM each in A and 2.9 mM in B.

As shown in Figure 4.3A, the four labeled amine compounds are separated using an untreated fused silica capillary with a total separation length of 70 cm (50 cm to the detector) within 17 min. It is noted that the peak originated from AF350 dye is well resolved (peak 5) from the AF350-amines at 20 min. Afterwards, the separation is successfully performed on a 50 μm wet chemical etched chip as shown in Figure 4.3B. As we can see from Figure 4.3, the migration time obtainable using MCE (separation within 102 s) is 11-times faster in comparison with CE system (separation within 1200s).

Similar experiments are then performed using 100 μm wc-chips. It is observed that the 40 mM phosphate buffer led to a very high electrical current as 100 μm channels are used rather than the 50 μm ones. This results in a Joule heating which causes undesirable effects such as bubble formation and backflow from SI. As a consequence, a dye solution leakage and a baseline drift occur. The sample leakage can be monitored by a video microscopy during the measurement as shown in Figure 4.4. For these reasons, the results do not provide an acceptable separation as shown in Figure 4.5.

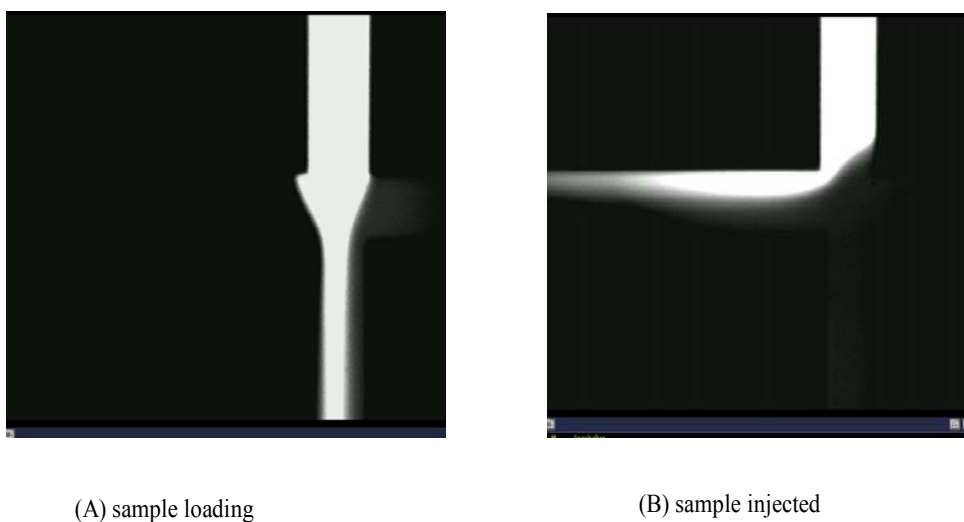


Figure 4.4: Video image of the leakage through the 100 μm channel.

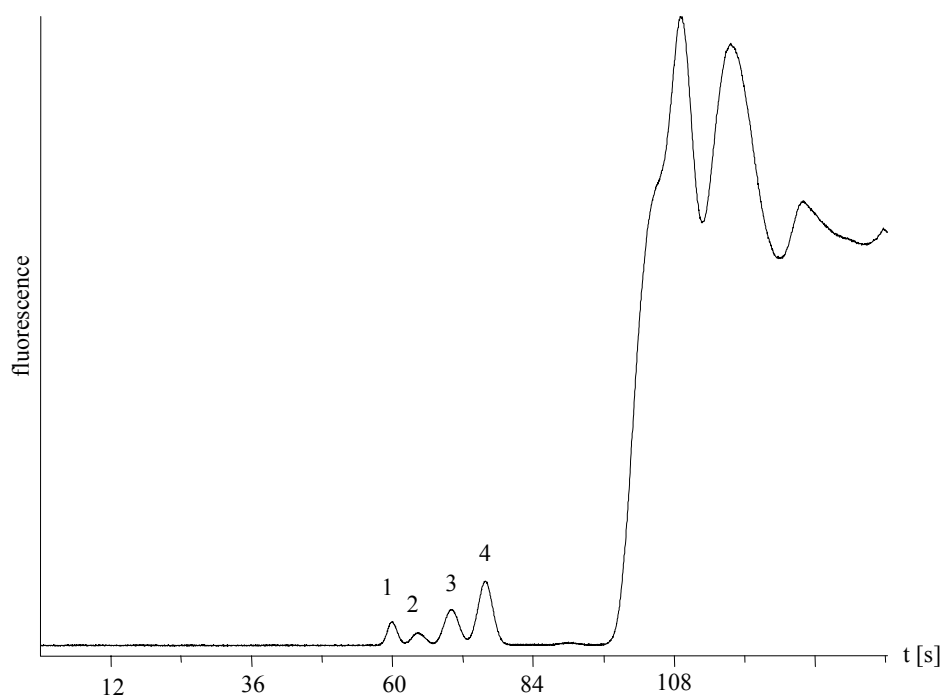


Figure 4.5: Baseline drifts due to leakage through the 100 μm channel with an effective separation length of 4 cm and other conditions as in Figure 4.3B.

In order to obtain stable conditions and reproducible results, a 10 mM phosphate buffer at pH 6 is used. Video images shown in Figure 4.6 reveal a successful pinched injection when 10 mM phosphate buffer at pH 6 is used (in both wc and pb chips). The corresponding electropherograms are shown in Figure 4.7.

As depicted in Figure 4.7, the four compounds are not completely resolved. Therefore, only two test compounds are used rather than four in order to ensure complete peak resolution and reliable peak analyses which are important for consistent determination of plate numbers. For this purpose, peak 1 (AF350-metoprolol) and peak 4 (AF350-2-butylamine) are chosen in the current study. The corresponding electropherograms using different chips (100 μm channels) are shown in Figure 4.8.

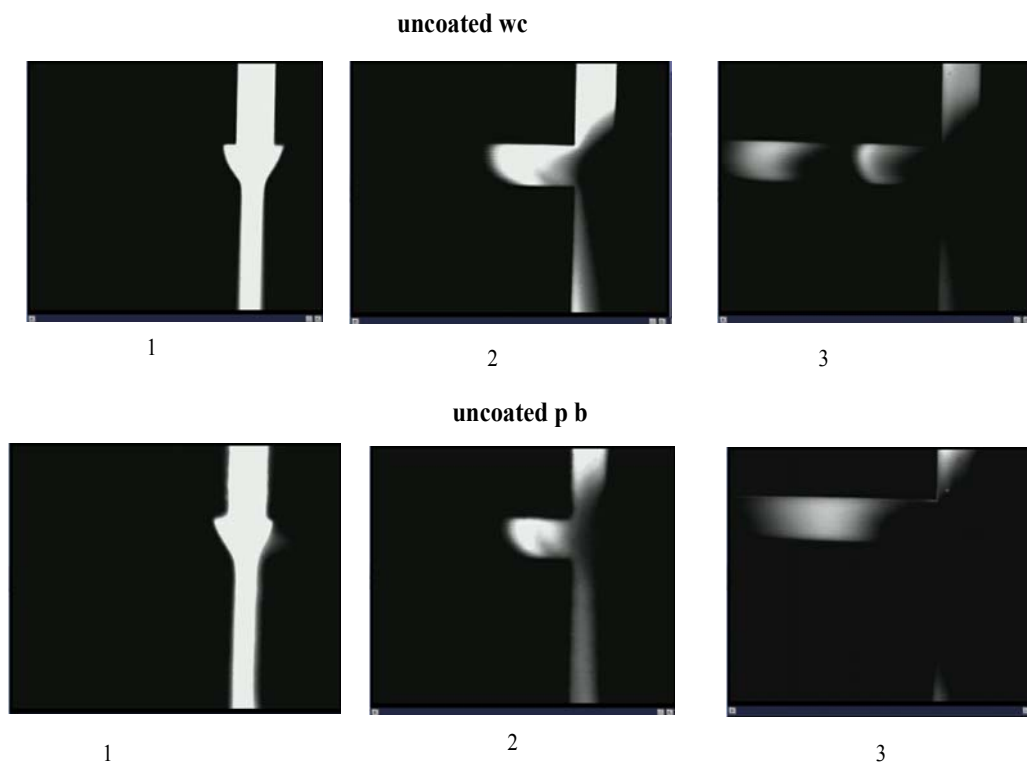


Figure 4.6: Video images of the injection process using uncoated 100 μm wc- and pb-chips.

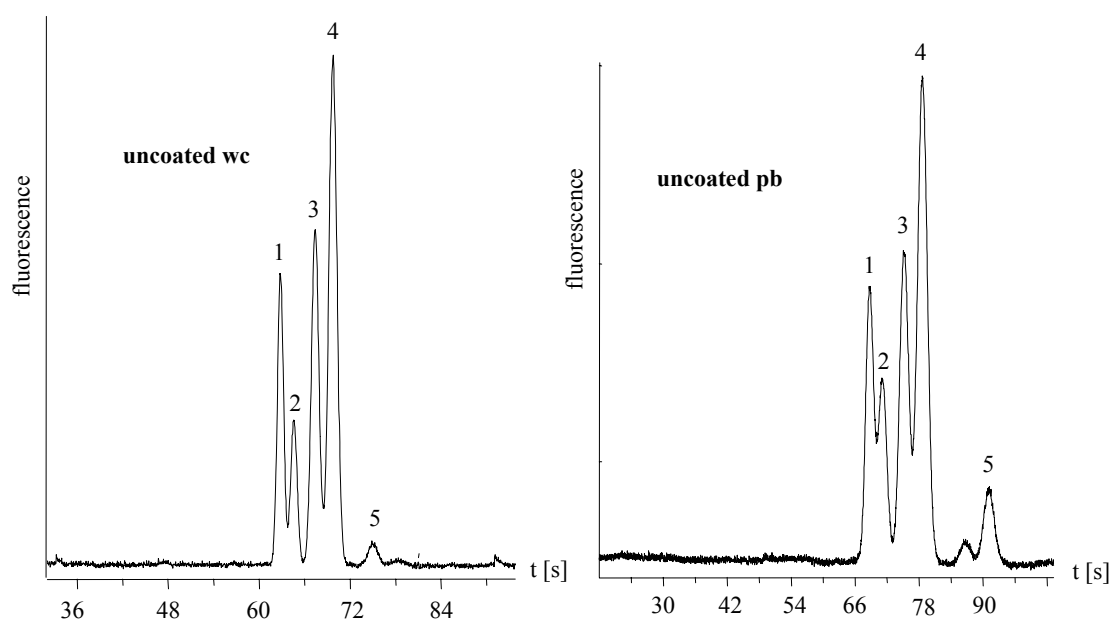


Figure 4.7: Electropherograms of the AF350 labeled amines using uncoated 100 μm wc- and pb-chips, effective separation length, 4 cm. Other conditions and peak identification are as in Figure 4.3B.

As expected, AF350-metoprolol and AF350-2-butylamine compounds are well resolved in a 100 μm uncoated wc-chip (Figure 4.8A) with a resolution of 3.79 and separation efficiencies of $N_1=24000$, $N_2=19000$, respectively. These values are relatively high compared to the uncoated pb-chip (Figure 4.8C) which provides a resolution of 2.73 and separation efficiencies of $N_1=5000$, $N_2=5000$.

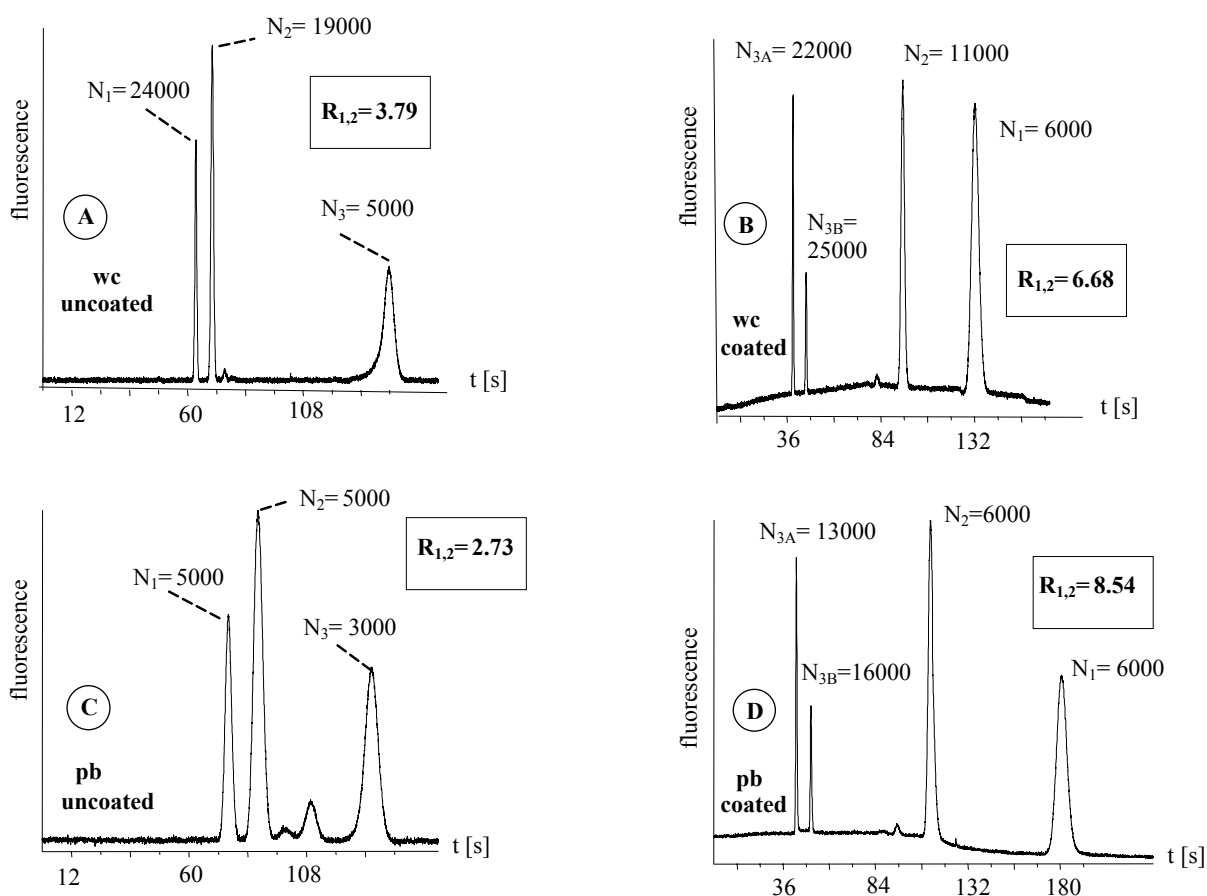


Figure 4.8: Efficiencies and resolutions of the separation of AF350-labeled amines using coated and uncoated wc- and pb-chips, respectively. In case of coated chips the polarity is reversed; peak identification: (1) AF350-metoprolol, (2) AF350-2-butylamine, (3) originating from the fluorescent dye, 2.9 mM each. Effective separation length, 4 cm. Other conditions are as in Figure 4.3B.

It is observed that the uncoated wc-chip provides a separation efficiency of almost 4.5-times higher compared to results in an uncoated pb-chip (Figures 4.8A and C). This can be explained as the surface roughness of the pb-channel leads to a non uniform EOF, which leads to band broadening with the results of a reduced resolution

and separation efficiency. These values are in good agreement with the published reports on the limited separation performance of pb-chips [10, 149, 152].

After the separation of AF350-labeled amines is performed on different uncoated chips, these chips are permanently coated using PVA [164]. This is applied in order to examine the improvement of the separation performance by covering the rough surface with an internal coating. For this purpose, the chips are slowly rinsed with a 3% aqueous solution of PVA. The adsorbed PVA layer is then dried in a nitrogen gas stream and immobilized by a heating step at 160 °C [164]. This procedure is performed twice in order ensure a complete coating efficiency. Afterwards, the separation of the AF350-labeled amines is checked using the prepared double coated chips.

For the application of PVA coated chips, the polarity is reversed as the EOF is suppressed resulting in an anionic net mobility of the analytes and a reversed migration order (see Figures 4.8B and D). Comparing Figures 4.8A and B, the resolution in a wc-coated chip is enhanced from 3.79 to 6.68 and the dye signals are now well resolved. These results agree well with the published work utilizing 50 μm wc-chips [164], in which up to a 3-times increase in separation efficiency can be observed using PVA-coated chips for the analysis of fluorescently labeled amines.

For a pb-coated chip, the resolution is also enhanced from 2.73 to 8.54 which is highly improved compared to the results of a coated wc-chip. Although the resolutions in wc- and pb-coated chips are improved, there is a diverse effect on the separation efficiencies. While the separation efficiencies of compounds 1 and 2 are reduced, a significant improvement in the separation efficiencies of the dye signals is observed (Figures 4.8B and D). This can be explained by the increased joule heating in 100 μm channels leading to an extra band broadening. As Joule heating is time-dependent, the compounds that migrate slower will be more affected than the fast migrating ones.

Finally, from Figures 4.8C and D it can be concluded that coating of pb-channels greatly improves the resolution, making coated pb-chips comparable to wc-devices.

Effect of dynamic coating

In order to examine if the improved separation performance found in devices coated permanently with PVA is also observed with uncoated pb-chips, dynamic coatings for EOF suppression such as hydroxypropylmethylcellulose (HPMC) and polyvinyl

alcohol (PVA) are applied.

In this experiment, 1% PVA and 1% HPMC are prepared in warm deionized water then diluted with the running buffer with a ratio of 1:10 to obtain 0.1% solutions. The corresponding electropherograms are shown in Figure 4.9. It is surprising that PVA has no effect on the EOF suppression in pb-chips as shown in Figure 4.9A. The addition of HPMC resulted in a strongly reduced EOF (Figure 4.9B) and in similar migration patterns in comparison to the permanently PVA-coated pb-chip (Figure 4.8D). The observed separation efficiency is, however, higher for the permanently PVA-coated device, indicating that covering the rough surface with a permanent layer of a hydrophilic polymer is more effective than dynamic coating.

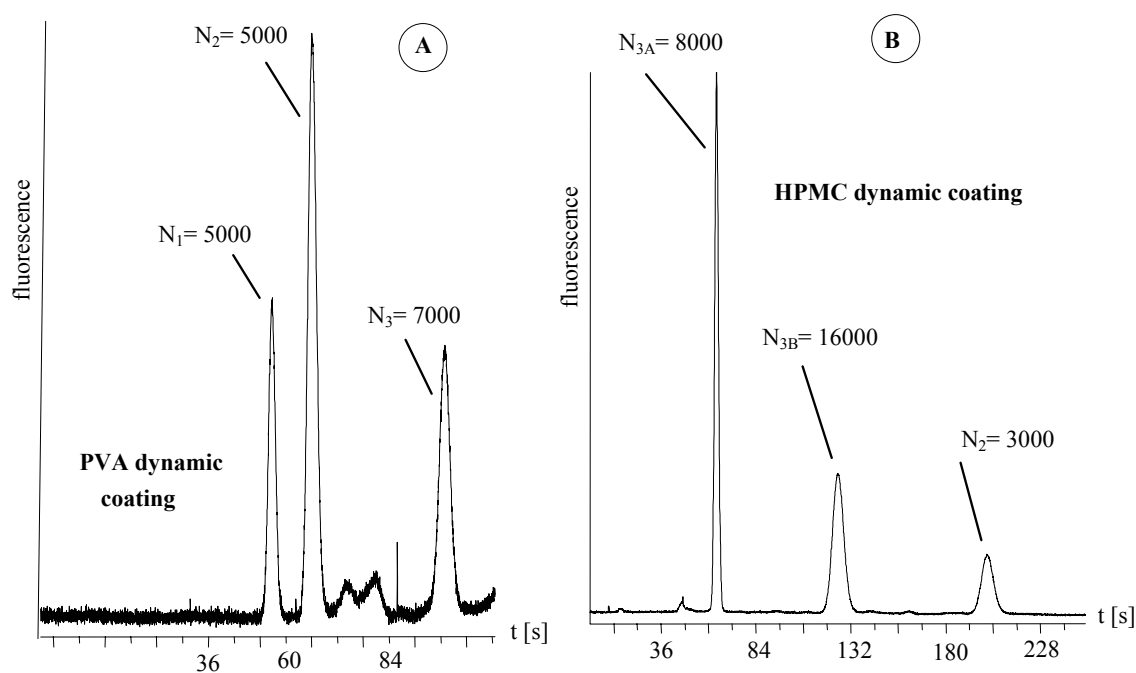


Figure 4.9: Effect of dynamic coating on the separation of AF350-labeled amines using bare pb-chips. Buffer, 10 mM phosphate, pH 6 with 1% PVA or 1%HPMC, effective separation length, 4 cm; injection potentials, BI 1.1, BO 3.3, SI 1.2, SO 0.0 kV, separation potentials, BI 2.4, BO 0.0, SI 2.0, SO 2.0 kV, in case of an HPMC-modified buffer the polarity is reversed due to a suppressed EOF. Other conditions are as in Figure 4.3B.

FITC-labeled amine test compounds

The results shown above indicate that the resolution of the labeled AF350-amines obtained in coated pb-chips is highly improved compared to results in coated wc-chips. To confirm this, additional work is performed using FITC-amine test mixtures on different blasted microchips. Such test mixtures consist of FITC-metoprolol, FITC-2-octylamine and FITC-2-butylamine as shown in Figure 4.10.

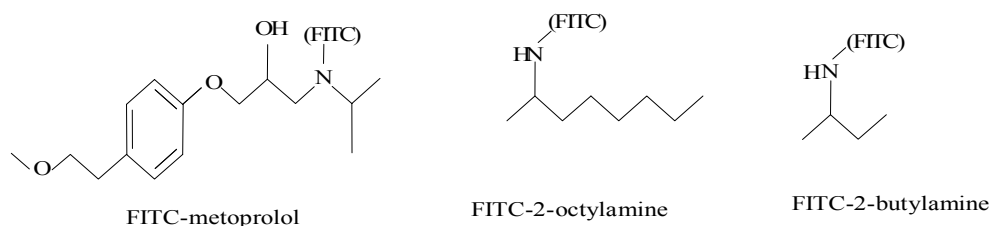


Figure 4.10: Chemical structure of the FITC-amine test compounds.

Here, different microchips involving pb (4 bar), pb (5.6 bar) and wc-chips are used. The corresponding electropherograms are shown in Figure 4.11.

It is observed that partial separation of the test mixture is possible with both types of pb-chips utilizing a separation length of 7 cm, as shown in Figures 4.11A and B. The separation efficiencies, as well as the resolution, obtained in structures manufactured at high pressure are slightly lower to that obtained for channels blasted with lower pressure. In details, the FITC-amine compounds are partially resolved with a resolution of 1.2 of the FITC-metoprolol and FITC-2-octylamine utilizing the uncoated pb-chip (4 bar) with a separation efficiency of 10000 (Figure 4.11A). Partial separation of FITC-labeled amines is also possible in an uncoated pb-chip (5.6 bar) with a separation efficiency and resolution values of 9000 and 1.1, respectively (Figure 4.11B). Errors for the determination of the separation efficiency as well as for the resolution are about 10% ($n = 3$). As a result, the differences in mean values of separation performance, $N_{4\text{bar}} = 10\ 000$ to $N_{5.6\text{bar}} = 9000$ and resolution $R_{4\text{bar}} = 1.2$ to $R_{5.6\text{bar}} = 1.1$ are not significant [153].

Using the uncoated wc-chip, the three signals are well resolved and the plate number is with $N = 36\ 000$ about three times higher compared to that obtainable in pb-chips, as shown in Figure 4.11C. Also the resolution R of signal 1 and 2 is significantly improved from about $R_{1,2} = 1.2$ for pb-chips to $R_{1,2} = 1.9$.

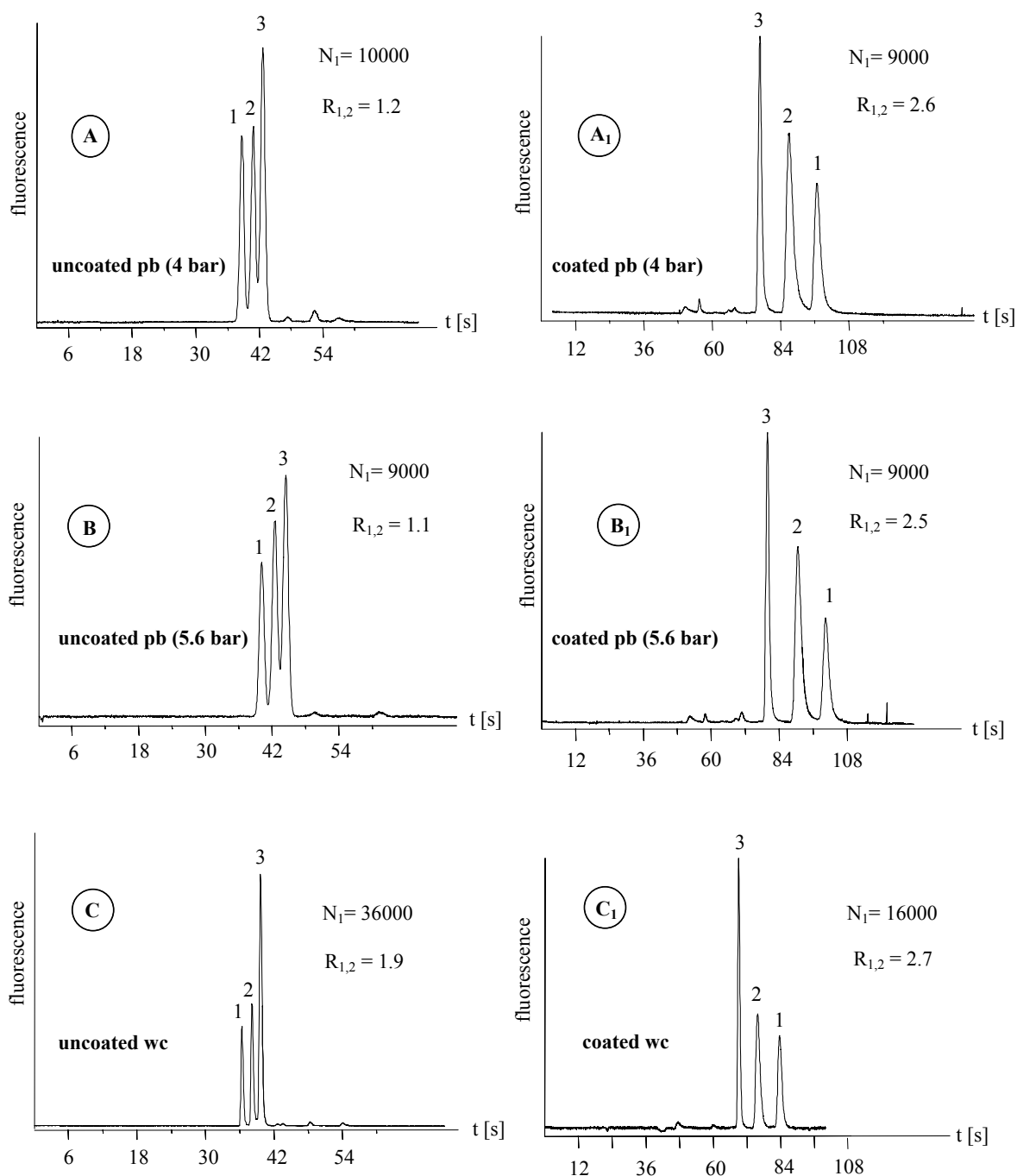


Figure 4.11: Efficiencies and resolutions of separation of FITC-labeled amines using uncoated and coated wc- and pb-chips. In case of coated chips the polarity is reversed; Buffer, 40 mM CHES, pH 9.2; effective separation length, 7 cm; injection potentials, BI 1.35, BO 4.1, SI 1.5 SO 0.0 kV, separation potentials, BI 4.0, BO 0.0, SI 3.4, SO 3.4 kV; peak identification: (1) FITC-metoprolol, (2) FITC-2-octylamine, (3) FITC-2-butylamine, 0.2 mM each.

These values are not surprising because the surface roughness of the wc-chips is in the nm-range while it is in μm -range for pb chips. In addition, these results match well with the AF350-amines results in terms of lower resolution in pb-chips.

After the separation of FITC-labeled amines is performed on different uncoated chips, these chips are permanently coated using PVA as described in the previous section. As the EOF is suppressed in PVA-coated chips, the anionic compounds have now to be detected at the anode by switching the polarity of the HV-source. The suppression of EOF results also in an increase of the migration time.

The separation performance of the FITC-labeled amines is then checked using the prepared coated chips. With such coated chips, a significantly improved resolution of the pb-chips of the test compounds is observed as shown in Figures 4.11A₁ and B₁. The resolution of the test compounds is significantly improved ($R_{1,2}= 2.6$) which is even higher than the value obtained with the uncoated wc-chips ($R_{1,2}= 1.9$). Although the resolution value obtained in coated pb-chips is 2-times higher than the uncoated ones ($R_{1,2}= 1.2$), the separation efficiency is not improved significantly.

Also with the coated wc-chips, an improved resolution with a value of 2.7 is observed (Figure 4.11C₁). However, it is surprising that the separation efficiency in the coated wc-chips (Figure 4.11C₁) is significantly lower compared to the respective uncoated chips (Figure 4.11C). This does not agree with the published work [164] where a significant increase in separation efficiencies with PVA-coated wc-chips is observed. Reasons for this are different experimental conditions such as larger channel dimensions with channel width of 100 μm in this work and 50 μm in the published work [164]. A comparison of the data of the PVA-coated wc-chip (Figure 4.11C₁) with the coated pb-chips (Figures 4.11A₁,B₁) shows that wc-chips provide better separation performance, especially with regard to the separation efficiency, which is about 2-times higher.

Chiral separation

While the lower resolution of uncoated pb-chips might be acceptable for some applications it is especially problematic for more demanding applications like chiral separations. For this purpose, hydroxypropyl- γ -cyclodextrin (HP- γ -CD) is used as a chiral selector for the separations of FITC-labeled cyclohexylethylamine enantiomers. When the chiral separation of enantiomers is performed in an uncoated

pb-chip it is found that the chiral compounds are resolved as a single peak (Figure 4.12C) while they are partially resolved ($R=0.9$) in an uncoated wc-chip as shown in Figure 4.12A. Applying permanent PVA coating, the two enantiomers are well resolved in both coated wc- and pb-chips (Figures 4.12B, D). In a coated wc-chip, the enantiomers provide a resolution of 1.5 which is relatively higher compared to results in coated pb-chip ($R=1.2$). In addition, a relatively shorter migration time is obtained with the coated wc-chip. The separation time is 125 s while it is 156 s with the coated pb-chip.

Concluding it can be said that the coated pb-chips are well suited in chiral separations although they provide a lower resolution compared to coated wc-chips.

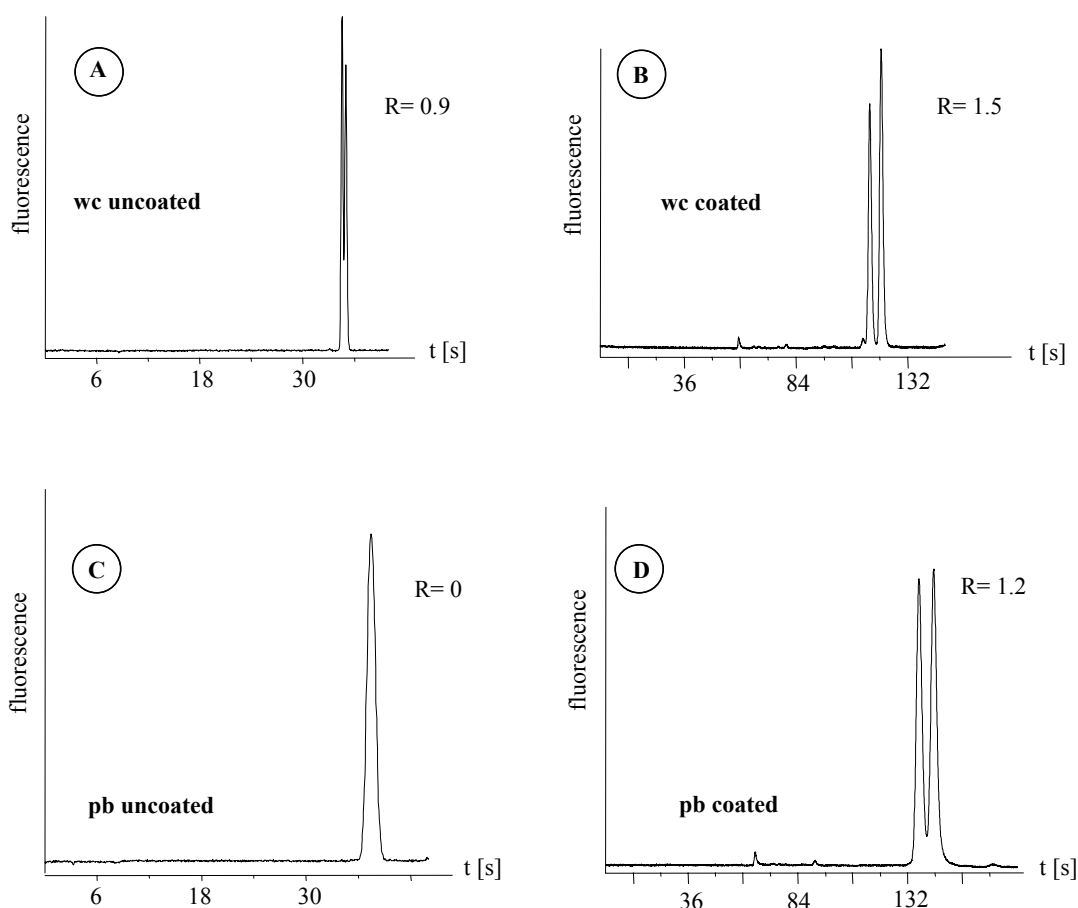


Figure 4.12: Chiral separation of (R)2(2) and (S)2(2)-FITC-1-cyclohexylethylamine (0.2 mM each) using coated and uncoated wc- and pb-chips, respectively. Buffer, 40mM CHES, 6.25mM HP- γ -CD, pH 9.2. Other conditions are as in Figure 4.11, except in the case of coated chips the polarity is reversed.

4.2 Application to drug analysis

Currently, the need of a commercial instrument for drug analysis will support the emergence of microfluidics from pure research to application. This will ensure increasing acceptance of “chips” by clinical and forensic analytical communities, and hopefully encourage further exciting developments like those presented below. While a substantial effort has been expended in the development of clinical devices for point-of-care (POC) applications, much less attention has been developed to forensic applications.

For this reason, on-a-chip methods for some abuse and therapeutic drugs will be described below. The application to pharmaceutical formulations and biological fluid are also studied. The linearity, reproducibility and applicability of those methods are then evaluated. Such methods can be used in clinical toxicology, therapeutic drug monitoring, forensic science and doping control.

4.2.1 Application to central nervous system stimulant drugs

It is well known that ephedrine and its diastereoisomer pseudoephedrine have stimulating effects [169-171] on the central nervous system (CNS). These compounds are not only accepted for medical purposes but also classified as drugs of abuse. Ephedrine and pseudoephedrine (Figure 4.13) are generally the most abundant alkaloids found in ephedra, and they typically constitute more than 80% of the alkaloid content of the dried plant material [172, 173].

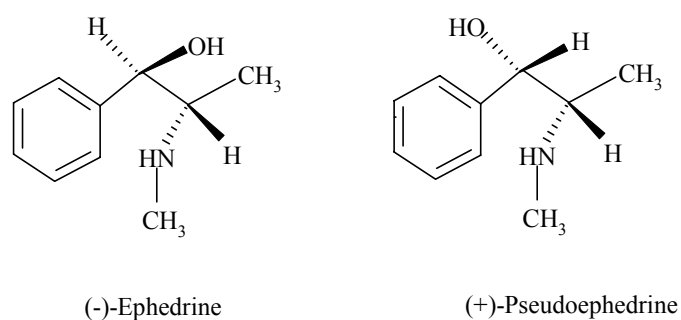


Figure 4.13: Chemical structure of (-)-ephedrine and (+)-pseudoephedrine.

Ephedrine is used as a sympathomimetic drug to treat asthma or bronchitis while pseudoephedrine is prescribed for symptoms of cold and flu including nasal congestion, cough, fever, and chills [174–177].

Concerns about the safety of ephedra-containing products have led to the development of a variety of analytical methods to assess their alkaloid content. For the quality control of ephedra herbs, high performance liquid chromatography (HPLC) is the most common analytical technique [178, 179]. However, this technique is a time-consuming analysis and needs relatively large amounts of sample.

Recently studies indicated that capillary electrophoresis (CE) provides good results in the analysis of Chinese traditional herbal medicine [180-183]. Currently, several CE methods have been developed for the separation and determination of ephedrine and pseudoephedrine in ephedra herbs, formulations, foods and human urine [184-191].

In this section, an argon ion laser operating at 488 nm coupled with a microscope based chip electrophoresis system is used for sensitive detection of labeled ephedrine and pseudoephedrine drugs. Development and validation of a fast micellar electrokinetic capillary chromatography (MEKC) method on a chip is also described for the simultaneous determination of the two alkaloids in pharmaceutical formulations and human urine.

4.2.1.1 Method development

Derivatization of ephedrine and pseudoephedrine

Most alkaloids that usually occur in plants are either weakly fluorescent or nonfluorescent compounds making trace analysis difficult without fluorogenic derivatization. In this study, since native fluorescence is insufficient for the detection of ephedrine and pseudoephedrine, more sensitive measurements are possible after a simple derivatization reaction. In this work, FITC is chosen to derivatize ephedrine and pseudoephedrine because of (i) its efficiency for the derivatization of secondary amines, (ii) the match of its excitation and emission wavelengths with a 488/520 nm argon ion laser optical system, and (iii) its high fluorescence quantum yield and molecular absorption coefficient [192].

Effect of SDS concentration on the separation performance

After derivatization of the two isomers, the selection of a suitable buffer is studied to achieve the best resolution, the highest sensitivity and the shortest analysis time. In the first stage of this work, the separation of the labeled ephedrine and pseudoephedrine is performed using a classical CE system with a buffer containing 10 mM borate at pH 9.5. However, the results do not provide an acceptable separation as shown in Figure 4.14A. This may be attributed to the fact that all analytes migrate according to their mass-to-size ratios in CE, which are in this case very similar. For this reason, it is necessary to further improve the method using sodium dodecyl sulfate (SDS) with 10 mM borate at pH 9.5. For this purpose, the concentration of a SDS surfactant is varied from 0 to 50 mM within the method development. It is found that addition of 10 mM SDS to the buffer results in a complete resolution of the two compounds (Figure 4.14B). However, it is still not suited for chip separation because the shorter separation length of a chip format can lead to unacceptable separation and possible overlapping peaks. A higher concentration of SDS like 35 mM SDS results in an acceptable peak resolution (Figure 4.14C) which can be transferred to the MCE system. Higher concentrations of SDS, such as 50 mM, result in an unacceptable resolution as shown in Figure 4.14D. As the peak 2 and peak 3 shown in Figure 4.14D are very close, they are also not suited for chip measurements.

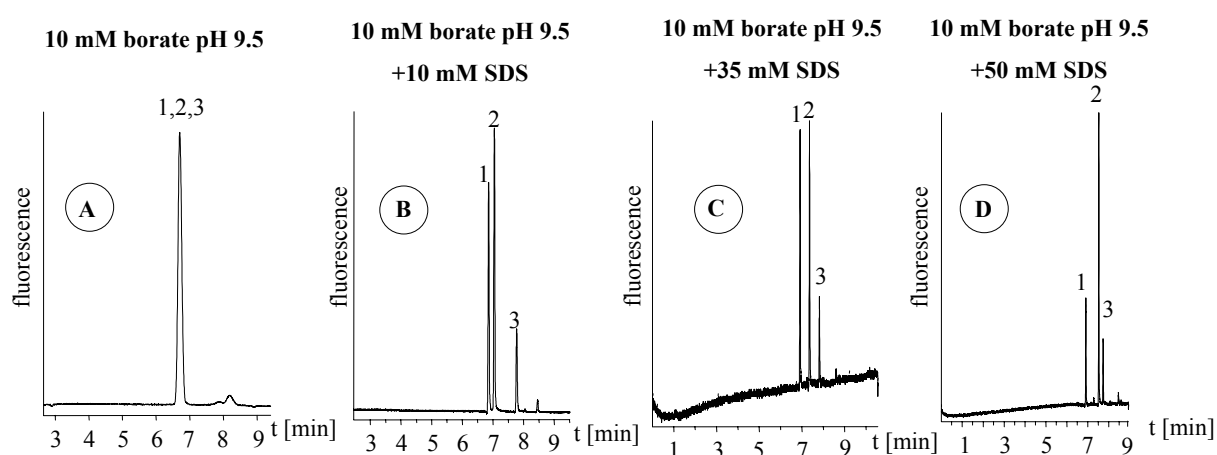


Figure 4.14: Electropherograms of FITC labeled stimulant drugs obtained using classical CE system. Conditions: Capillary, 60 cm effective, 80 cm total length, 50 μm i.d. Injection, 2 s hydrodynamic injection. Separation, 30 kV. Detection using Argos system at 477 nm exci/495 nm emis. Compounds and concentrations: (1) 6.25 $\mu\text{g}/\text{mL}$ FITC-ephedrine (2) 6.25 $\mu\text{g}/\text{mL}$ FITC-pseudoephedrine. (3) FITC dye.

This is due to the fact that the separation channel in MCE has a fixed length of only several centimeters (up to 7 cm) while in classical CE the capillary length is flexible and long separation capillaries are usually used (60 cm in this case).

Therefore, a 35 mM SDS solution added to 10 mM borate buffer at pH 9.5 is chosen as the optimal concentration that provides both good resolution and sensitive detection of the compounds. As shown in Figures 4.14B, C, D, the addition of SDS to the buffer enhances the resolution of the FITC-E, the FITC-PE and the FITC-dye as well. This is important especially in quantitative analysis to assure correct calculation of peak areas. This can be explained by the fact that the micelle phase (SDS) has mobility against the EOF. This results in an increase in the migration time of FITC-E and FITC-PE compounds with an increase in SDS concentration. In this case, the resolution can be enhanced by enlarging the effective migration distance of the analytes and as a result, increasing the mobility differences between FITC-E and FITC-PE.

Effect of chip type

After selection of the suitable buffer, the effect of the pb-chip compared to wc-chip on the separation performance of the two isomers is also examined within the method development. For this purpose, three different glass chips are utilized such as 100 μm pb, 100 μm wc and 50 μm wc-chips as well as fused silica (FS) chips. The separation of the two drugs is successfully performed using such chips with the previously selected buffer. The corresponding electropherograms are shown in Figures 4.15, 4.16. As described before, the pb-chips provide lower resolution due to their surface roughness. The influence of the surface roughness is shown by the separation of labeled ephedrine and pseudoephedrine on a pb-chip which results in a low resolution value of 1.5 (Figure 4.15A). This value is comparable with that obtained using a 100 μm wc-chip (Figure 4.15C).

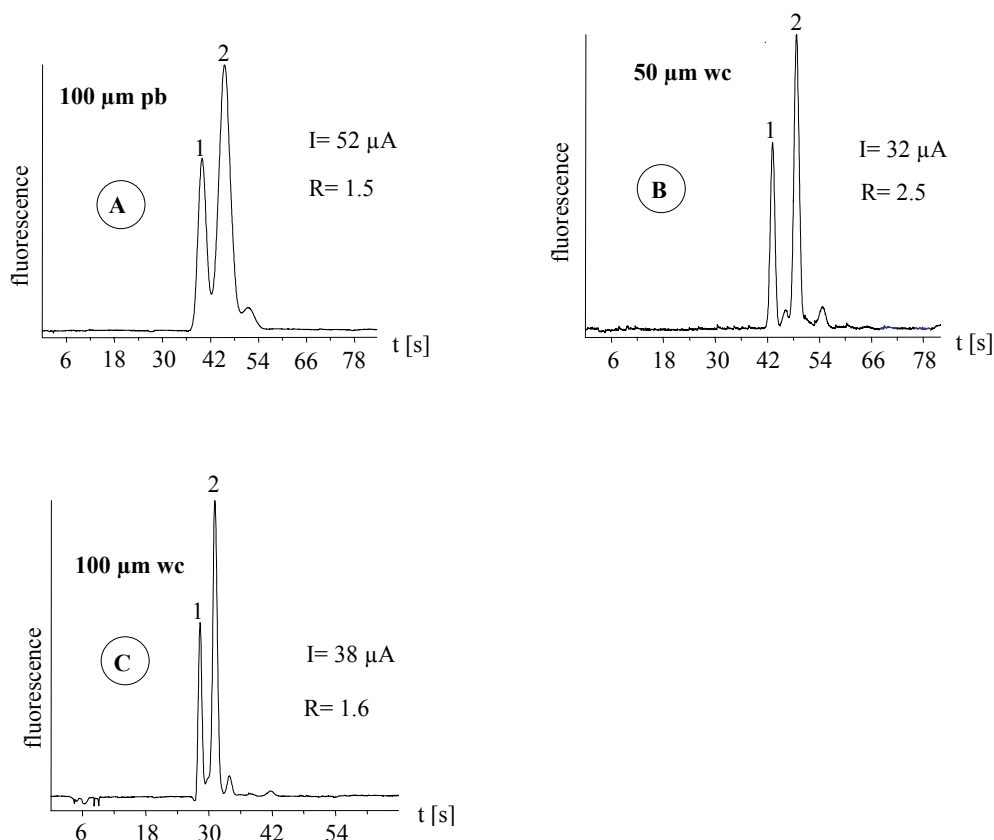


Figure 4.15: Electropherograms of FITC labeled stimulant drugs obtained in different chips. Conditions: BGE is 10 mM borate buffer at pH 9.5+35 mM SDS. Effective separation length, 2 cm. Injection potentials, BI 0.65, BO 2.050, SI 0.75, and SO 0.00 (kV); separation potentials, BI 2.00, BO 0.00, SI and SO 0.7 (kV). Compounds and concentrations: (1) 1.2 $\mu\text{g/mL}$ FITC-ephedrine (2) 1.2 $\mu\text{g/mL}$ FITC-pseudoephedrine. Mercury lamp at 450-480 nm is used as excitation light source.

The 50 $\mu\text{m wc}$ -chip seems to be well suited in this study in terms of better resolution ($R=2.5$) and lower current value ($I= 32 \mu\text{A}$) as shown in Figure 4.15B. As a result, the lower electric current value leads to low electrical conductivity allowing to work at high field strengths without typical problems in chip separations due to Joule heating. In addition, by using a FS-chip an improvement in the separation efficiency by a factor of two is achieved. Also, a faster separation time (within 40 s) is observed compared to borofloat (BF) chips (within 55 s) as shown in Figure 4.16. The higher separation efficiency obtained in a FS-chip may be attributed to the effect of Joule heating. As Joule heating is time-dependent, the compounds that migrate slower (Figure 4.16A) will be more affected than the fast migrating ones (Figure 4.16B). Both microchips are used in the current study, however, a FS-chip is more favorable

because it has good transmittance and low autofluorescence properties in the deep UV spectral region.

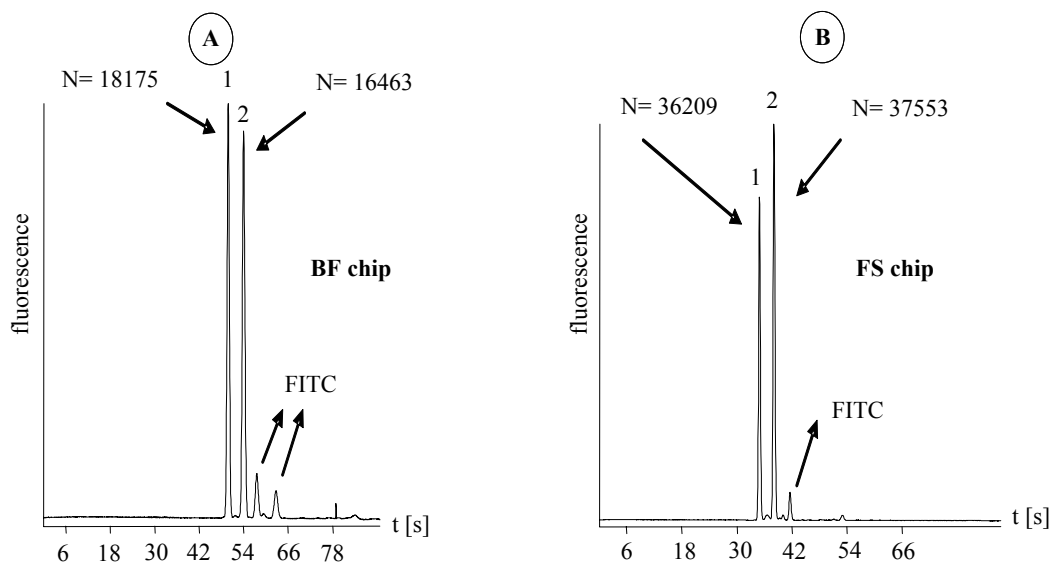


Figure 4.16: Electropherograms of FITC labeled stimulant drugs obtained in a BF-chip (A) and a FS-chip (B). Conditions: BGE is 10 mM borate buffer at pH 9.5+35 mM SDS. Effective separation length, 5 cm Injection potentials, BI 0.65, BO 2.050, SI 0.75, and SO 0.00 (kV); separation potentials, BI 4.00, BO 0.00, SI and SO 3.4 (kV). Other conditions and peak identification are as in Figure 4.15.

Effect of SDS on sensitivity and efficiency

SDS similarly, as any anionic species, does not interact with the negatively charged surface of the channels, which is favorable especially in chip measurements. MEKC in a chip format is not applied very often and uses micelles only for controlling the selectivity and the migration of analytes. The solubilization of the analyte in the micellar phase alters its properties significantly [127]. On this account, additional work is performed to study the effect of SDS on the sensitivity and peak efficiency, for example addition of SDS to the buffer can improve the sensitivity and separation efficiency. In Figure 4.17, FITC-E is used for these measurements, in which the S/N ratio is improved by a factor of 4 after addition of SDS to the buffer. This is due to the fact that in different applications SDS is reported to be a good fluorescence enhancer [193, 194], which is caused by the higher viscosity inside the micelles compared to the outside environment. Increased viscosity restricts the relaxational motion of molecules and thus enhances the fluorescence yield [194]. Improvement in the

separation efficiency by a factor of 6 is achieved as well. It can be concluded that MEKC is the method of choice in this study because it has the benefit of a higher sensitivity compared with the CZE method (Figure 4.17A).

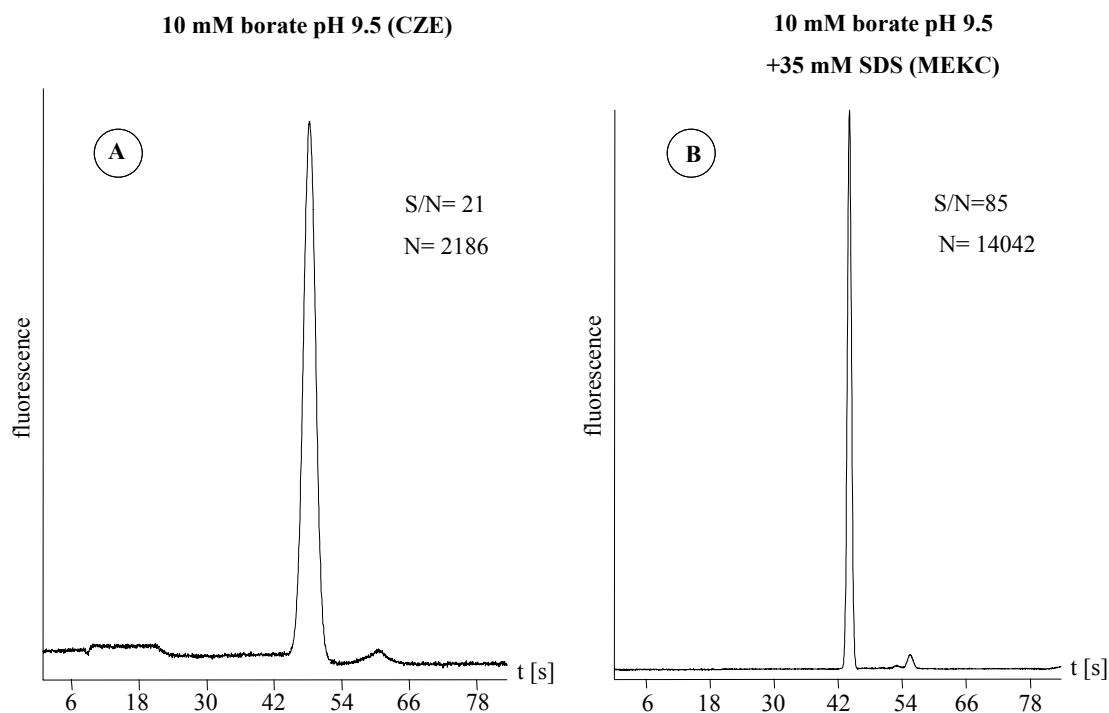


Figure 4.17: Electropherograms of 1.2 $\mu\text{g/mL}$ FITC-ephedrine: (A) in 10 mM borate buffer at pH 9.5 on a BF chip, (B) in 10 mM borate buffer at pH 9.5+35 mM SDS on a BF chip and other conditions are as in Figure 4.16.

Effect of the light source

As described previously (section 3.2.3), the setup of the MCE system can be coupled with different light sources allowing different applications. For this purpose, an epifluorescence setup is used enabling the coupling of an argon-ion laser into a commercial fluorescence microscope. The detection of the analytes is performed by laser-induced fluorescence (LIF) using an argon ion laser with an excitation wavelength of 488 nm (with an emission filter at 520 nm) in comparison to lamp based fluorescence detection at 450–480 nm (with an emission filter >515 nm). It is found that LIF detection provided a 40-fold higher sensitivity in relation to a lamp

based fluorescence detection. As shown in Figure 4.18, the LOD of the standard compounds is determined to be 140 pg/mL using an argon ion laser while it is at 6 ng/mL using a mercury lamp. Nevertheless, both detection methods are used for the sensitive determination of the two alkaloids in formulations and human urine.

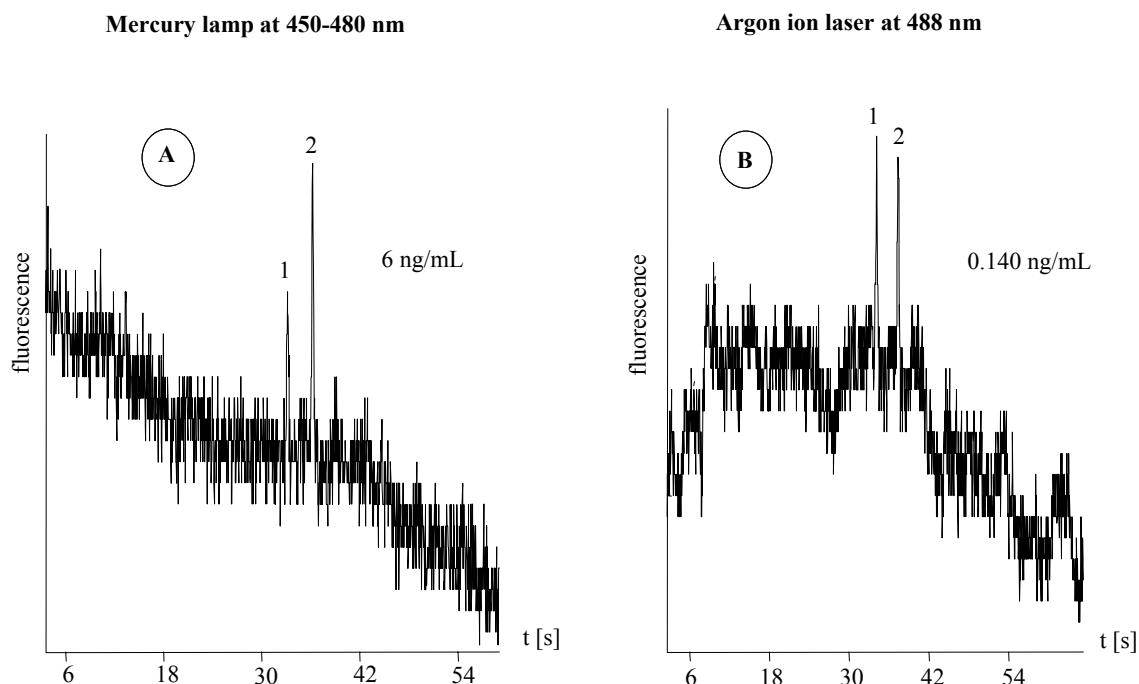


Figure 4.18: Electropherograms of standard ephedrine and pseudoephedrine at the limit of detection: (A) 6 ng/mL FITC-ephedrine (peak 1) and 6 ng/mL FITC-pseudoephedrine (peak 2) on a FS-chip using mercury lamp detection, (B) 140 pg/mL FITC-ephedrine (peak 1) and 140 pg/mL FITC-pseudoephedrine (peak 2) on a FS-chip using argon ion laser, other conditions are as in Figure 4.16.

4.2.1.2 Application to pharmaceutical formulations

Fast determination of the active ingredient in a drug is very useful in the manufacture and quality control of medicines. In order to quantify the amount of ephedrine and pseudoephedrine in commercial tablets, the previously developed MCE methods are validated with regard to precision, linearity, LOD, LOQ and accuracy.

For the determination of calibration plots, standard samples of labeled ephedrine and pseudoephedrine at eight different concentration levels are prepared covering the range from 0.5-4000 ng/mL of each labeled compound. Each sample is analyzed three

times and the mean peak areas are calculated.

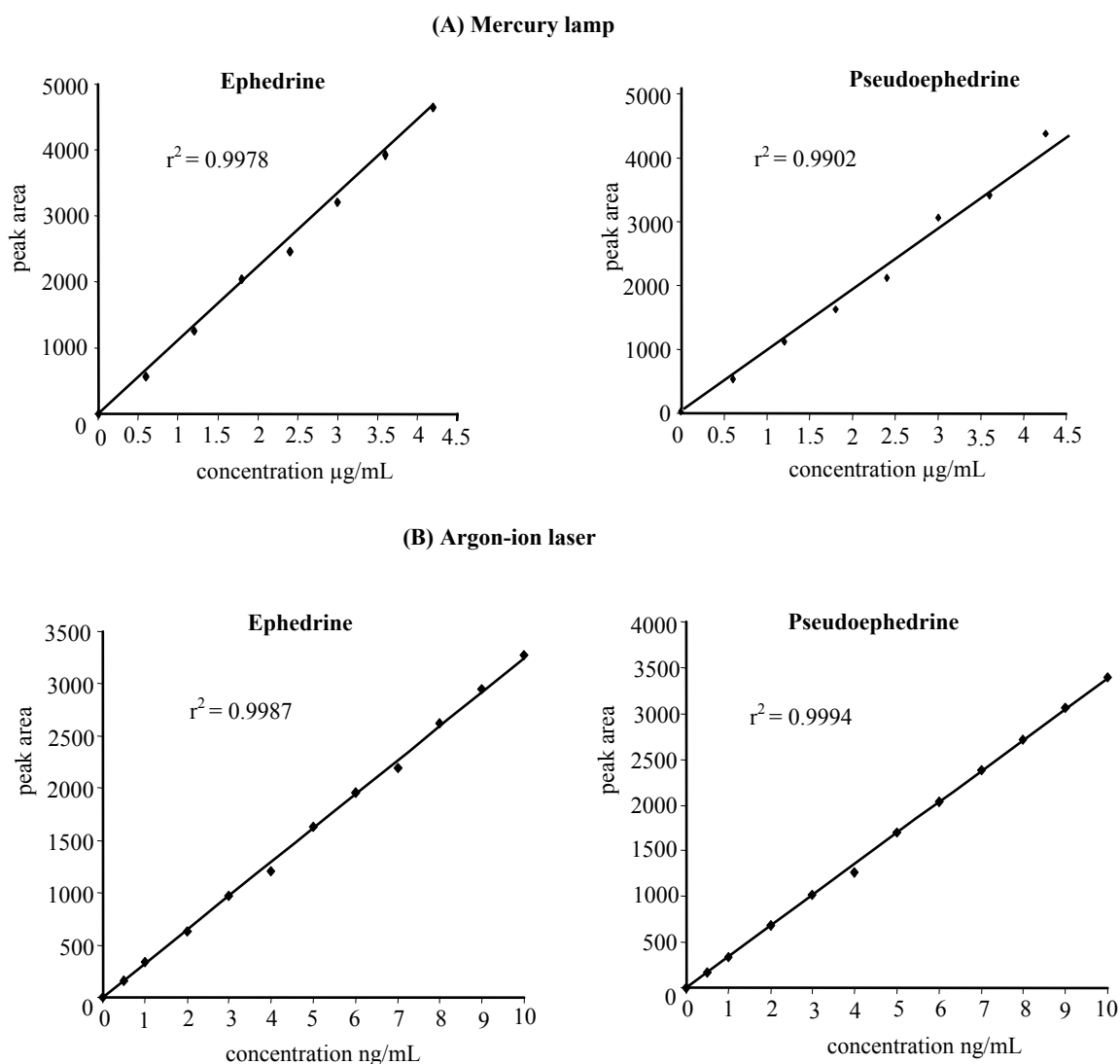


Figure 4.19: Standard calibration plots for standard ephedrine and pseudoephedrine: (A) using mercury lamp on a BF-chip, (B) using argon ion laser on a FS-chip and other conditions are as in Figure 4.16.

Calibration lines are obtained by plotting the concentration on the abscissa versus the mean peak area. The resultant calibration plots exhibit good linearity as shown in Figure 4.19. The regression parameters which are calculated from the calibration curves are reported in Table 4.1. As seen in Table 4.1, calibration curves of ephedrine and pseudoephedrine provide good correlation coefficients ($r^2 > 0.990$ for both compounds) ensuring a linear response over the concentrations range.

The limit of detection (LOD) is defined as the analyte concentration which leads to an

S/N ratio of 3:1. These values are measured for both drugs to either be 6 ng/mL by using the mercury lamp or 0.14 ng/mL using the argon ion laser for excitation. The corresponding electropherograms are shown in Figure 4.18. The limit of quantification (LOQ) is defined as the analyte concentration that can be analyzed with acceptable precision and accuracy usually determined from a series of diluted solutions exhibiting an $S/N \geq 10$. The typical LOQ values for both drugs are determined on one hand at 0.6 $\mu\text{g/mL}$ with the mercury lamp or on the other hand at 0.5 ng/mL with the argon ion laser, as shown in Figure 4.20. All values of LOD and LOQ are listed in Table 4.1.

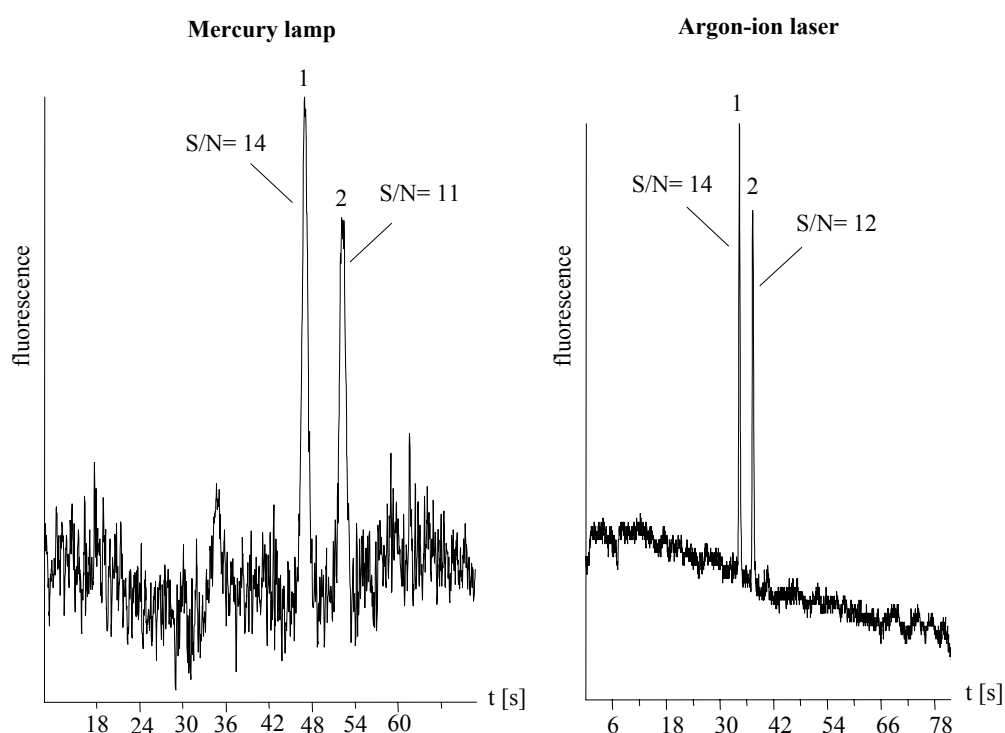


Figure 4.20: Electropherograms of standard ephedrine and pseudoephedrine at LOQ: (A) 0.6 $\mu\text{g/mL}$ FITC-E (peak 1) and 0.6 $\mu\text{g/mL}$ FITC-pseudoephedrine (peak 2) on a BF-chip using mercury lamp detection, (B) 0.5 ng/mL FITC-ephedrine (peak 1) and 0.5 ng/mL FITC-pseudoephedrine (peak 2) on a FS-chip using argon ion laser, other conditions are as in Figure 4.16.

The intraday accuracy and precision of the method are determined by running three replicates of the standard (3.6 $\mu\text{g/mL}$ of E, PE or 2 ng/mL E, PE using either mercury lamp or argon ion laser, respectively). The measurement with each FITC-derivatized drug shows high reproducibility in terms of peak areas and migration times. The relative standard deviation (RSD) is a statistical term to measure the precision for a

series of repetitive measurements. For this reason the RSDs of the peak areas (Table 4.1) are calculated to be less than 3% or less than 2% for migration time revealing that the method is highly precise.

Table 4.1: Method validation for quantitative determination of ephedrine and pseudoephedrine (* n= 3 measurements).

Parameter	Mercury lamp at 480 nm		Argon ion laser at 488 nm	
	Ephedrine	Pseudoephedrine	Ephedrine	Pseudoephedrine
Linearity	0.6-4 µg/mL	0.6-4 µg/mL	0.5-10 ng/mL	0.5-10 ng/mL
LOD	6 ng/mL	6 ng/mL	0.14 ng/mL	0.14 ng/mL
LOQ	0.6 µg/mL	0.6 µg/mL	0.5 ng/mL	0.5 ng/mL
RSD% peak area*	2.35	2.55	1.96	1.50
RSD% migration time*	0.79	1.85	1.44	1.82
Correlation coefficient	0.9978	0.9902	0.9987	0.9994
Intercept	- 48883	-115511	- 16247	- 10582
Slope	417031	985449	326454	339993

The validated MCE methods are then applied to the commercially available tablets containing ephedrine and pseudoephedrine such as Asmoline (20 mg/tablet ephedrine) and Congestal (60 mg/tablet pseudoephedrine) tablets. The tablets are powdered and dissolved in methanol using an ultrasonic bath for 20 min. The resulting solutions are filtered and diluted to give stock solutions with concentrations of 1 mg/mL for each drug under examination. After labeling with FITC, the obtained electropherograms of the tablets are shown in Figure 4.21. The results reveal that the larger amounts of excipients, generally used in tablets, do not interfere with the drugs under investigation. As depicted in Figure 4.21, it is obvious that the resultant peaks are well resolved without interfering by-products. Furthermore, no shifts in migration time

relative to pure ephedrine and pseudoephedrine standards are observed.

The applicability of the methods for determination of ephedrine and pseudoephedrine in tablets is carried out using the standard addition technique as a check for accuracy.

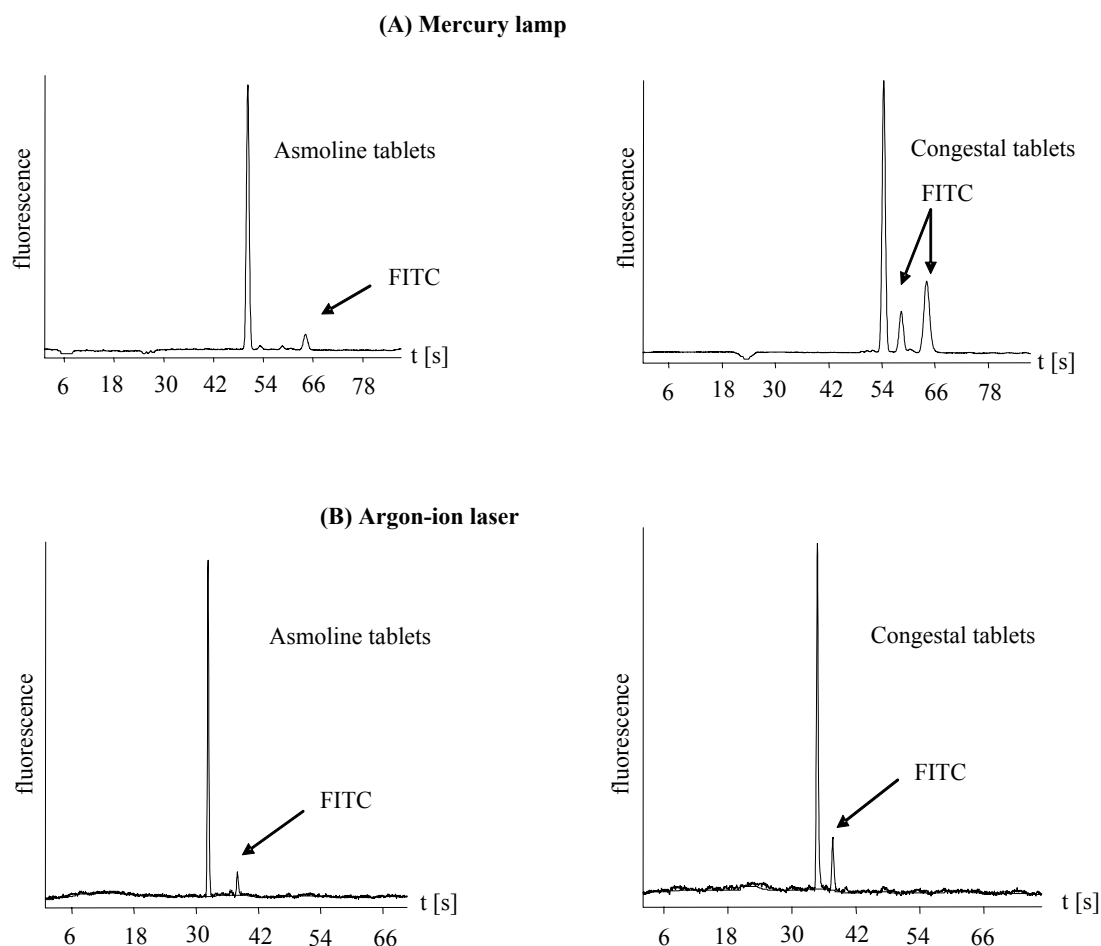


Figure 4.21: Electropherograms of ephedrine and pseudoephedrine in commercial tablets: (A) Asmoline tablets: 1.2 $\mu\text{g/mL}$ FITC-ephedrine and Congestal tablets: 1.2 $\mu\text{g/mL}$ FITC-pseudoephedrine on a BF-chip using mercury lamp, (B) Asmoline tablets: 5 ng/mL FITC-ephedrine and Congestal tablets: 5 ng/mL FITC-pseudoephedrine on a FS-chip using argon ion laser. Other conditions are as in Figure 4.16.

For this purpose, four different amounts of the standard solutions are added to solutions of the tablets, and then the recovery of each drug in tablets is calculated. The produced results are reproducible with low relative standard deviations (RSDs) as shown in Table 4.2. The values of average recovery of ephedrine and pseudoephedrine in formulations are about 100.69 and 100.49%, respectively (see Table 4.2). RSD, (is an indicator of precision) of the mean recoveries is less than 4%. The average amount of ephedrine and pseudoephedrine in tablets is calculated to be

20.13 and 60.29 mg/tablet respectively. Such results are described in details in Table 4.2. The results obtained for the content of E and PE in the pharmaceutical formulations are in good agreement with the labeled amount in tablets. This indicates that the method is robust and can be employed as a routine method for quality control of ephedrine and pseudoephedrine dosage forms.

Table 4.2: Determination of ephedrine and pseudoephedrine in pharmaceutical formulations ($n= 4$ measurements).

Formulation	Amount of standard added	Amount of standard found	Recovery %	Light source
Asmoline tablets (20 mg/tablet E)	1.20 $\mu\text{g/mL}$	1.19 $\mu\text{g/mL}$	99.17	Mercury lamp
	1.80 $\mu\text{g/mL}$	1.85 $\mu\text{g/mL}$	102.78	
	2.40 $\mu\text{g/mL}$	2.44 $\mu\text{g/mL}$	101.67	
	3 $\mu\text{g/mL}$	3.02 $\mu\text{g/mL}$	100.67	
Mean recovery%			101.05	
RSD%			1.51	
Congestal tablets (60 mg/tablet PE)	1.20 $\mu\text{g/mL}$	1.17 $\mu\text{g/mL}$	97.50	
	1.80 $\mu\text{g/mL}$	1.85 $\mu\text{g/mL}$	102.78	
	2.40 $\mu\text{g/mL}$	2.36 $\mu\text{g/mL}$	98.33	
	3 $\mu\text{g/mL}$	3.14 $\mu\text{g/mL}$	104.67	
Mean recovery%			100.82	
RSD%			3.42	
Asmoline tablets (20 mg/tablet E)	1 ng/mL	0.98 ng/mL	98	Argon-ion laser
	2 ng/mL	2 ng/mL	100	
	3 ng/mL	3.1 ng/mL	103.33	
	4 ng/mL	4 ng/mL	100	
Mean recovery%			100.33	
RSD%			2.21	
Congestal tablets (60 mg/tablet PE)	1 ng/mL	0.99 ng/mL	99	
	2 ng/mL	1.95 ng/mL	97.50	
	3 ng/mL	3.05 ng/mL	101.67	
	4 ng/mL	4.1 ng/mL	102.50	
Mean recovery%			100.17	
RSD%			2.32	

4.2.1.3 Application to human urine

With the development of modern sports games and the increasing number of doping cases, it is demanding to develop fast and highly sensitive screening methods for doping control. In 1990, the Medical Commission of the International Olympic Committee included the ephedrine and pseudoephedrine in the list of forbidden substances [69]. Recently, the commission has adopted the following limits of concentration in urine above which an athlete is considered to be “positive”: 25 $\mu\text{g/mL}$ for pseudoephedrine and 10 $\mu\text{g/mL}$ for ephedrine. Antidoping controls are routinely carried out on the urine and thus a fast, simple and reliable analytical method is needed for identifying the abuse of such compounds by athletes.

However, analysis of drugs in body fluids using microfluidic devices presents a special challenge, both in terms of sensitivity and fouling of microchannels by matrix components. In addition the derivatization of the compounds in pure urine without extraction is a problematic issue due to inhibition of the derivatization process by endogenous urine components. The dilution of urine with water (1:1) and a concurrent alkalization with basic buffer can solve this problem. Several other methods have been described in the literature for the determination of ephedrine in urine [195-197]. However, there are no available techniques for the determination of ephedrine or pseudoephedrine without extraction. The previously developed MCE methods can be also used for quantitative determination of both drugs in human urine.

In vitro analysis

For *in vitro* analysis, ephedrine and pseudoephedrine with known concentrations in urine are derivatized as previously described (section 3.7). The calibration plots are performed within the concentration ranges 2-4200 ng/mL for each compound. As shown in Figure 4.22, the calibration plots exhibited good linearity. The linearity of the calibration curves provides correlation coefficient values higher than 0.995 as shown in Table 4.3. RSD of peak area ($n= 3$) is calculated to be less than 4%. All regression parameters and RSD values are listed in Table 4.3.

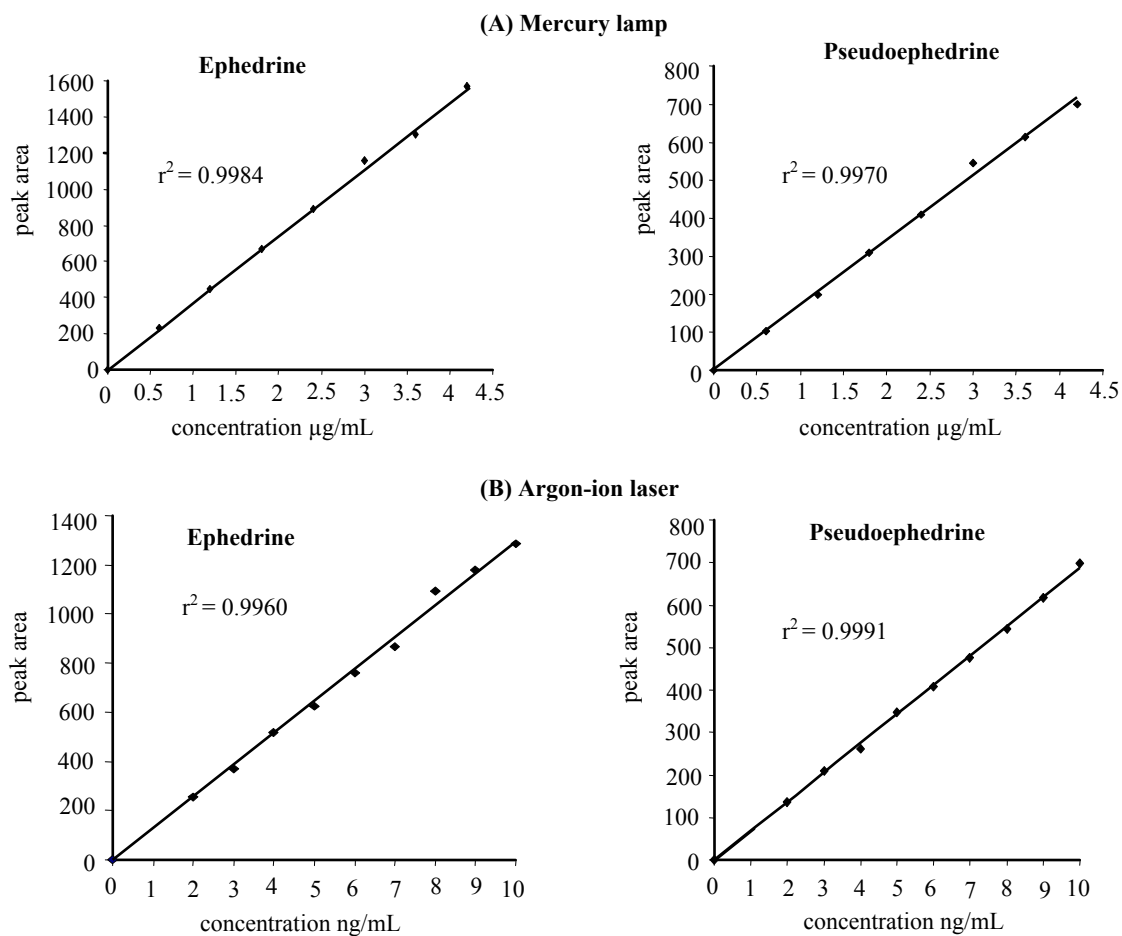


Figure 4.22: Standard calibration plots for ephedrine and pseudoephedrine in human urine: (A) using mercury lamp on a BF-chip, (B) using argon ion laser on a FS-chip and other conditions are as in Figure 4.16.

Table 4.3: Determination of ephedrine and pseudoephedrine in human urine (* n= 3).

Parameter	Mercury lamp at 480 nm		Argon ion laser at 488 nm	
	Ephedrine	Pseudoephedrine	Ephedrine	Pseudoephedrine
Linearity	0.6-4.2 µg/mL	0.6-4.2 µg/mL	2-10 ng/mL	2-10 ng/mL
LOD	20 ng/mL	120 ng/mL	0.5 ng/mL	1 ng/mL
LOQ	0.6 µg/mL	0.6 µg/mL	2 ng/mL	2 ng/mL
RSD% peak area*	2.60	3.25	2.16	2.85
Correlation coefficient	0.9984	0.9970	0.9960	0.9991
Intercept	6068	1936	- 13299	- 3789
Slope	370244	170443	131141	69224

The corresponding electropherogram for *in vitro* analysis is shown in Figure 4.23. Using the mercury lamp (Figure 4.23A), the two stimulant drugs are completely resolved, however, peak broadening is observed which is expected due to the high ionic strength of the urine. Using an argon ion laser, Figure 4.23B, the two compounds are resolved providing very sharp peaks which are well resolved from the endogenous urine components.

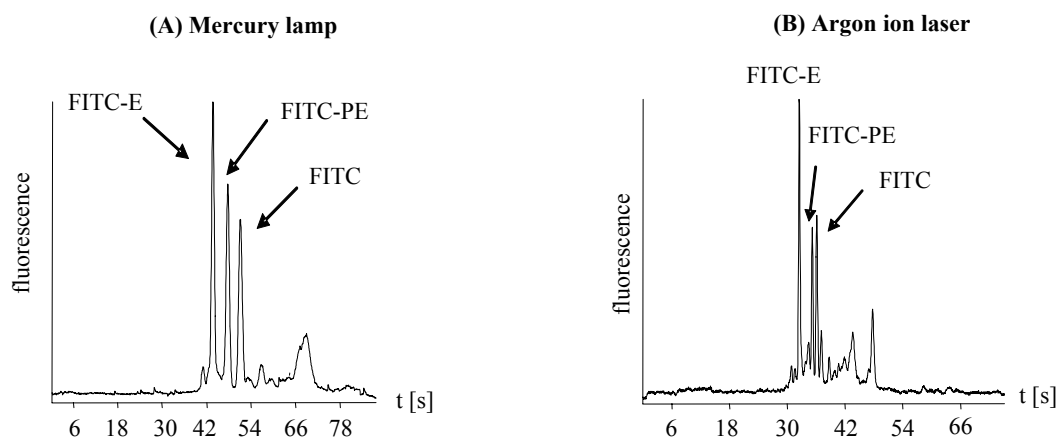


Figure 4.23: Electropherograms of FITC-ephedrine and FITC-pseudoephedrine *in vitro* human urine: (A) 1.2 $\mu\text{g/mL}$ FITC-ephedrine and 1.2 $\mu\text{g/mL}$ FITC-pseudoephedrine on a BF-chip using mercury lamp or (B) 10 ng/mL FITC-ephedrine and 10 ng/mL FITC-pseudoephedrine on a FS-chip using argon ion laser. Other conditions are as in Figure 4.16.

Due to the fact that the urine background is different from the water background, many amino-containing substrates in urine will compete in the derivatization and the labeling efficiency may not be as high as in pure water. Therefore, LODs are determined in urine by using a mercury lamp to be 20 and 120 ng/mL for E and PE, respectively, as shown in Figure 4.24A (6 ng/mL in aqueous solution). All values of LODs in urine are reported in Table 4.3.

Using argon ion laser, very low concentrations of E and PE in urine are measured to be 0.5 and 1 ng/mL, respectively, as shown in Figure 4.24B. These data reveal that LIF utilizing an argon ion laser is the best approach for sensitive detection of ephedrine and pseudoephedrine in urine. The practical detection limits are lower than expected and fulfill the requirements for stimulants screening with a threshold of 10 $\mu\text{g/mL}$.

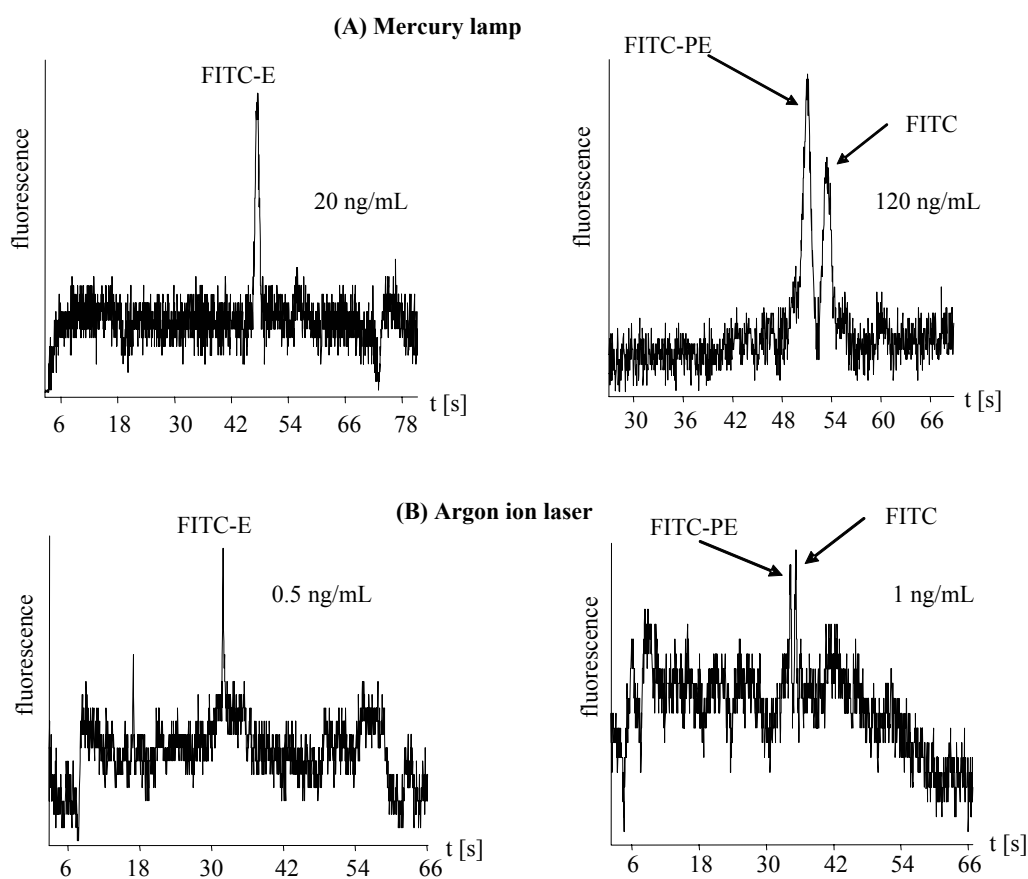


Figure 4.24: Electropherograms of standard ephedrine and pseudoephedrine in human urine at the limit of detection: (A) 20 ng/mL FITC-ephedrine and 120 ng/mL FITC-pseudoephedrine on a BF-chip using mercury lamp, (B) 0.5 ng/mL FITC-ephedrine and 1 ng/mL FITC-pseudoephedrine on a FS-chip using argon ion laser. Other conditions are as in Figure 4.16.

In vivo analysis

For *in vivo* analysis, the assay described under *in vitro* analysis is applied to urine samples collected from human volunteers after oral intake (after 12h) of 20 mg ephedrine and 60 mg pseudoephedrine. It is well known that 70-80% of ephedrine and pseudoephedrine dose is excreted unmetabolized in the urine within 48 hours [188-191]. According to the calibration curves and the associated regression equations, the unknown concentrations in patient urine are calculated to be 0.6 $\mu\text{g/mL}$ and 0.9 $\mu\text{g/mL}$ for ephedrine and pseudoephedrine, respectively. Figures 4.25A and B represent the typical electropherograms obtained with the human urine where the migration time remains unchanged whilst peak separation is still satisfactory.

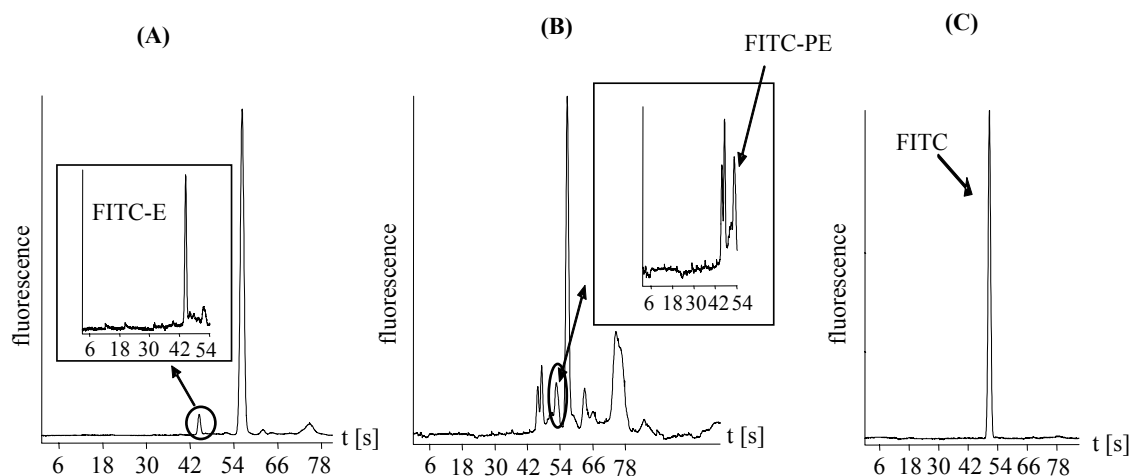


Figure 4.25: Electropherograms of FITC-ephedrine and FITC-pseudoephedrine (A,B) in vitro human urine on a BF-chip using mercury lamp (C) FITC-urine blank. Other conditions are as in Figure 4.16.

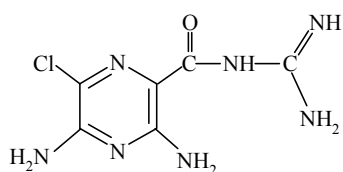
For *in vivo* analysis, small peaks of the stimulants are detected as shown in Figures 4.25A and B. This is attributed to the fact that drugs in biological fluid are present at low concentration levels because of metabolic processes or the low therapeutic doses of the drugs. For FITC-E, only a small peak of the drug is observed at 42 s which is well resolved from the peak originating from the dye as shown in Figure 4.25A. On the other hand two small endogenous peaks are observed in case of FITC-PE (Figure 4.25B), however, they do not interfere. The electropherogram obtained from the analysis of the blank urine spiked with FITC is shown in Figure 4.25C which demonstrates that no major endogenous components are detected in the time range of the drugs of interest. Therefore, direct urine analysis is feasible without significant sample treatment. Furthermore, the obtained MCE results can be considered to be more sensitive compared to those obtained by CZE [197] or by solid phase micro-extraction method [195].

It can be concluded that the developed MCE-fluorescence methods provide several advantages over conventional chromatography methods. The analysis time using MCE is usually within several seconds in contrast to GC or HPLC, where the analysis time is usually 30-60 min. In MCE measurements, only a few μL of aqueous buffer are employed, showing that the method is economic and environmentally friendlier. Furthermore, with the use of fluorescence detection, a small amount of analytes in

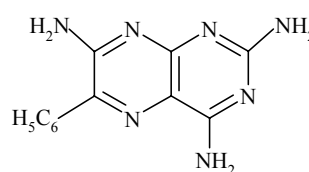
microchip can be determined with high sensitivity. Based on these advantages, microchip analysis is well suited for doping control as well as in pharmaceutical labs.

4.2.2 Application to diuretic drugs

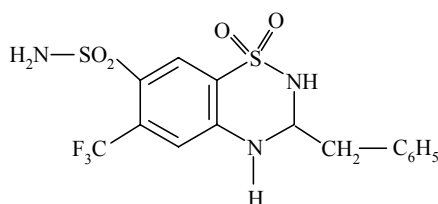
Diuretics are a heterogeneous group of compounds widely used in the treatment of congestive heart failure and hypertension [198]. Diuretics have been misused in sports in recent years, for two reasons: (1) athletes may wish to reduce their body weight quickly in order to qualify for a lower mass class (2) athletes may wish to dilute their urine to avoid a positive doping result [198]. Diuretics are classified according to their chemical structure, their mechanism and site of action within the nephron, and their diuretic potency. They are classified as thiazides (e.g., bendroflumethiazide), loop diuretics (e.g., bumetanide), potassium sparing diuretics (e.g., amiloride and triamterene) [198]. The chemical structures of the four diuretics under investigation are shown in Figure 4.26.



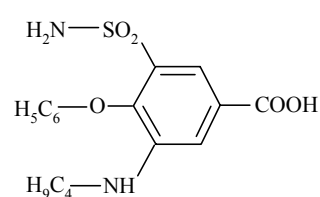
Amiloride (229.6 g/mol)



Triamterene (253.3 g/mol)



Bendroflumethiazide (421.4 g/mol)



Bumetanide (364.4 g/mol)

Figure 4.26: Chemical structure of the diuretic drugs.

In literature, several chromatography methods such as HPLC [199, 200], GC [201, 202], and TLC [203, 204] have been reported for the separation, detection, and determination of diuretics. Among these methods, RP HPLC with UV-detection is the most common one and has been adapted as the standard screening method for doping

control. In recent years, CE methods for diuretics analysis have been developed applying CZE [205, 206] or MEKC [207, 208].

In this section, development and validation of a fast MCE method is introduced for the simultaneous determination of unlabeled diuretic drugs in pharmaceutical formulations and human urine.

4.2.2.1 Method development

Native fluorescence of diuretics

In the first part of this section, in order to optimize the detection setup, the excitation-emission wavelengths of the diuretics are determined using fluorescence spectroscopy as shown in Figure 4.27.

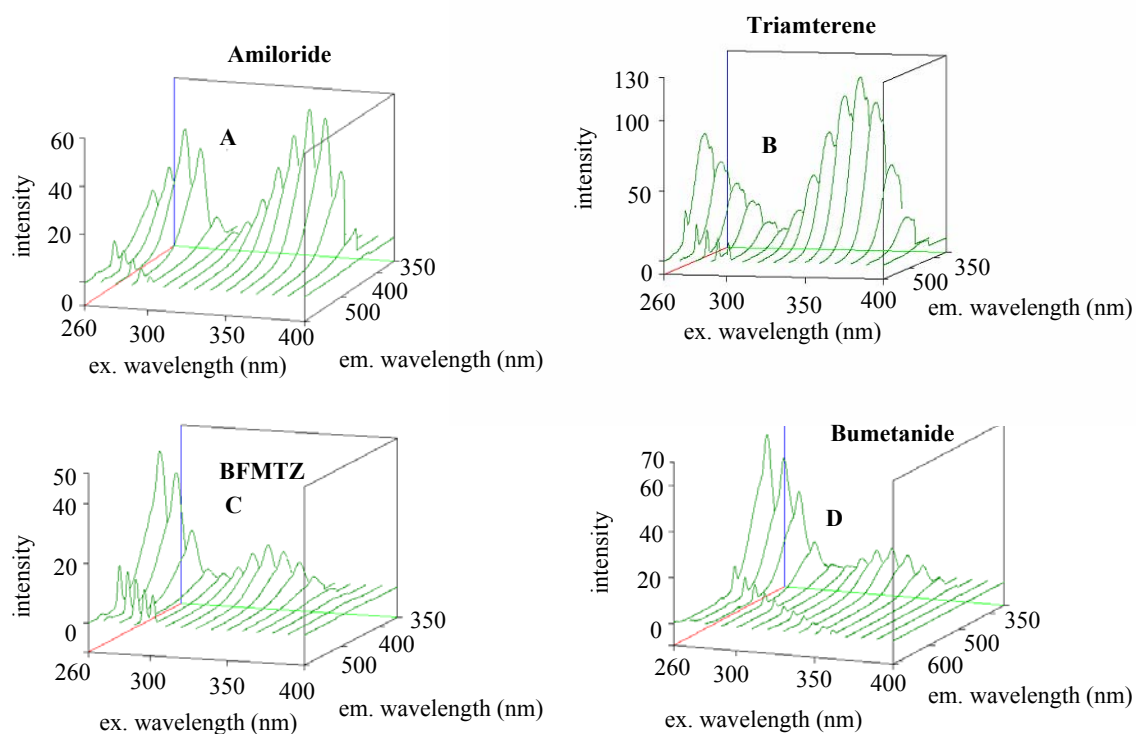


Figure 4.27: 3-D measurements of the excitation-emission spectra of the diuretic drugs under analysis: (A) 1 $\mu\text{g/mL}$ Amiloride in MES pH 5.5, (B) 0.08 $\mu\text{g/mL}$ Triamterene in MES pH 5.5, (C) 1 $\mu\text{g/mL}$ BFMTZ in MES pH 5.5, (D) 1 $\mu\text{g/mL}$ Bumetanide in MES pH 5.5.

In these experiments, 0.2 mg/mL diuretic standard solutions are used. A series of diluted solutions in MES buffer at pH 5.5 is then prepared that include 1 $\mu\text{g/mL}$ amiloride, 0.08 $\mu\text{g/mL}$ triamterene, 1 $\mu\text{g/mL}$ BFMTZ, and 1 $\mu\text{g/mL}$ bumetanide. The corresponding excitation-emission spectra shown in Figure 4.26 reveal that the four diuretics under examination provided native fluorescence which can be measured using CE or MCE with different fluorescence excitation light sources.

Effect of pH on the separation performance

The separation of the four diuretics is performed with a classical capillary electrophoresis instrument using a previously described 15 mM borate buffer at pH 8 [206]. Separation of the diuretics is performed in the mode of CZE which has the benefit of simplicity and rapid analysis for charged compounds. The separation is performed on a chip within 15 s (Figure 4.28B) rather than 7 min using a classical CE system (Figure 4.28A). This makes MCE an attractive alternative to CE, especially when fast separations are required.

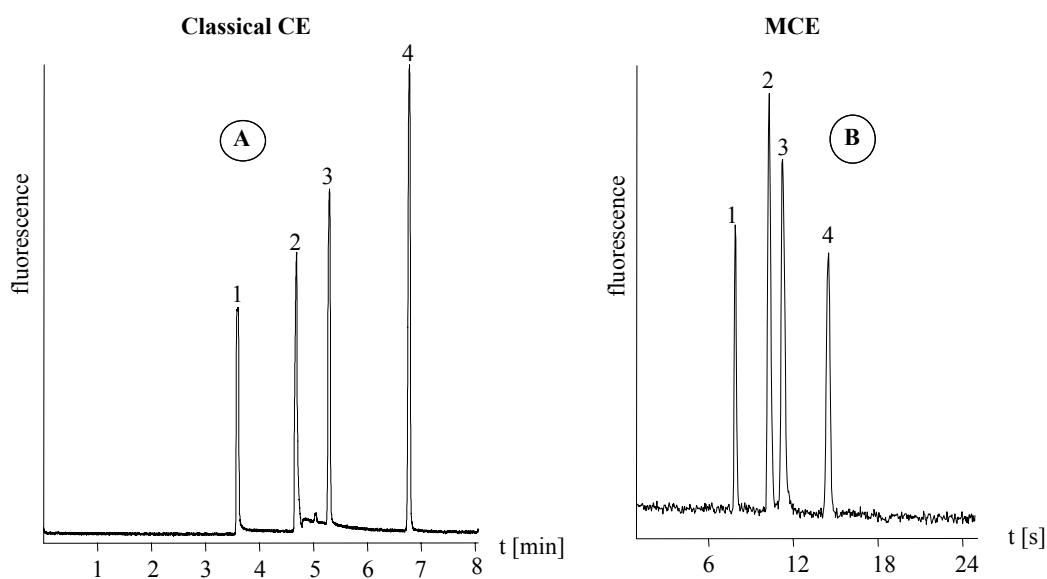


Figure 4.28: Comparison of electropherograms of standard diuretic compounds obtained with classical CE (A) and MCE (B) in 15 mM borate buffer pH 8. Conditions: (A): Capillary, 60 cm effective, 80 cm total length, 50 μm i.d. Injection, 10 kV, 5 s. Separation, 30 kV. Fluorescence detection using an Argos 250B Detector, excitation at 325 nm, emission light collected with a high pass filter at 385 nm. Compounds and concentrations: (1) 25 $\mu\text{g/mL}$ amiloride, (2) 2 $\mu\text{g/mL}$ triamterene, (3) 25 $\mu\text{g/mL}$ bendrofluomethiazide, and (4) 25 $\mu\text{g/mL}$ bumetanide. Conditions: (B): Effective separation length, 2 cm. Injection potentials, BI 1.35, BO 4.10, SI 1.50, and SO 0.00 (kV); separation potentials, BI 4.00, BO 0.00, SI and SO 3.2 (kV). Compounds and concentrations: (1) 5 $\mu\text{g/mL}$ amiloride, (2) 1 $\mu\text{g/mL}$ triamterene, (3) 15 $\mu\text{g/mL}$ bendrofluomethiazide, and (4) 5 $\mu\text{g/mL}$ bumetanide. Detection using HeCd laser at 325 nm.

In Figure 4.28, the same buffer system is used but with analytes concentration of 5 times lower for on-chip separations (e.g. 5 $\mu\text{g/mL}$ for amiloride). This is due to the fact that a HeCd laser is utilized as excitation source while a commercial lamp based fluorescence detection system is used in classical CE.

In order to improve the detection sensitivity and electrophoretic resolution, different buffer systems at different pHs and ionic strengths are studied. In electrophoresis, the pH of the buffer medium affects the electrophoretic mobility which modifies the migration velocity, separation efficiency and detection sensitivity [206]. For the drugs of interest, the effect of pH is studied in the pH range from 3-7 with Na-phosphate buffer, at pH 8 with borate buffer and at pH 9 with CHES buffer. The corresponding electropherograms are shown in Figure 4.29.

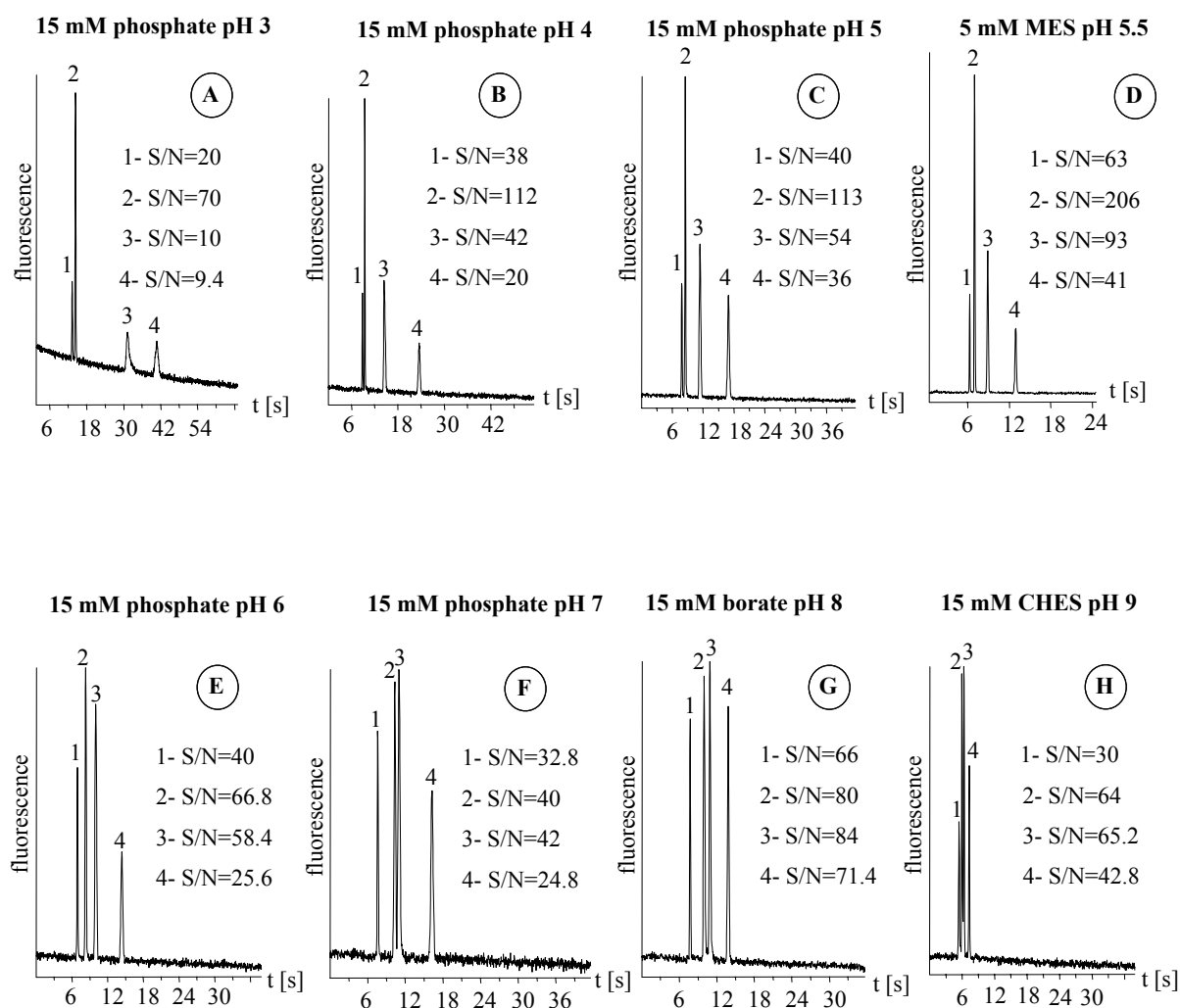


Figure 4.29: Electropherograms of diuretics using different pH buffers. Conditions and peak identification are as in Figure 4.28B.

For the drugs under examination, a decrease in pH results in an increase in migration time (Figure 4.29A). This observation agrees well with the fact that the electroosmotic mobility in capillaries has a sigmoid relationship with the pH [206, 209, 210]. At pH 3, the four compounds are separated within 42 s providing a low S/N ratio. At pH 4 (Figure 4.29B), the compounds are partially resolved within 24 s along with an enhancement in sensitivity (S/N=112 for triamterene while it is 70 at pH 3). At pH 5 (Figure 4.29C), the compounds are well resolved within 18 s with a S/N ratio of 113 for triamterene which is comparable with those obtained at pH 4. Using MES buffer at pH 5.5 (Figure 4.29D), it is found that the S/N ratios of all diuretics are highly improved by a factor of about two (206 for triamterene) compared to their values at pH 5 and a fast separation is also obtained (14 s). At pH 6, the compounds provide better resolution but a lower sensitivity (Figure 4.29E). In the pH range from 7-9 (Figures 4.29F,G,H), the compounds are partially resolved and they do not provide a complete baseline separation, especially at pH 9.

The migration order of the diuretics is shown to be related to the molecular structure and the mass of the drugs (see Figure 4.25). Diuretics containing amine groups such as amiloride and triamterene are present as cations in acidic pH buffers. Respective acidic buffers are however less suited for diuretics containing carboxylic or sulphonamide groups such as bendroflumethiazide and bumetanide.

Effect of additives and organic solvents

Also additives like native cyclodextrins and SDS are studied within the method development. It is found that the addition of SDS does not improve the separation sensitivity as expected but results in longer migration times (108 or 30 s) as shown in Figures 4.30A and B. Addition of native α , β and γ -cyclodextrins results in faster separation time, however, they do not improve the sensitivity and resolution. In these experiments, it is found that the four diuretics are not resolved completely in case of β or γ -cyclodextrin (Figures 4.30F and G) while a complete resolution is obtained with the addition of α -cyclodextrin (Figure 4.30E). Dimethyl sulfoxide (DMSO) and acetonitrile (ACN) as solvents are also studied; however, the compounds do not provide acceptable baseline separation using these solvents (Figures 4.30C and D). Finally a 5 mM MES buffer at pH 5.5 is chosen as an optimal buffer providing both, good resolution and sensitive detection of the compounds (Figure 4.29D).

Furthermore the selection of a MES buffer is advantageous because of the relatively low electrical conductivity, allowing to work at high field strengths without typical problems in chip separations due to Joule heating.

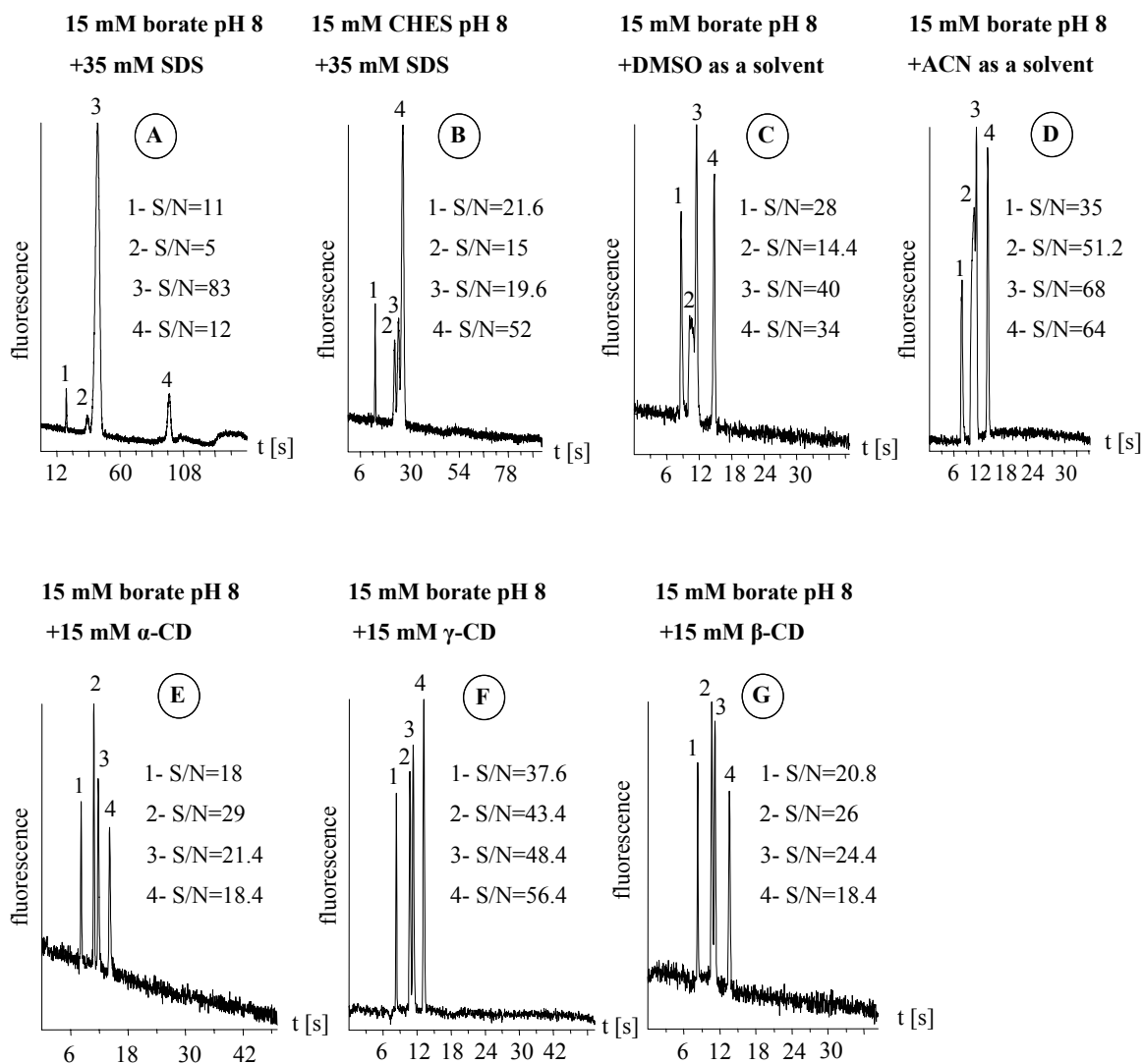


Figure 4.30: Electropherograms of diuretics using some additives to the buffer system. Conditions and peak identification are as in Figure 4.28B.

Effect of the light source

After adjusting the buffer system, different lasers besides laser based fluorescence detection are used to enhance the detection limit of the diuretics. For the analysis of diuretics, the performance of the detection sensitivity is compared using either a

mercury lamp (330-380 nm exc. with an emission filter >420 nm), a HeCd laser (325 nm exc. with an emission filter >350 nm) or a pulsed frequency doubled Nd:YAG-laser (266 nm exc. with an emission filter >320 nm). A comparison of different electropherograms obtained is shown in Figure 4.31.

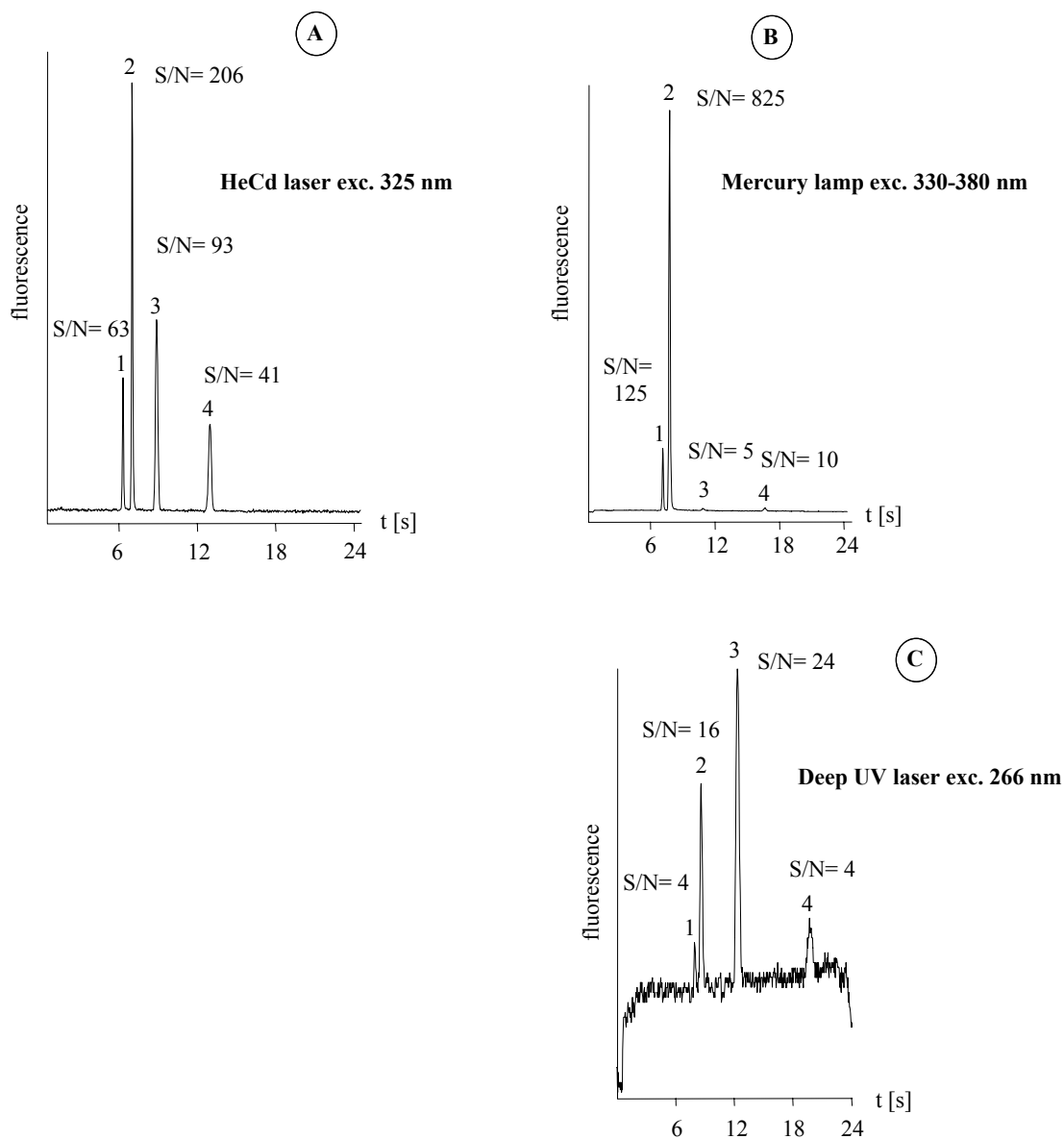


Figure 4.31: Comparison of sensitivities obtained with different light sources for excitation in MCE, Buffer, 5 mM MES, pH 5.5. Other conditions and peak identification are as in Figure 4. 28B.

As shown in Figure 4.31, different electropherograms are obtained using different light sources due to the different spectral properties of the analytes (see Figure 4.27). Using a lamp based fluorescence detection (Figure 4.31B) the sensitivity of amiloride

is improved by a factor of two and by a factor of four for triamterene compared to the HeCd laser (Figure 4.31A). This is not surprising due to the fact that their excitation wavelengths (360 nm) fit well to the excitation wavelength of the filter (330-380 nm) which is used in the instrumental setup. Although the two compounds are excited at the same wavelength (see Figure 4.27), the triamterene compound provides a higher fluorescence quantum yield than amiloride. This can explain why the sensitivity of triamterene using the mercury lamp is much better than amiloride. The four compounds are completely detected using a HeCd laser (Figure 4.31A) in comparison with the mercury lamp with an improvement in the sensitivity of BFMTZ by a factor of eighteen and by a factor of four for bumetanide. Detection of all compounds can also be performed utilizing a 266 nm Nd:YAG-laser with lower sensitivity for all compounds as in Figure 4.31C.

LIF utilizing a HeCd laser is the best approach for sensitive detection of diuretics for the current application.

4.2.2.2 Quantitative analysis of diuretics in tablets

The developed MCE method is then applied to the pharmaceutical preparations after validation. To validate this method, first, the calibration curves for the standard compounds are determined covering the concentration ranges of 1-20 $\mu\text{g/mL}$ amiloride, 50-1000 ng/mL triamterene, 1-20 $\mu\text{g/mL}$ bendroflumethiazide and 2-20 $\mu\text{g/mL}$ bumetanide. At least eight concentration levels are examined. For each level, four measurements are taken and the average peak area is used to make the calibration curve. The obtained calibration plots shown in Figures 4.32 exhibit a good linearity with the correlation coefficients of 0.9965, 0.9959, 0.9962, and 0.9969 for amiloride, triamterene, BFMTZ and bumetanide, respectively. The other regression parameters involving slopes and intercepts of the obtained calibration curves are listed in Table 4.4. The statistical data reported in Table 4.4, reveal a good linearity and precision. Intra-day relative standard deviations (RSD) are calculated ($n=4$) in Table 4.4 for the peak area and migration time. In all cases, the RSD values are less than 2 % for peak area and 3 % for migration time.

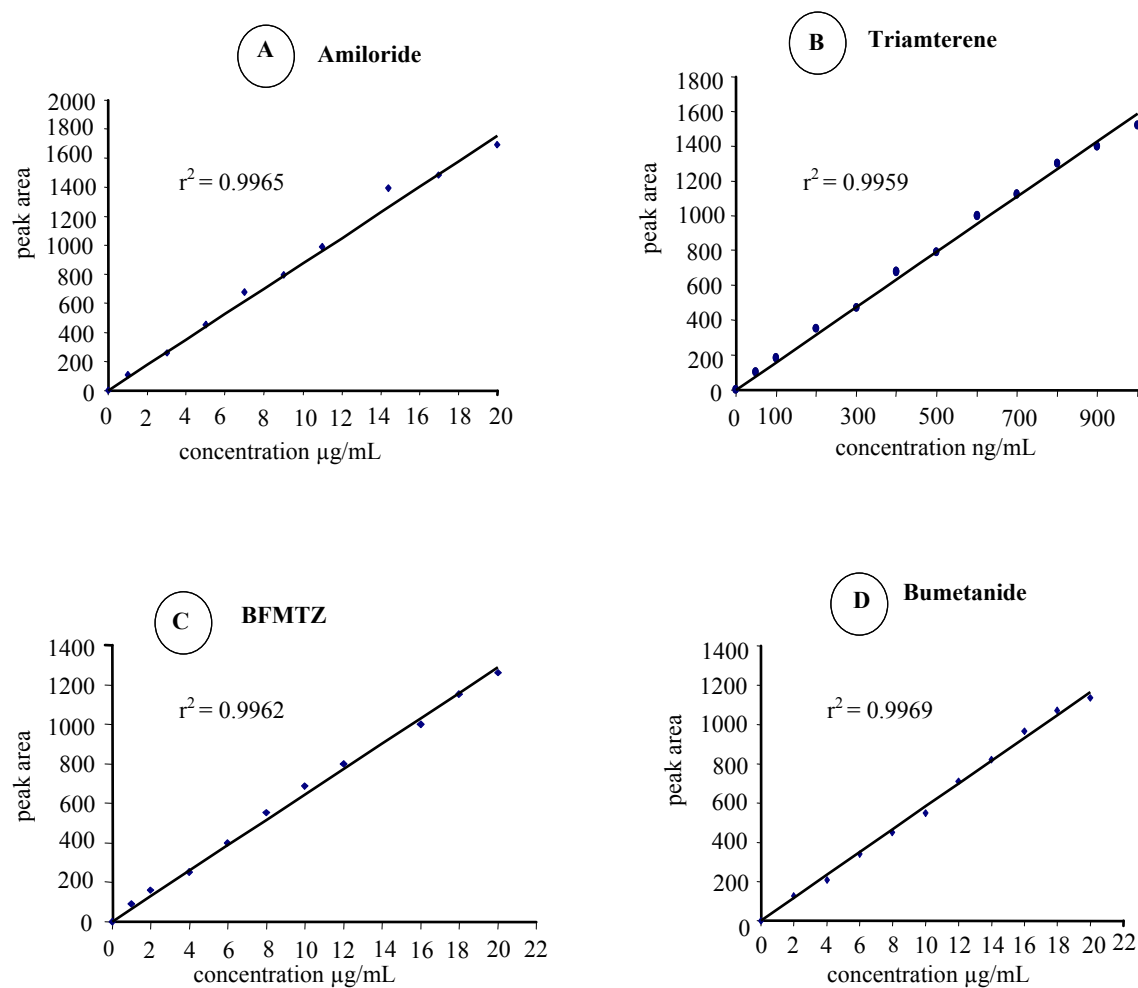


Figure 4.32: Standard calibration plots for standard diuretic drugs using HeCd laser and other conditions are as in Figure 4.28B.

Table 4.4: Method validation for quantitative determination of diuretic drugs (* n= 4).

Parameters	Amiloride	Triamterene	BFMTZ	Bumetanide
Sensitivity range	1-20 µg/mL	50-1000 ng/mL	1-20 µg/mL	2-20 µg/mL
LOQ	1 µg/mL	50 ng/mL	1 µg/mL	2 µg/mL
LOD	250 ng/mL	12.5 ng/mL	300 ng/mL	900 ng/mL
RSD% peak area*	1.85	1.61	1.02	1.11
RSD% migration time*	1.66	1.94	1.23	2.30
Correlation coefficient	0.9965	0.9959	0.9962	0.9969
Intercept	23752	28449	25482	-7949
Slope	85793	1544	62549	58797

The limits of detection (LOD) are given in Table 4.4. These values are confirmed by injection of a standard solution close to the LODs, resulting in a peak height for all diuretics which is equal to or less than three times of the baseline noise. The corresponding electropherograms are shown in Figure 4.33.

As described above, the HeCd laser provides better sensitivities for amiloride and triamterene. As a result, LODs for amiloride and triamterene are determined to be 250 ng/mL and 12.5 ng/mL, respectively (Figures 4.33A and B). It is observed that, the measured LOD of triamterene is twenty times better than amiloride. This means that the proposed method is highly sensitive for quantitative determination of triamterene comparing with amiloride. It is also observed that less sensitivities are obtained for BMFTZ and bumetanide, whose LODs are determined to be 300 ng/mL and 900 ng/mL, respectively (Figures 4.33C and D).

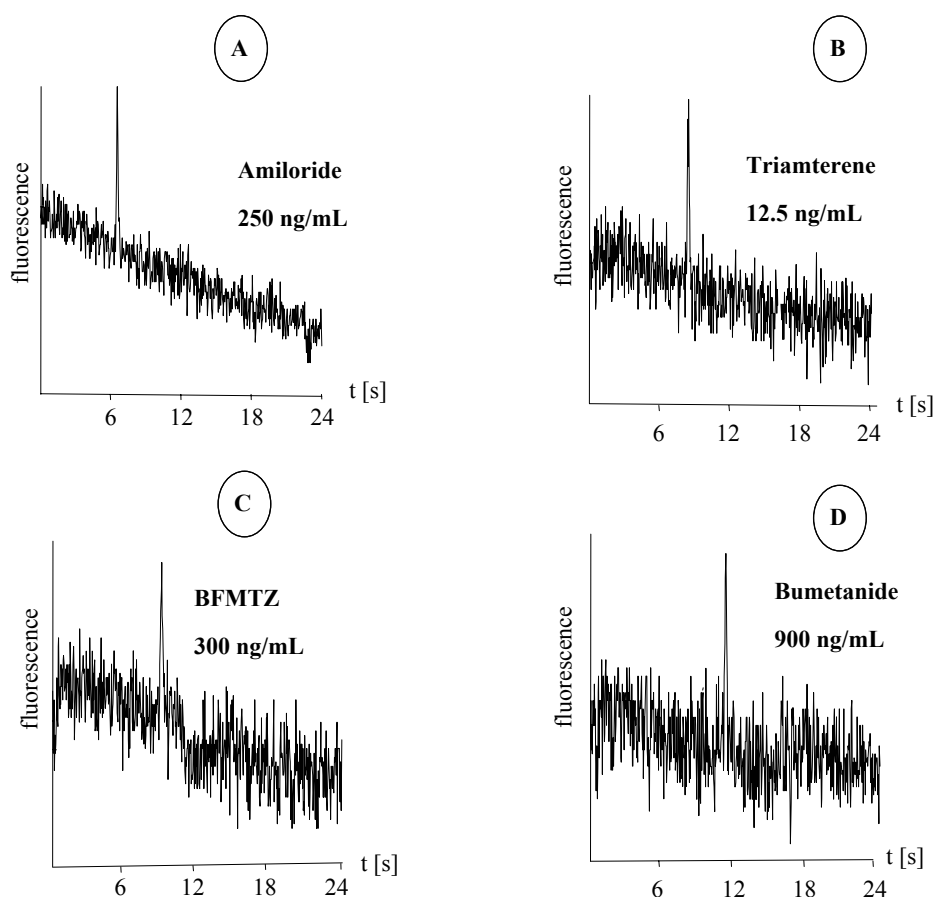


Figure 4.33: Electropherograms of standard diuretics at the limit of detection: (A) 250 ng/mL amiloride, (B) 12.5 ng/mL triamterene, (C) 300 ng/mL bendroflumethiazide, (D) 0.9 μ g/mL bumetanide, and other conditions are as in Figure 4.28B.

The limits of quantitation (LOQ) are calculated from a series of diluted solutions exhibiting an $S/N \approx 10$. These values are determined to be $1 \mu\text{g/mL}$ amiloride, 50 ng/mL triamterene, $1 \mu\text{g/mL}$ BFMTZ and $2 \mu\text{g/mL}$ bumetanid as shown in Figure 4.34.

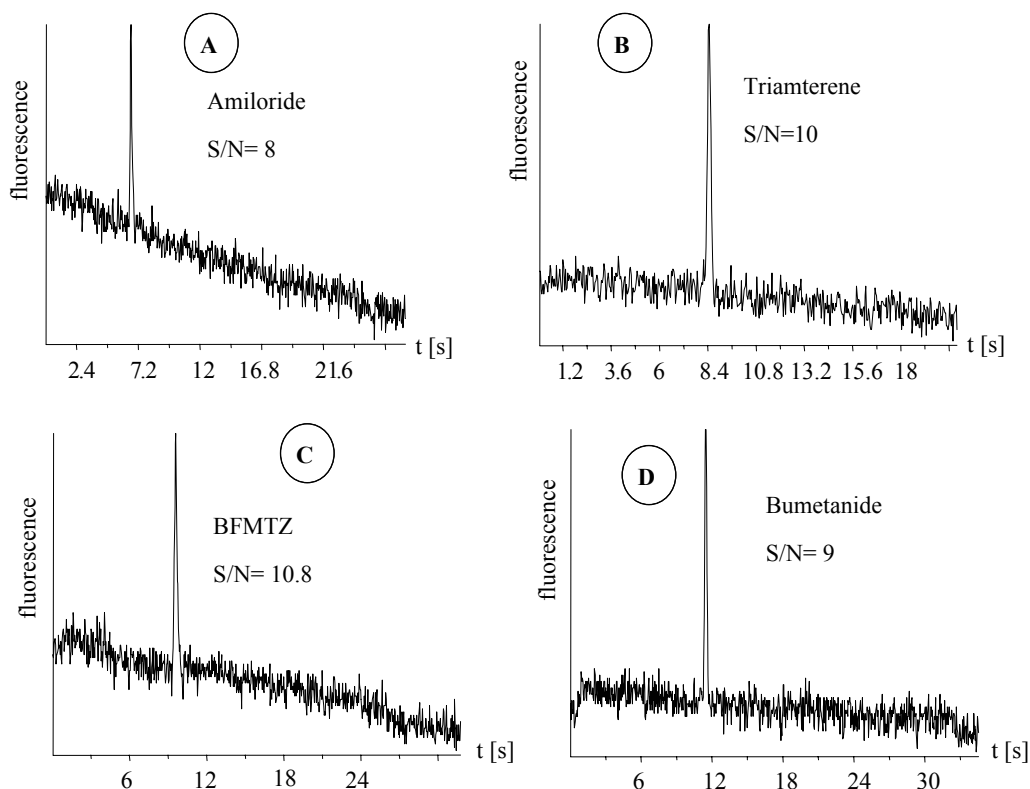


Figure 4.34: Electropherograms of standard diuretics at LOQ. (A) 250 ng/mL amiloride, (B) 12.5 ng/mL triamterene, (C) 300 ng/mL BFMTZ, (D) 900 ng/mL bumetanide. Other conditions are as in Figure 4.28B.

The validated method is then applied to the commercially available tablets such as Hydikal (5 mg/tablet amiloride and 50 mg/tablet HCTZ), Epitens (30 mg/tablet triamterene and 10 mg/tablet xipamide) and Edemex tablets (1 mg/tablet bumetanide). The tablets are finely powdered, dissolved in methanol and then diluted to give stock solutions with concentrations of 0.2 mg/mL according to the labeled amount of the drug. Afterwards, all solutions are filtered before being introduced into the chip in order to avoid any contaminations from the tablets coating materials. The corresponding electropherograms obtained for each tablet are shown in Figure 4.35.

In the electropherogram representing the hydikal tablets (Figure 4.35A), the peak of amiloride is well resolved from the other compound, HCTZ, without interfering. In electropherograms of Epitens and Edemex tablets (Figures 4.35B and C) only the respective signals of triamterene and bumetanide are obtained. Currently, the formulations containing BFMTZ is not available in the market. The interday reproducibility of migration times, as evident from the comparison of respective migration times in Figures 4.33–4.35, is poorer as expected due to fluctuations in EOF and ambient temperatures.

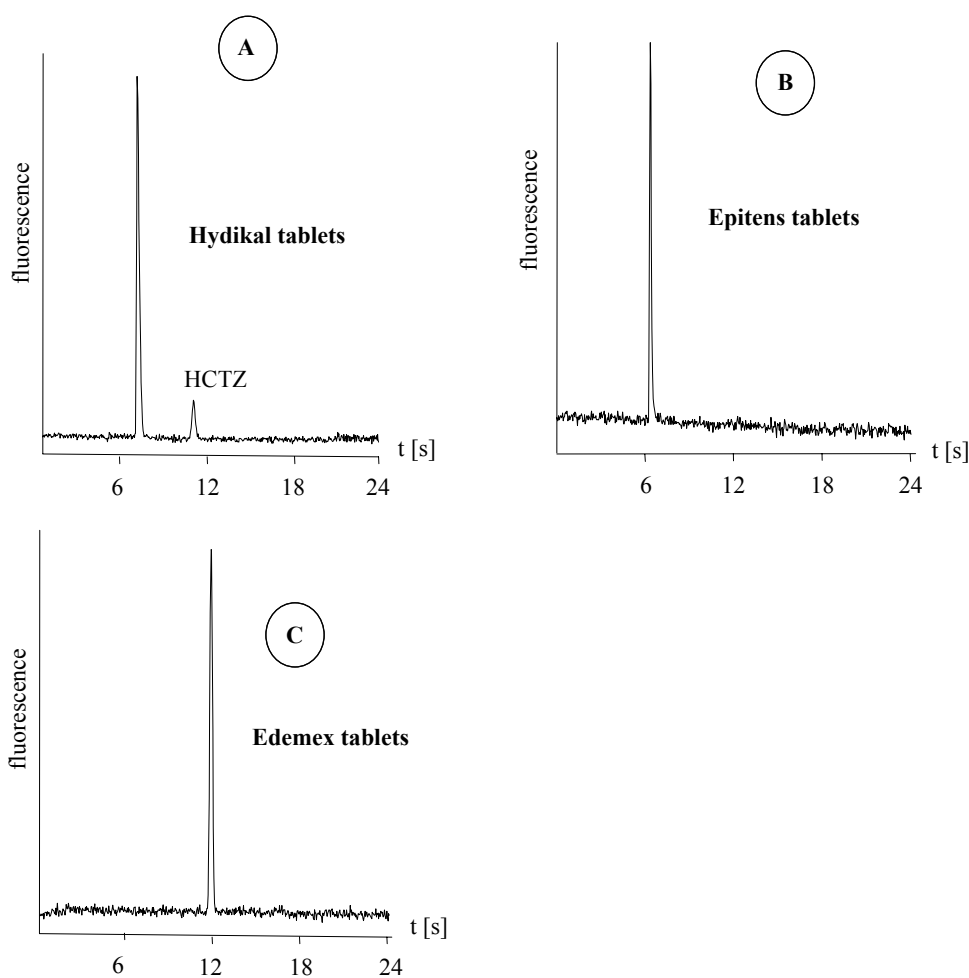


Figure 4.35: Electropherograms of the diuretics in commercial tablets: (A) Hydikal tablet: 10 $\mu\text{g}/\text{mL}$ amiloride, (B) Epitens tablet: 250 ng/mL triamterene, (C) Edemex tablet: 10 $\mu\text{g}/\text{mL}$ bumetanide. Other conditions are as in Figure 4.28B.

Quantitative determination of the diuretics in tablets is performed using the standard addition technique as described in Table 4.5. For this purpose, four different amounts of each standard are added to the solutions of the pharmaceutical formulations. Each MCE-experiment for quantitation is repeated four times. The values of the average recovery for

diuretics in formulation ranged from 99.96 to 100.74 % indicating the reproducibility of the method with relative standard deviations less than 2%. The amount of drugs is calculated in tablets to be 5.01, 30.22 and 0.99 mg/tablet for amiloride, triamterene and bumetanide, respectively. These results are in good agreement with the labeled amount of diuretics in formulations as described in Table 4.5. These data show that chip electrophoresis is well suited for quantitative determination of drugs in formulations within seconds.

Table 4.5: Determination of diuretics in pharmaceutical formulations ($n=4$).

Formulation	Amount of standard added	Amount of standard found	Recovery %
Hydikal tablets (5 mg/tablet amiloride)	5 µg/mL	5.02 µg/mL	100.40
	7 µg/mL	6.90 µg/mL	98.75
	9 µg/mL	9.13 µg/mL	101.44
	11 µg/mL	11.10 µg/mL	100.90
Mean recovery%			100.32
RSD%			1.24
Epitens tablets (30 mg/tablet triamterene)	200 ng/mL	198.06 ng/mL	99.03
	300 ng/mL	303.36 ng/mL	101.12
	400 ng/mL	408 ng/mL	102
	500 ng/mL	504 ng/mL	100.80
Mean recovery%			100.74
RSD%			1.25
Edemex tablets (1 mg/tablet bumetanide).	4 µg/mL	4.10 µg/mL	102.50
	6 µg/mL	5.90 µg/mL	98.33
	8 µg/mL	8 µg/mL	100
	10 µg/mL	9.90 µg/mL	99
Mean recovery%			99.96
RSD%			1.83

4.2.2.3 Analysis of diuretics in human urine

As described above, diuretics are used illegally by athletes to avoid detection of banned substances by reducing their concentration in urine. For this reason, the Medical Commission of the International Olympic Committee added diuretics to the banned substance list in April 1986, and they scheduled within a doping class from the 1988 Olympic Games [69, 209]. Recently, the World Anti-doping Agency (WADA), in its 2005 version, has included diuretics in the prohibited substances [211].

Many techniques have been developed for doping analysis such as automated solid phase extraction [212], HPLC [213] and recently capillary zone electrophoresis (CZE) [214-217]. However most of these techniques are time-consuming. Most of diuretics are excreted unchanged in urine [200]; therefore, the screening method for diuretics in human urine can be mainly developed to detect the native compounds (unmetabolized form).

For this purpose, the developed MCE method can also be applied to the analysis of the diuretics dissolved in human urine. The electropherogram in Figure 4.36A corresponds to the drug standards dissolved in human urine after dilution with water (1:1) to avoid the matrix effect.

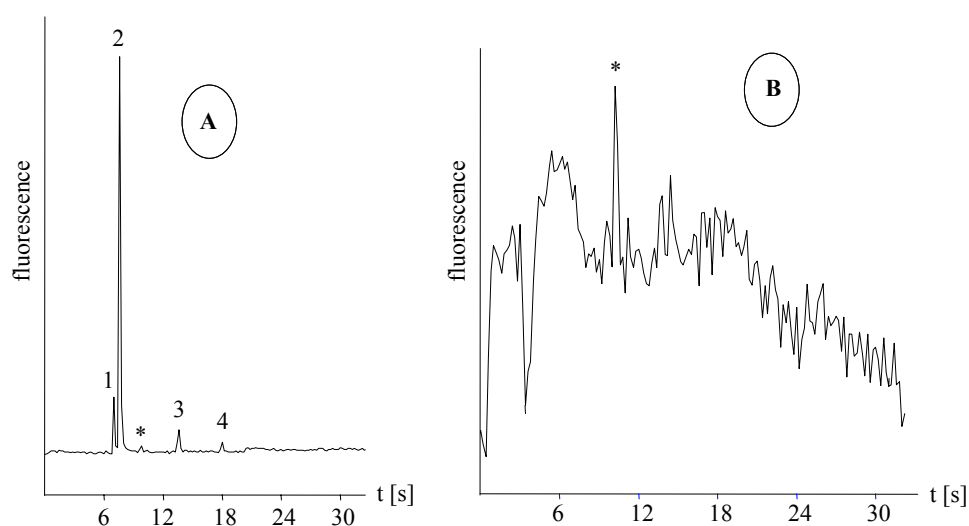


Figure 4.36: (A) Electropherogram of the standard diuretic drugs in human urine (1) 5 $\mu\text{g/mL}$ amiloride, (2) 1 $\mu\text{g/mL}$ triamterene, (3) 15 $\mu\text{g/mL}$ bendrofluomethiazide, (4) 5 $\mu\text{g/mL}$ bumetanide, and (*) peak originated from endogenous urine components, (B) Electropherogram of the urine blank. Detection using mercury lamp at 330-380 nm, other conditions are as in Figure 4.28B.

In comparison with the electropherogram of the drug standard dissolved in running buffer (Figure 4.31B), the migration time remains unchanged and the separation is still satisfactory. The only significant difference is that the peaks are broadened when dissolved in urine which is expected due to the high ionic strength of the urine. In Figure 4.36B, the electropherogram of the blank urine is shown for comparison. No interferences from endogenous urine components are observed.

In comparison with the GC-MS technique [218], which is commonly used in doping analysis, the developed MCE achieves a very fast separation (within 18 s), while in GC-MS the separation is achieved within minutes. However, the later method was used in the Sydney 2000 Olympic Games to analyze 3000 samples in 4 weeks [217] which is relatively slow and time consuming comparing to the developed MCE method. These results show that MCE can be used as a faster analytical principle for screening and confirmatory analysis in doping control. In addition, the advantage of detecting native fluorescence is the elimination of derivatization steps simplifying the proposed method and reducing the time of the total analysis. As a result, the introduced method shows good promise for applying it to the detection of trace levels of abused drugs in forensic analysis.

Chapter 5 Summary and conclusions

The aim of this work was:

1- Improvement of the performance of powder-blasted (pb) microchips by applying polyvinyl alcohol (PVA) as a permanent coating.

It was found that the limited electrophoretic resolution obtained in powder-blasted (pb) chips could significantly be improved by coating the channels with polyvinyl alcohol. The performance of coated and uncoated powder-blasted (pb) devices as well as coated and uncoated wet chemical etched (wc) chips was compared in electrophoretic separations of fluorescently labeled test compounds.

It was found that the uncoated powder-blasted chips provided lower theoretical plate numbers and poorer resolutions. Applying the coating process to powder-blasted chips, the resolution of test compounds in such coated powder-blasted devices was higher than in uncoated wet chemical etched chips.

Dynamic coating of powder-blasted chips was also applied using hydroxypropylmethylcellulose (HPMC) and polyvinyl alcohol. The latter was found to be not effective for dynamic coating while hydroxypropylmethylcellulose resulted in a strongly reduced EOF.

PVA-coated pb-chips could also be applied in chiral separations. In an uncoated pb-chip with a hydroxypropyl- γ -cyclodextrin (HP- γ -CD) buffer, only one broad signal was obtained while two well-resolved signals were obtained in a coated device.

It can be concluded that, coated powder-blasted chips can become an economic alternative to wet chemical etched chips for many applications, especially in protein separations.

2- Development and validation of fast methods based on microchip capillary electrophoresis (MCE) to determine some therapeutic and abuse drugs in formulations and human urine. Drugs such as central nervous system stimulants (ephedrine and pseudoephedrine) and diuretics were successfully determined using MCE. A fast micellar electrokinetic capillary chromatography (MEKC) method was introduced for the determination of FITC-labeled ephedrine and pseudoephedrine. Different light sources were used for excitation such as an argon ion laser and a mercury lamp. It was found that LIF utilizing an argon ion laser is the best approach for sensitive detection of ephedrine and pseudoephedrine in comparison to a mercury lamp. The method was

successfully applied to the analysis of the respective drugs in pharmaceutical formulations and human urine.

Furthermore, a fast MCE method was developed for the determination of diuretics in formulations and human urine. Different light sources were used utilizing either a mercury lamp (330-380 nm), a HeCd laser (325 nm) or a pulsed frequency doubled Nd:YAG-laser (266 nm). The HeCd was chosen as an excitation light source which provided a higher sensitivity for the detection of the diuretics. The developed MCE method was successfully applied to formulations and human urine without interference from other active ingredients.

It can be concluded that, MCE-separations of drugs are completed within seconds rather than several minutes as in HPLC. Furthermore as a chip electrophoresis can be integrated into portable analytical devices, this approach appears to be especially attractive for field analysis and point of care diagnostics.

Chapter 6 Curriculum vitae

Surname	Tolba
First Name	Kamal
Date of birth	13.06 .1972
Martial Status	Married
Place of birth	Bani-Suef (Egypt)
Nationality	Egyptian
Education	
09/1978 – 07/1984	Primary School, Bani-Suef/Egypt
09/1984 – 07/1990	Secondary School, Bani-Suef/Egypt
07/1990	Degree: Abitur
Studies	
09/1990 – 07/1994	Chemistry at the Faculty of Science (Cairo University).
07/1994	Bachelor Diploma
09/1994– 07/1995	Degree: Master Diploma of Chemistry
10/1997–01/2001	Master Work at the National organization for Drug Control and Research
01/2002	Master Degree of Chemistry
09/1995 – 10/2004	Research staff at the National organization for Drug Control and Research
10/2004 – 06/2006	PhD Work at Max-Planck Institute of Coal Research
06/2006 – 08/2007	PhD Work at the Institute of Analytical Chemistry, Chemo- and Biosensors (Prof. Belder) at the University of Regensburg

References

- [1] <http://en.wikipedia.org/wiki/Lab-on-a-chip#Journals>.
- [2] Harrison, D. J., Fluri, K., Seiler, K., Fan, Z. H., Effenhauser, C. S., Manz, A., *Science* 1993, 261, 895-897.
- [3] Schmalzing, D., Koutny, L., Adourian, A., Belgrader, P., Matsudaira, P., Ehrlich, D., *Proc. Natl. Sci. USA* 1997, 94, 10273–10278.
- [4] Jacobson, S. C., Culbertson, C. T., Daer, J. E., Ramsey, J. M., *Anal. Chem.* 1998, 70, 3476–3480.
- [5] Liu, S. R., Ren, H. J., Gao, Q. F., Roach, D. J., Loder, R. T., Armstrong, T. M., Mao, Q. L., Blaga, I., Barker, D. L., Jovanovich, S. B., *Proc. Natl. Sci. USA* 2000, 97, 5369–5374.
- [6] Wallenborg, S. R., Bailey, C. G., *Anal. Chem.* 2000, 72, 1872–1878.
- [7] Rodriguez, I., Jin, L. J., Li, S. F. Y., *Electrophoresis* 2000, 21, 211–219.
- [8] Reetz, M. T., Kühling, K. M., Deege, A., Hinrichs, H., Belder, D., *Angew. Chem. Int. Ed.* 2000, 39, 3891–3893.
- [9] Dolník, V., Liu, S. R., Jovanovich, S., *Electrophoresis* 2000, 21, 41–54.
- [10] Pu, Q. S., Luttge, R., Gardeniers, H. J. G. E., van den Berg, A., *Electrophoresis* 2003, 24, 162–171.
- [11] Wensink, H., Schlautmann, S., Goedbloed, M. H., Elwenspoek, M. C., *J. Micromech. Microeng.* 2002, 12, 616–620.
- [12] Belder, D., Ludwig, M., *Electrophoresis* 2003, 24, 3595–3606.
- [13] Berridge, J. C., *J. Pharm. Pharmacol.* 1993, 45, 361.
- [14] Chamberlain, J., *The Analysis of Drugs in Biological Fluids*, CRC Press, Boca Raton, FL, 2nd edn., 1995.
- [15] Baselt, R. C., Cravey, R. H., *Disposition of Toxic Drugs and Chemicals in Man*, Chemical Toxicology Institute, Foster City, CA, USA, 4th edn., 1995.
- [16] Mehta, A. C., *Analyst* 1997, 122, 83R–88R.
- [17] Baselt, R. C., *Analytical Procedures for Therapeutic Drug Monitoring and Emergency Toxicology*, PSG, Littleton, MA, USA, 2nd edn., 1987.
- [18] Mehta, A. C., *Anal. Proc.*, 1995, 32, 347.
- [19] Uges, D. R. A., Bouma, P., Pietersma, H., Meijer-Koens, J., *Eur. Hosp. Pharm.* 1996, 2, 4.

- [20] Lai, C. K., Lee, T., Au, K. M., Chan, A. Y. W., *Clin. Chem.* 1997, 43, 312.
- [21] Song, W., Dou, C., *J. Anal. Toxicol.* 2003, 27, 366.
- [22] Papatheodoridis, G. V., Papadelli, D., Cholongitas, E., Vassilopoulos, D., Mentis, A., Hadziyannis, S. J., *Am. J. Med.* 2004, 116, 601.
- [23] Ferreira, H., Lucio, M., de Castro, B., Gameiro, P., Lima, J. L., Reis, S., *Anal. Bioanal. Chem.* 2003, 377, 293.
- [24] Erk, N., *J. Pharm. Biomed. Anal.* 1999, 21, 429.
- [25] Maurer, H. H., *J. Chromatogr. B* 1999, 733, 3.
- [26] Maurer, H. H., Tauvel, F. X., Kraemer, T., *J. Anal. Toxicol.* 2001, 25, 237.
- [27] Kim, K. R., Yoon, H. R., *J. Chromatogr. B* 1996, 682, 55.
- [28] Gioino, G., Hansen, C., Pacchioni, A., Rocca, F., Barrios, S. M., Brocca, E., Cancela, L. M., *Ther. Drug Monit.* 2003, 25, 99.
- [29] Chmielewska, A., Konieczna, L., Plenis, A., Bieniecki, M., Lamparczyk, H., *Biomed. Chromatogr.* 2005, 20, 119.
- [30] Alnouti, Y., Srinivasan, K., Waddell, D., Bi, H., Kavetskaia, O., Gusev, A. I., *J. Chromatogr. A* 2005, 1080, 99.
- [31] Hurtado, F. K., Nogueira, D. R., Bortolini, F., Magalhaes da Silva, L., Zimmermann, E., Jost e Souza, M., de Melo, J., Rolim, C. M. B., *J. Liq. Chromatogr.* 2007, 30, 1981-1989.
- [32] Rebiere, H., Mazel, B., Civade, C., Bonnet, P., *J. Chromatogr. B* 2007, 850, 376-383.
- [33] Golubitskii, G. B., Budko, E. V., *J. Pharm. Chem.* 2006, 40, 633-637.
- [34] Demirkaya, F., Kadioglu, Y., *J. Pharm. Sci.* 2005, 30, 78-82.
- [35] Doherty, B., O'Donnell, F., Smyth, W. F., Leslie, J. C., Ramachandran, V. N., Boyd, N. S., Hack, C. J., O'Kane, E., McClean, S., *Talanta* 2007, 72, 755-761.
- [36] Ciavarella, A. B., Gupta, A., Sayeed, V. A., Khan, M. A., Faustino, P. J., *J. Pharma. and Biomed. Analysis* 2007, 43, 1647-1653.
- [37] Pedrouzo, M., Reverte, S., Borrull, F., Pocurull, E., Marce, R. M., *J. Sep. Sci.* 2007, 30, 297-303.
- [38] Ulu, S. T., *J. Pharm. Sci.* 2006, 3, 123-139.
- [39] El-Sherbiny, D. T., El-Enany, N., Belal, F. F., Hansen, S. H., *J. Pharma. and Biomed. Analysis* 2007, 43, 1236-1242.
- [40] Iqbal, M. S., Shad, M. A., Ashraf, M. W., Bilal, M., Saeed, M., *Chromatographia* 2006, 64, 219-222.

- [41] Bahrami, G., Mirzaeei, S., Kiani, A., *J. Chromatogr. B* 2005, 816, 327-331.
- [42] Srinubabu, G., Raju, C. A. I., Sarath, N., Kumar, P. K., Rao, J. S., *Talanta* 2007, 71, 1424-1429.
- [43] SciFinder Scholar 2006, Search for Scientific Information, Regensburg University.
- [44] Spyridaki, M.-H., Kiouisi, P., Vonaparti, A., Valavani, P., Zonaras, V., Zahariou, M., Sianos, E., Tsoupras, G., Georgakopoulos, C., *Anal. Chim. Acta* 2006, 573, 242-249.
- [45] Thevis, M., Sigmund, G., Schiffer, A., Schaenzer, W., *European Journal of Mass Spectrometry* 2006, 12, 129-136.
- [46] Thevis, M., Thomas, A., Delahaut, P., Bosseloir, A., Schaenzer, W., *Anal. Chem.* 2006, 78, 1897-1903.
- [47] Thevis, M., Schaenzer, W., *J. Chromatogr. Sci.* 2005, 43, 22-31.
- [48] Thieme, D., Grosse, J., Lang, R., Mueller, R. K., Wahl, A., *J. Chromatogr. B* 2001, 757, 49-57.
- [49] Statheropoulos, M., Tzamtzis, N., Miki, K. *J. Chromatogr. B* 1998, 706, 245-251.
- [50] Statheropoulos, M., Smaragdis, E., Tzamtzis, N., Georgakopoulos, C., *Anal. Chim. Acta* 1996, 331, 53-61.
- [51] Lyris, E., Tsiakatouras, G., Angelis, Y., Koupparis, M., Spyridaki, M., Georgakopoulos, C., *J. Chromatogr. B* 2005, 827, 199-204.
- [52] Cherkaoui, S., Veuthey, J. L., *J. Chromatogr. A* 2000, 874, 121.
- [53] Desiderio, C., Fanali, S., *J. Chromatogr. A* 2000, 895, 123.
- [54] Zaugg, S., Zhang, X., Sweedler, J., Thormann, W., *J. Chromatogr. B* 2001, 752, 17.
- [55] Makino, K., Yano, T., Maiguma, T., Teshima, D., Sendo, T., Itoh, Y., Oishi, R., *Ther. Drug Monit.* 2003, 25, 574.
- [56] Macia, A., Borrull, F., Aguilar, C., Calull, M., *Electrophoresis* 2004, 25, 428.
- [57] Macia, A., Borrull, F., Calull, M., Aguilar, C., *Electrophoresis* 2005, 26, 970.
- [58] Chen, Y. L., Wu, S. M., *Anal. Bioanal. Chem.* 2005, 381, 907.
- [59] Rios, A., Escarpa, A., Gonzalez, M. C., Crevillen, A. G., *TrAC Trends Anal. Chem.* 2006, 25, 467.
- [60] Kutter, J. P., *Trends Anal. Chem.* 2000, 352-363.
- [61] Bruin, G. J. M., *Electrophoresis* 2000, 21, 3931-3951.

- [62] Reyes, D. R., Iossifidis, D., Auroux, P. A., Manz, A., *Anal. Chem.* 2002, *74*, 2623–2636.
- [63] Auroux, P. A., Iossifidis, D., Reyes, D. R., Manz, A., *Anal. Chem.* 2002, *74*, 2637–2652.
- [64] Jacobson, S. C., Hergenroder, R., Koutny, L. B., Warmack, R. J., Ramsey, J. M., *Anal. Chem.* 1994, *66*, 1107–1113.
- [65] Wooley, A. T., Sensabaugh, G. F., Mathies, R. A., *Anal. Chem.* 1997, *69*, 2181–2186.
- [66] Shi, Y., Simpson, P. C., Scherer, J. R., Wexler, D., Skibola, C., Smith, M. T., Mathies, R. A., *Anal. Chem.* 1999, *71*, 5354–5361.
- [67] Simpson, J. W., Ruiz-Martinez, M. C., Mulhern, T. G., Berka, J., Latimer, D. R., Ball, J. A., Rothberg, J. M., Went, G. T., *Electrophoresis* 2000, *21*, 135–149.
- [68] Zhang, C.-X., Manz, A., *Anal. Chem.* 2001, *73*, 2656–2662.
- [69] International Olympic Committee, *Antidoping Code of the Olympic Movement*, IOC, Lausanne 1999.
- [70] Compton, S. W., Brownlee, R. G., *Biotechniques* 1988, *6*, 432-440.
- [71] Kohlrausch, F., *Ann. Physik* 1897, *62*, 209-239.
- [72] Tiselius, A., *Kolloid-Z.* 1932, *59*, 306-309.
- [73] Hjerten, S., *Chromatogr. Rev.* 1967, *9*, 122-219.
- [74] Virtanen, R., Nanto, V., *Scand. J., Clin. Lab. Invest.* 1971, *27*, 27-30.
- [75] Virtanen, R., *Acta Polytech. Scand.* 1974, *123*, 1-76.
- [76] Mikkers, F. E. P., Everaets, F. M., Verheggen, T. P. E. M., *J. Chromatogr.* 1979, *169*, 1-10.
- [77] Mikkers, F. E. P., Everaets, F. M., Verheggen, T. P. E. M., *J. Chromatogr.* 1979, *169*, 11-20.
- [78] Giddings, J. C., *J. Sep. Sci.* 1969, *4*, 181-189.
- [79] Jorgenson, J. W., Lukacs, K. D., *Anal. Chem.* 1981, *53*, 1298-1302.
- [80] Jorgenson, J. W., Lukacs, K. D., *J. Chromatogr.* 1981, *218*, 209-216.
- [81] Jorgenson, J. W., Lukacs, K. D., *J. High Resolut. Chromatogr., Chromatogr. Commun.* 1981, *4*, 230-231.
- [82] Winberger, R., *CE Technologies*, Chappaqua, New York 1993, p. 41.
- [83] Schulze, P., *Diploma Thesis*, MPI of Coal Research 2004, p. 7.

- [84] Brad, A., Faulkner, L. R., *Electrochemical methods*, John Wiley & Sons, New York 1980.
- [85] Hunter, R. J., *Zeta potential in colloid science, principles and applications*, Academic Press, New York 1981.
- [86] Davies, J. T., Rideal, E. K., *Interfacial Phenomena*, Academic Press, New York 1961.
- [87] Saloman, K., Burgi, D. S., Helmer, Z. C., *J. Chromatogr.* 1991, 559, 69-80.
- [88] Van der Goor, A. A. M., Wanders, B. J., Everaets, F. M., *J. Chromatogr.* 1989, 470, 95-104.
- [89] Adamson, A. W., *Physical Chemistry of surface*, Wiley Interscience, New York 1967.
- [90] Issaq, H. J., Atamna, I. Z., Muschik, G. M., Janini, G. M., *Chromatographia* 1991, 32, 155-161.
- [91] Pau, P. C. F., Berg, J. O., McMillan, W. G., *J. Phys. Chem.* 1990, 94, 2671-2679.
- [92] Wallingford, R. A., Ewing, A. G., *Adv. Chromatogr.* 1989, 29, 1.
- [93] Heiger, D., *Hewlett Packard*, Avondale, PA 1993.
- [94] Végvári, Á, *PhD Thesis*, Uppsala 2002, p 19-20.
- [95] Hjertén, S., *Electrophoresis* 1990, 11, 665-690.
- [96] Guttman, A., Paulus, A., Cohen, A. S., Grinberg, N., Karger, B. L., *J. Chromatogr.* 1988, 448, 41-53.
- [97] Gústafsson, Ó., *MSc. Thesis*, Technical University of Denmark 2004, p. 17.
- [98] Knox, J. H., Grant, I. H., *Chromatographia* 1987, 24, 135-143.
- [99] Nelson, R. J., Paulus, A., Cohen, A. S., Gutman, A. B., Karger, B. L., *J. Chromatogr.* 1989, 480, 111-127.
- [100] Rush, R. S., Cohen, A. S., Karger, B. L., *Anal. Chem.* 1991, 63, 1346-1350.
- [101] Vinther, A., Soeberg, H., Nielsen, L., Pedersen, J., Bidermann, K., *Anal. Chem.* 1992, 64, 187-191.
- [102] Reijena, J. C., Aben, G. V. A., Everaets, F. M., Verheggen, T. P. E. M., *J. Chromatogr.* 1983, 260, 241-254.
- [103] Jones, A. E., Grushka, E., *J. Chromatogr.* 1989, 466, 219-225.
- [104] Grushka, E., McCormick, R. M., Kirkland, J. J., *Anal. Chem.* 1989, 61, 241-246.

- [105] Schmitt, T., Engelhardt, H., Schneider, H. J., *Würzburger Kolloquium in Chromatography and Electrophoresis*, Bertsch Verlag, Straubing 1993, p. 21-28.
- [106] Sepaniak, M. J., Cole, R. O., Clark, B. K., *J. Liq. Chromatogr.* 1992, 15, 1023-1040.
- [107] Schure, M. R., Lenhoff, A. M., *Anal. Chem.* 1993, 65, 3024-3036.
- [108] Green, S., Jorgenson, J. W., *J. Chromatogr.* 1989, 478, 63-70.
- [109] Bushy, M. M., Jorgenson, J. W., *J. Chromatogr.* 1989, 480, 301-310.
- [110] Emmer, A., Jansson, M., Roeraade, J., *J. High Resolut. Chromatogr.* 1991, 14, 738-740.
- [111] Belder, D., Schomburg, G., *J. High Resolut. Chromatogr.* 1992, 15, 686.
- [112] Gilges, M., Husmann, H., Kleemiß, M. H., Motch, S. R., Schomburg, G., *J. High Resolut. Chromatogr.* 1992, 15, 452.
- [113] Gilges, M., Kleemiß, M. H., Schomburg, G., *Anal. Chem.* 1994, 66, 2038.
- [114] Hjerten, S., *J. Chromatogr.* 1985, 347, 191-198.
- [115] Chankvetadze, B., *Capillary Electrophoresis in Chiral Analysis*, Tbilis State University, Republic of Georgia, 1997, p. 35.
- [116] Chankvetadze, B., *Capillary Electrophoresis in Chiral Analysis*, Tbilis State University, Republic of Georgia, 1997, p. 37.
- [117] http://www.chemsoc.org/ExemplarChem/entries/2003/leeds_chromatography/chromatography/complete.htm.
- [118] Rasmussen, H. T., McNair, H. M., *J. Chromatogr.* 1990, 516, 223-231.
- [119] Dolník, V., *Electrophoresis* 1997, 18, 2353-2361.
- [120] Dolník, V., *Electrophoresis* 1999, 20, 3106-3115.
- [121] Dolník, V., Hutterer, K. M., *Electrophoresis* 2001, 22, 4163-4178.
- [122] Hutterer, K., Dolník, V., *Electrophoresis* 2003, 24, 3998-4012.
- [123] Kim, J., Zand, R., Lubman, D. M., *Electrophoresis* 2003, 24, 782-793.
- [124] Morzunova, T. G., *J. Pharma. Chem.* 2006, 158-170.
- [125] Geiser, L., Veuthey, J., *Electrophoresis* 2006, 28, 45-57.
- [126] Terabe, S., Otsuka, K., Ichikawa, K., Tsuchiya, A., Ando, T., *Anal. Chem.* 1984, 56, 111.
- [127] Otsuka, K., Terabe, S., *Bull. Chem. Soc. Jpn.* 1998, 71, 2465-2481.
- [128] Albin, M., Weinberger, R., Sapp, E., Moring, S., *Anal. Chem.* 1991, 63, 417-422.

- [129] Wu, S., Dovichi, N. J., *Talanta* 1992, 39, 173-178.
- [130] Schulze, P., *Diploma Thesis*, MPI of Carbon Research 2004, p. 20.
- [131] Terry, S. C., Jeman, J. H., Angell, J. B., *IEEE Trans, Electron Devices* 1979, 26, 1880.
- [132] Manz, A., Graber, N., Widmer, H. M., *Sensors and Actuators, B: Chemical B* 1990, 1, 244-248.
- [133] Manz, A., Harrison, D. J., Lüdi, H., Widmer, H. M., *Anal.Chem.* 1992, 64, 1926-1932.
- [134] Manz, A., Harrison, D. J., Verpoorte, E. M. J., *J. Chromatogr.* 1992, 593, 253-258.
- [135] Verpoorte, E., *Electrophoresis* 2002, 23, 677-712.
- [136] Lichtenberg, J., de Rooij, N. F., Verpoorte, E., *Talanta* 2002, 56, 233-266.
- [137] Lacher, N. A., Garrison, K. E., Martin, R. S., Lunte, S. M., *Electrophoresis* 2001, 22, 2526-2536.
- [138] Becker, H., Locascio, L. E., *Talanta* 2002, 56, 267-287.
- [139] Freemantle, M., *Chem. Eng. News* 1999, 27-36.
- [140] Belder, D., Ludwig, M., *Electrophoresis* 2003, 24, 2422-2430.
- [141] Tolba, K., Belder, D., *Electrophoresis* 2007, accepted.
- [142] Tachibana, Y., Otsuka, K., Terabe, S., Arai, A., Suzuki, K., Nakamura, S., *J. Chromatogr. A* 2003, 1011, 181-192.
- [143] Guihen, E., Sisk, G. D., Scully, N. M., Glennon, J. D., *Electrophoresis* 2006, 27, 2338-2347.
- [144] Ding, Y., Garcia, C. D., *Electroanalysis* 2006, 18, 2202-2209.
- [145] Belder, D., Ludwig, M., Wang, L.-W., Reetz, M. T., *Angew. Chem. Int. Ed.* 2006, 45, 2463-2466.
- [146] Roberts, M. A., Rossier, J. S., Bercier, P., Girault, H., *Anal. Chem.* 1997, 69, 2035-2042.
- [147] Becker, H., Deitz, W., *Proc. SPIE* 1998, 3515, 177.
- [148] McCormick, R. M., Nelson, R. J., Alonso-Amigo, M. G., Benvegna, J., Hooper, H. H., *Anal. Chem.* 1997, 69, 2626-2630.
- [149] Belloy, E., Thurre, S., Walckiers, E., Sayah, A., Gijs, M. A. M., *Sens. Actuators A* 2000, 84, 330-337.
- [150] Solognac, D., Sayah, A., Constantin, S., Freitag, R., Gijs, M. A. M., *Sens. Actuators A* 2001, 92, 388-393.

- [151] Belloy, E., Sayah, A., Gijs, M. A. M., *Sens. Actuators A* 2000, 86, 231–237.
- [152] Schlautmann, S., Wensink, H., Schasfoort, R., Elwenspoek, M., van den Berg, A., *J. Micromech. Microeng.* 2001, 11, 386–389.
- [153] Belder, D., Kohler, F., Ludwig, M., Tolba, K., Piehl, N., *Electrophoresis* 2006, 27, 3277–3283.
- [154] McDonald, J. C., Duffy, D. C., Anderson, J. R., Chiu, D. T., Wu, H., Schueller, O. J. A., Whitesides, G. M., *Electrophoresis* 2000, 21, 27–40.
- [155] Jacobson, S. C., Koutny, L. B., Hergenrder, R., Moore, A. W., Ramsey, J. M., *Anal. Chem.* 1994, 66, 3472–3476.
- [156] Gooijer, C., Mank, A. J. G., *Anal. Chim. Acta* 1999, 400, 281–295.
- [157] Fister, J. C., Jacobson, S. C., Davis, L. M., Ramsey, J. M., *Anal. Chem.* 1998, 70, 431.
- [158] Ocvirk, G., Tang, T., Harrison, D. J., *Analyst* 1998, 123, 1429.
- [159] Jiang, G. F., Attiya, S., Ocvirk, G., Lee, W. E., Harrison, D. J., *Biosens. Bioelecton.* 2000, 14, 861.
- [160] Schulze, P., Ludwig, M., Kohler, F., Belder, D., *Anal. Chem.* 2005, 77, 1325–1329.
- [161] Belder, D., Deege, A., Maass, M., Ludwig, M., *Electrophoresis* 2002, 23, 2355–2361.
- [162] Ludwig, M., *Diploma Thesis*, MPI of Coal Research 2001, p. 47.
- [163] Ludwig, M., *PhD Thesis*, MPI of Coal Research 2005.
- [164] Belder, D., Deege, A., Kohler, F., Ludwig, M., *Electrophoresis* 2002, 23, 3567–3573.
- [165] <http://probes.invitrogen.com/handbook/sections/0103.html>.
- [166] <http://probes.invitrogen.com/resources/spectraviewer>.
- [167] Ludwig, M., Belder, D., *Electrophoresis* 2003, 24, 2481–2486.
- [168] Varjo, S. J. O., Ludwig, M., Belder, D., Riekkola, M. L., *Electrophoresis* 2004, 25, 1901–1906.
- [169] Betz, J. M., Gay, M. L., Mossoba, M. M., Adams, S., Portz, B. S., *J. AOAC Int.* 1997, 80, 303.
- [170] Karch, S. B., in: Cupp, M. J. (Ed.), *Toxicology and Clinical Pharmacology of Herbal Products*, Humana Press, Totowa 2000, p. 11.
- [171] Abourashed, E. A., El-Alfy, A. T., Khan, I. A., Walker, L., *Phytother. Res.* 2003, 17, 703–712.

- [172] Sheu, S. J., *J. Food Drug Anal.* 1997, 5, 285.
- [173] Liu, Y. M., Sheu, S. J., Chiou, S. H., Chang, H. C., Chen, Y. P., *Planta Med.* 1992, 59, 376.
- [174] Castleman, M., *The Healing Herbs: The Ultimate Guide to the Curative Power of Nature's Medicines.* New York 1995, p. 230.
- [175] Kasahara, Y., Hikino, H., *J. Chromatogr.* 1985, 324, 503–507.
- [176] Liu, Y. M., Sheu, S. J., *J. Chromatogr.* 1992, 600, 370–372.
- [177] Yamasaki, K., Fujita, K., *Chem. Pharm Bull* 1979, 27, 43–47.
- [178] Harada, M., Ogihara, Y., Kano, Y., Akahori, A., Ochio, Y., Miura, O., Yamamoto, K., Suzuki, H., *Iyakuhin Kenkyu* 1989, 20, 1300.
- [179] Hu, J., *Yaowu Fenxi Zazhi* 1994, 14, 33.
- [180] LI, F. Q., Zhang, J. Y., Chen, X. G., Hu, Z. D., *Anal. Lett.* 2001, 34, 2447.
- [181] Liu, H. T., Wang, K. T., Chen, X. G., Hu, Z. D., *Anal. Lett.* 2000, 33, 1105.
- [182] Liu, H. T., Wang, K. T., Zhang, H. Y., Chen, X. G., Hu, Z. D., *Analyst* 2000, 125, 1083.
- [183] Liu, S. H., Li, Q. F., Chen, X. G., Hu, Z. D., *Electrophoresis* 2002, 23, 3392.
- [184] Li, G. B., Zhang, Z. P., Chen, X. G., Hu, Z. D., Zhao, Z. F., Hooper, M., *Talanta* 1999, 48, 1023.
- [185] Liu, Y. M., Sheu, S. J., *J. Chromatogr.* 1993, 637, 219.
- [186] Huang, H. Y., Hsich, Y. Z., *Anal. Chem. Acta* 1997, 351, 49.
- [187] Jelinek, I., *Chem. Listy.* 1999, 93, 800.
- [188] Flurer, C. L., Lin, L. A., Satzger, R. D., Wolnik, K. A., *J. Chromatogr.* 1995, 669, 133.
- [189] Chicharro, M., Zapardiel, A., Bermejo, E., Pérez-lópez, J. A., Hernández, L., *J. Chromatogr.* 1993, 622, 103.
- [190] Chicharro, M., Zapardiel, A., Bermejo, E., Pérez-lópez, J. A., Hernández, L., *Quim. Anal. (Barcelona)* 1994, 13, 134.
- [191] Chicharro, M., Zapardiel, A., Bermejo, E., Pérez-lópez, J. A., Hernández, L., *J. Liq. Chromatogr.* 1995, 18, 136.
- [192] Jin, L. J., Rodriguez, I., Li, S. F. Y., *Electrophoresis* 1999, 20, 1538–1545.
- [193] Subbiah, D., Kala, S., Mishra, A. K., *Chemosphere* 2005, 61, 1580–1586.
- [194] Zhao, Y., Baeyens, W. R. G., van der Weken, G., García-Campana, A. M., *Biomed. Chromatogr.* 1999, 13, 143–144.
- [195] Lokhanauth, K., Snow, H., *J. Sep. Sci.* 2005, 28, 612–618.

- [196] Van Eenoo, P., Delbeke, F. T., Roels, K., De Backer, P., *J. Chromatogr. B* 2001, 760, 255-261.
- [197] Yang, X., Wang, X., Zhang, X., *Anal. Chem. Acta* 2005, 549, 81-87.
- [198] Goebel, C., Trout, G., Kazlauskas, R., *Anal. Chem. Acta* 2004, 502, 65-74.
- [199] Herraizhernandez, R., Campinsfalco, P., Sevillanocabeza, A., *Chromatographia*, 1992, 33, 177-185.
- [200] Ventura, R., Segura, J., *J. Chromatogr. B* 1996, 687, 127-144.
- [201] Lisi, A. M., Trout, G. J., Kazlauskas, R., *J. Chromatogr. B* 1991, 563, 257-270.
- [202] Carreras, D., Imaz, C., Navajas, R., Garcia, M. A. et al., *J. Chromatogr. A* 1994, 683, 195-202.
- [203] Maurer, H. H., *J. Chromatogr. B* 1999, 733, 3-25.
- [204] Mohrke, W., Knauf, H., Mutschler, E., *Int. J. Clin. Pharmacol.* 1997, 35, 447-452.
- [205] Caslavaska, J., Thormann, W., *J. Chromatogr. B* 2002, 770, 207-216.
- [206] González, E., Becerra, A., Laserna, J. J., *J. Chromatogr. B* 1996, 687, 145-150.
- [207] Luis, M. L., Corujedo, S., Blanco, D., Fraga, J. M. G. et al., *Talanta* 2002, 57, 223-231.
- [208] González, E., Montes, R., Laserna, J. J., *Anal. Chim. Acta* 1993, 282, 687-693.
- [209] Luckas, K. D., Jorgenson, J. W., *J. High Resolut. Chromatogr., Chromatogr. Commun.* 1985, 8, 407.
- [210] Lambert, W. J., Middleton, D. L., *Anal. Chem.* 1990, 62, 1585.
- [211] The World Anti-Doping Agency (WADA), *The World Anti-Doping Code*, The 2005 prohibited list 2005, 1-9.
- [212] Goebel, C., Trout, G. J., Kazlauskas, R., *Anal. Chim. Acta* 2004, 502, 65-74.
- [213] Hemiez, R., Campfns, P., Sevillano, A., *Chromatographia* 1992, 33, 177.
- [214] Guzman, H. A. J., Moschera, K., Malick, A.W., *J. Chromatogr.* 1991 559, 307.
- [215] González, E., Lasema, J. J., *Electrophoresis* 1994, 15, 240.
- [216] Chicharro, M., Zapardiel, A., Bermejo, E., Perez J. A., Hernandez, L., *Anal. Lett.* 1994, 27, 1809.
- [217] Jumppanen, J., Siren, H., Riekkola, M.-L., *J. Chromatogr. A* 1993, 652, 441.
- [218] Lisi, A. M., Kazlauskas, R., Trout, G. J., *J. Chromatogr.* 1992, 581, 57-63.